THESIS
2
2007

This is to certify that the
dissertation entitled

MODELING OF DELAY INDUCED BY DOWNSTREAM TRAFFIC DISTURBANCES AT SIGNALIZED INTERSECTION

presented by

KAMRAN AHMED

has been accepted towards fulfillment
of the requirements for the

Ph.D. degree in Civil Engineering

Major Professor's Signature

8/17/2006

Date

MSU is an Affirmative Action/Equal Opportunity Institution

LIBRARY
Michigan State
University

PLACE IN RETURN BOX to remove this checkout from your record.
TO AVOID FINES return on or before date due.
MAY BE RECALLED with earlier due date if requested.

DATE DUE	DATE DUE	DATE DUE

2/05 p:/CIRC/DateDue.indd-p.1

MODELING OF DELAY INDUCED BY DOWNSTREAM TRAFFIC DISTURBANCES AT SIGNALIZED INTERSECTION

By

Kamran Ahmed

A DISSERTATION

Submitted to
Michigan State University
in partial fulfillment of the requirements
for the degree of

DOCTOR OF PHILOSOPHY

Department of Civil and Environmental Engineering

2006

ABSTRACT

MODELING OF DELAY INDUCED BY DOWNSTREAM TRAFFIC DISTURBANCES AT SIGNALIZED INTERSECTION

By

Kamran Ahmed

Macroscopic models are presented to estimate delay during extended control periods (multiple cycles) when downstream traffic queues are both changing over time and significant enough to disrupt traffic flow from an upstream intersection. The models consist of an upstream demand estimation algorithm, a downstream queue build-up prediction algorithm, a shockwaves propagation and dissipation tracking algorithm, and a mechanism to explicitly capture and feed traffic conditions of current cycles into subsequent cycle's control design. Basic traffic flow properties, signal control parameters, and link geometry are used as inputs. The models are modular and can be incorporated in any size system for one or multiple cycles. The models were applied to a hypothetical system of closely spaced intersections and tested for different traffic flow, control, and geometric conditions. The results show that the delay induced by downstream traffic operations on an upstream intersection can be significant and that it may change with each cycle and could reach equilibrium once traffic flow, downstream queues, and signal control measures stabilize and start replicating over time. Cycle-by-cycle analysis of delay values shows that delay is sensitive to assumed initial traffic conditions. The results show that the green ratio, offsets, and spacing between intersections have significant effects on this delay. The macroscopic delay models are

validated using a microscopic traffic simulation model. There is a close association between delay and queue lengths from both models.

DEDICATION

To my father, Chaudhry Niaz Ali, my mother Mrs. Shamshad Niaz, and my brothers Imran Tipu and Adnan Ahmed, for their guidance, support, love and passion. Without these things this thesis could not have been possible.

ACKNOWLEDGMENTS

First and foremost, I wish to thank my advisor Ghassan Abu-Lebdeh for his valuable support and guidance. I am proud to be his first doctoral student, and have learned a lot from his approach of conducting research and high professionalism.

The effort needed to produce this thesis was prodigious. It could not have occurred without the diligence, dedication and commitments of time from many people I would like to express my personal gratitude to Dr. Taylor for his cooperation, genuine, and thoughtfulness.

I would also like to thank my committee members Drs; William C. Taylor, Francois Dion, Bruce Pigozzi, and Rahim Benekohal, for their guidance and help.

I am also grateful to my parents, brothers and other family members, Nadia, Abida, Abubakar, Haleema, Sadia and Maryam, for praying my success and acheivements. To my spouse, Ayesha, thank you for your loving understanding and sacrifice of many evenings and weekends of family time.

At the last but not least my special thanks to National University of Science and Technology (NUST), Pakistan for providing me opportunity and financial support to complete my studies and research work in Michigan State University, USA

TABLE OF CONTENT

LIST OF TABLES ix

LIST OF FIGURES x

CHAPTER 1
Introduction 1
1.1 Background 1
1.2 Problem statement and motivation for study 3
1.3 Research objectives 4
1.4 Research contribution 5
1.5 Research approach and layout 6

CHAPTER 2
Literature Review 7

CHAPTER 3
Delay at Signalized Intersections 14
3.1 Introduction 14
3.2 Uninterrupted flow 14
3.3 Interrupted flow 15
3.4 Signalized intersection 15
3.5 Delay as measure of effectiveness 18
3.5.1 Types of delay 18
3.5.1.1 Stopped-time delay 18
3.5.1.2 Approach delay 18
3.5.1.3 Time –in –queue delay 18
3.5.1.4 Travel time delay 18
3.5.1.5 Control delay 19
3.6 Estimation of delay at signalized intersections 19
3.6.1 Delay estimation using vertical queuing analysis 20
3.6.1.1 Deterministic queuing analysis 20
3.6.1.2 Stochastic queuing analysis 21
3.6.2 Delay estimation using microscopic simulation models 25
3.6.3 Delay estimation using shockwave 26
3.7 Delay estimation methods defined by different capacity guides 27
3.8 Delay models of the 2000 Highway Capacity Manual (HCM 2000) 28
3.8.1 Control delay 28
3.8.1.1 Uniform control delay (d_1) 29
3.8.1.2 Progression adjustment factor (PF) 29
3.8.1.3 Incremental delay (d_2) 31
3.8.1.4 Initial queue delay (d_3) 32
3.9 Summary of delay estimation models 33

3.10 Limitation of HCM 2000 delay methodology 33

CHAPTER 4
Formulation and Derivations of Downstream Induced-delay d4 Model 38
4.1 Introduction 38
4.2 Formation of shockwaves due to a downstream traffic disturbance 42
4.2.1 Mid-block stopping shock wave (MBW1) 44
4.2.2 Mid-block starting shock wave (MBW2) 48
4.2.3 Point of intersection of shock waves 49
4.3 Estimation of queue length between upstream and downstream intersections 51
4.3.1 Wasted green 52
4.3.2 Blockage 55
4.3.3 New traffic 55
4.3.4 Estimation of output from upstream and downstream approaches during a cycle 56
4.3.4.1 Regime 1 (wasted green, no blockage, no new traffic) 57
4.3.4.2 Regime 4 (no wasted green, no blockage, new traffic) 58
4.3.4.3 Regime 5 (no wasted green, blockage, no new traffic) 59
4.3.4.4 Regime 7 (wasted green, no blockage, new traffic) 60
4.3.4.5. Regime 8 (no wasted green, no blockage, no new traffic) 61
4.3.5 Assumptions for queue estimation at downstream approach 63
4.4. Expression for link average speed (Va) 64
4.4.1 Case 1: Vehicle accelerate to free flow speed, cruise, and finally decelerate . 65
4.4.2. Case 2: Vehicle accelerate for half of distance and then decelerates for other half 67
4.5 Length of delay d_4 at the upstream intersection due to downstream traffic disturbance 68
4.6. Estimation of delay for multiple cycles 71

CHAPTER 5
Results and Sensitivity Analysis of Downstream-Induced Delay 74
5.1. Introduction 74
5.2. Example application of the d4-model 75
5.3. Cycle-by-Cycle analysis 75
5.3.1 Variation of d4 and queue length during each cycle 77
5.3.1.1 Impact of link length on d4 80
5.3.1.2 Impact of offset on d4 86
5.3.1.3 Impact of g/c ratio of upstream and downstream approaches on d4 90
5.4 Average value of d4 for 15-minute analysis period 94
5.4.1 Impact of link length on average d4 value 94
5.4.2 Impact of g/c ratio of upstream and downstream approaches on average value of d4 97
5.4.3 Impact of offset on average value of d4 99
5.5 Summary of sensitivity analysis of d4 model 101

CHAPTER 6
Validation of d4 model **102**
6.1 Introduction 102
6.2 Simulation models 102
6.2.1 Microscopic simulation model 103
6.2.2 Macroscopic simulation model 104
6.2.3 Mesoscopic simulation model 104
6.3 CORSIM 105
6.3.1 Support programs 106
6.3.2 Simulation models 106
6.3.2.1 NETSIM 106
6.3.2.2 FRESIM 106
6.3.3 Measure of effectiveness (MOE'S) 107
6.4 Methodology for validation 107
6.5. Coding networks in CORSIM 107
6.5.1 Isolated signalized intersection network 109
6.5.2 Paired signalized intersections network 111
6.6 Significance and quantification of downstream disturbance and additional delay 113
6.7 Validation of the d4 delay model 117
6.7.1 Cycle by cycle comparison 118
6.7.2 Average d4 value for 15-minute analysis period 123
6.7.2.1 Varying Link Length 123
6.7.2.2 Varying g/c ratio 129
6.8 Summary of validation of d4 model 133

CHAPTER 7
Conclusion and Recommendations **134**
7.1 Introduction 134
7.2 Conclusions 135
7.3 Recommendations for further studies 138

References **140**

LIST OF TABLES

Table 3.1 Classification of transportation facilities by flow types (31) 15

Table 3.2 Classification of probability distribution used in stochastic queuing analysis . 23

Table 3.3 Level of service criteria for signalized intersection 28

Table 3.4 Relationship between arrival type and platoon ratio (4) 30

Table 3.5 Progression adjustment factors for uniform delay calculation (4) 31

Table 3.6 Control delay for upstream EB approach by varying link length (Cycle length = 120 sec and 0.67 g/c for both intersection, offset 0 sec) 35

Table 3.7 Control delay for upstream EB approach by offset (Cycle length = 120 sec and 0.67 g/c for both intersection, link length = 400 ft) 35

Table 4.1 Eight traffic flow regimes 56

Table 6.1 Comparison of delay between d4-model and CORSIM results (g/c 0.73-0.67) 126

LIST OF FIGURES

Figure 2.1 Flow chart to estimate degree of saturation and system throughput, Rouphail and Akcelik (5). 8

Figure 3.1 Conflicts points at two-way street (Vehicle conflicts , Pedestrian conflicts) 16

Figure 3.2 Flow chart to analysis operations at signalized intersection, according to HCM 17

Figure 3.3 Different types of delay at signalized intersection 19

Figure 3.4 vehicles arrival and departure verse time at signalized intersection (shaded area = total delay) 21

Figure 3.5 Flowchart of queuing analysis and delay estimation approaches (32) 24

Figure 3.6 shockwaves occurrence at signalized intersection 27

Figure 3.7 Paired signalized intersection system 34

Figure 3.8 Queue spillback from downstream link to the upstream intersection (snap shot of the microscopic simulation experiment) 36

Figure 4.1 Paired-Intersection system setup 38

Figure 4.2 Location and speed of four shockwaves 43

Figure 4.3 Shockwaves intersecting upstream of the upstream intersection ($d_4>0$ in this case) 43

Figure 4.4 Point of intersection located downstream of the upstream intersection ($d_4 = 0$ in this case) 44

Figure 4.5 Important coordinates of the mid block starting and stopping shockwaves 45

Figure 4.6 Two points (x_1, y_1) and (x_2, y_2) in xy plan 47

Figure 4.7 Coordinates of point of intersection of mid block stopping and starting shockwaves. 51

Figure 4.8 Wasted green due to late arrival at green of downstream approach 53

Figure 4.9 Wasted green due to gap between departure of existing queue and arrival of new traffic 53

Figure 4.10 Flow regime with wasted green, no blockage, and no new traffic (Regime 1) 58

Figure 4.11 Flow regime with new traffic, no wasted green and no blockage (Regime 4) 59

Figure 4.12 Flow regime for upstream intersection with blockage (Regime 5) 60

Figure 4.13 Flow regime for downstream intersection with wasted green and new traffic (Regime 7) 61

Figure 4.14 Flow regime for downstream approach for Regime 8 62

Figure 4.15 Flow regime for upstream approach for Regime 8 62

Figure 4.16 Speed profile for a vehicle that accelerates to free-flow speed, cruises and then decelerates to a stop (Case 1) 65

Figure 4.17 Speed profile for vehicle that accelerates to half of distance and then decelerates to a stop (Case 2) 68

Figure 4.18 Additional delay observed by first and second vehicle at upstream approach 69

Figure 4.19 Reduction of delay "d4" for the second vehicle at upstream approach 70

Figure 4.20 Flow chart for the estimation of delay d_4 for multiple cycles 73

Figure 5.1 Upstream and downstream intersection location 75

Figure 5.2 Variation of d4 at subject approach, and change of queue length at downstream link for each cycle. In this case g/c for upstream and downstream are 0.8 and 0.6, respectively; cycle length 150 sec, offset 20 sec, and link length 300 m. 78

Figure 5.3 Variation d4 at subject approach, and change of queue length at downstream link for each cycle. In this case g/c for upstream and downstream are 0.9 and 0.6, respectively; cycle length 120 sec, offset 20 sec, and link length 300 m. 78

Figure 5.4 Variation of d4 with link length (g/c for upstream and downstream are 0.8 and 0.6, respectively; offset 0 seconds; and cycle length is 150 sec) 81

Figure 5.4a Variation of d4 with link length (g/c for upstream and downstream are 0.8 and 0.6, respectively; offset 0 seconds; and cycle length is 150 sec) (Analysis period starts at third cycle) 81

Figure 5.5 Variation of d4 with link length (g/c for upstream and downstream are 0.8 and 0.6, respectively; offset 10 seconds; and cycle length is 150 sec) 82

Figure 5.6 Variation of d4 with link length (g/c for upstream and downstream is 0.8 and 0.6, respectively; offset 15 seconds; and cycle length is 150 sec) 82

Figure 5.7 Variation of d4 with link length (g/c for upstream and downstream are 0.8 and 0.6, respectively; offset 20 seconds; and cycle length is 150 sec) 83

Figure 5.8 Variation of d4 with link length (g/c for upstream and downstream are 0.9 and 0.6, respectively; offset –15 seconds, and cycle length is 150 sec) 85

Figure 5.9 Variation of d4 with link length (g/c for upstream and downstream are 0.9 and 0.6, respectively; offset 0 seconds, and cycle length is 150 sec) 85

Figure 5.10 Variation of d4 with offset for different cycles (g/c for upstream and downstream are 0.8 and 0.6, respectively; and link length is 300m) 88

Figure 5.11 Variation of d4 with offset for different cycles (g/c for upstream and downstream are 0.9 and 0.6, respectively; and link length is 300m) 88

Figure 5.12 Variation of d4 with offset for different cycles (g/c for upstream and downstream are 0.9 and 0.6, respectively; and link length is 400m) 89

Figure 5.13 Variation of d4 with offset for different cycles (g/c for upstream and downstream are 0.9 and 0.6, respectively; and link length is 500m) 89

Figure 5.14 Variation of d_4 with g/c ratios of upstream and downstream (link length 400m and offset –5 sec) 91

Figure 5.15 Variation of d_4 with g/c ratios of upstream and downstream approaches (link length 300m and offset 10 sec) 91

Figure 5.16 Variation of d_4 with g/c ratios of upstream and downstream (link length 500m and offset 10 sec) 92

Figure 5.17 Variation of d_4 with g/c ratios of upstream and downstream (link length 300m and offset 25 sec) 92

Figure 5.18 Variation of d_4 with upstream and downstream approaches g/c ratios (link length 300m and offset 35 sec) 93

Figure 5.19 Variation of ratio of queue length to link length and average d_4 with link length (g/c for upstream and downstream are 0.9 and 0.6, respectively; offset 10sec, and cycle length 150 sec) 96

Figure 5.20 Variation of ratio of queue length to link length and average d_4 with link length (g/c for upstream and downstream are 0.8 and 0.6, respectively; offset 5sec, and cycle length 150 sec) 96

Figure 5.21 Variation of average d_4 with g/c ratios of upstream and downstream approaches (offset –10 sec, link length 300m, and cycle length is 150 sec) 98

Figure 5.22 Variation of average d_4 with g/c ratios of upstream and downstream approaches (offset 20 sec, link length 200m, and cycle length is 150 sec) 98

Figure 5.23 Variation of average d_4 with offset (link length is 200m, cycle length 150 sec) 100

Figure 6.1 Snapshot of TSIS 108

Figure 6.2 Snapshot of TRAFVU 108

Figure 6.3 Isolated signalized intersection coded in CORSIM 109

Figure 6.4 Phasing diagram of isolated signalized intersection 110

Figure 6.5 Comparison of control delay from the individual runs for the isolated intersection 111

Figure 6.6 Paired signalized intersections coded in CORSIM 112

Figure 6.7 Phasing diagram of paired signalized intersections network 112

Figure 6.8 Comparison of vehicle trips discharged from the subject approach for the isolated and paired signalized intersection systems 114

Figure 6.9 Comparison of average speed at the subject approach for the isolated and paired signalized intersection systems 114

Figure 6.10 Comparison of total time (total time on the link for all vehicles) at the subject approach for the isolated and paired signalized intersection systems 115

Figure 6.11 Comparison of queue delay at the subject approach for the isolated and paired signalized intersection systems 115

Figure 6.12 Comparison of delay time (total delay per vehicle trip) at the subject approach for the isolated and paired signalized intersection systems 116

Figure 6.13 Comparison of control delay at the subject approach for the isolated and paired signalized intersections system 116

Figure 6.14 Comparison of d_4 values between CORSIM and the d4-model. In this case link length is 300 m, g/c ratios of upstream and downstream are 0.73 and 0.67, respectively; and offset 20 sec 119

Figure 6.15 Comparison of d_4 values between CORSIM and the d4-model. In this case link length is 300 m, g/c ratios of upstream and downstream are 0.8 and 0.6, respectively; and offset 20 sec 119

Figure 6.16 Comparison of d_4 values between CORSIM and the d4-model. In this case link length is 300 m, g/c ratios of upstream and downstream are 0.9 and 0.6, respectively; and offset 10 sec 120

Figure 6.18 Comparison of d4 values between CORSIM and the d4-model. In this case link length is 500 m, g/c ratios of upstream and downstream are 0.8 and 0.6, respectively; and offset 0 sec 121

Figure 6.19 Comparison of d_4 values between CORSIM and the d4-model. In this case link length is 500 m, g/c ratios of upstream and downstream are 0.9 are 0.6, respectively; and offset 0 sec 121

Figure 6.20 Comparison of d4 values between CORSIM and the d4-model. In this case link length is 400 m, g/c ratios of upstream and downstream are 0.73 and 0.67, respectively; and offset 10 sec. 122

Figure 6.21 Comparison of d_4 values between CORSIM and the d4-model. In this case link is length 400 m, g/c ratios of upstream and downstream are 0.8 and 0.6, respectively; and offset 10 sec 122

Figure 6.22 Comparison of d4 values between CORSIM and the d4-model. In this case link length is 400 m, g/c ratios of upstream and downstream are 0.9 and 0.6, respectively; and offset 10 sec 123

Figure 6.23 Comparison of d_4 values between CORSIM and the d4-model. In this case g/c ratios of upstream and downstream are 0.7 and 0.67, respectively; offset -15 sec, and cycle length 150sec 124

Figure 6.24 Comparison of d_4 values between CORSIM and the d4-model. In this case g/c ratios of upstream and downstream are 0.8 and 0.6, respectively; offset -15 sec, and cycle length 150sec 125

Figure 6.25 Comparison of d_4 values between CORSIM and the d4-model. In this case g/c ratios of upstream and downstream are 0.9 and 0.6, respectively; offset -15 sec, and cycle length 150sec 125

Figure 6.26 Comparison of d_4 values between CORSIM and the d4-model. In this case g/c ratios of upstream and downstream are 0.9 and 0.6, respectively; offset 0 sec, and cycle length 150sec 127

Figure 6.27 Comparison of d_4 values between CORSIM and the d4-model. In this case g/c ratios of upstream and downstream are 0.73 and 0.67, respectively; offset 0 sec, and cycle length 150sec 127

Figure 6.28 Comparison of d_4 values between CORSIM and the d4-model. In this case g/c ratios of upstream and downstream are 0.8 and 0.6, respectively; offset 10 sec, and cycle length 150sec. 128

Figure 6.29 Comparison of d_4 values between CORSIM and the d4-model. In this case g/c ratios of upstream and downstream are 0.9 and 0.6, respectively; offset 20 sec, and cycle length 150sec. 128

Figure 6.30a Comparison of average d4 between CORSIM and d4-model. In this case link length is 500m and offset = -15sec, ... 129

Figure 6.30b Comparison of average d4 between CORSIM and d4-model. In this case link length is 500m and offset = 0sec, ... 130

Figure 6.30c Comparison of average d4 between CORSIM and d4-model. In this case link length is 500m and offset = 10sec, ... 130

Figure 6.30d Comparison of average d4 between CORSIM and d4-model. In this case link length is 500m and offset = 20sec, ... 131

Figure 6.31a Comparison of average d4 between CORSIM and d4-model. In this case link length is 400m and offset = -15sec, ... 131

Figure 6.31b Comparison of average d4 between CORSIM and d4-model. In this case link length is 400m and offset = 0sec, ... 132

Figure 6.31c Comparison of average d4 between CORSIM and d4-model. In this case link length is 400m and offset = 10sec, ... 132

Figure 6.31d Comparison of average d4 between CORSIM and d4-model. In this case link length is 400m and offset = 20sec, ... 133

CHAPTER 1

Introduction

1.1 Background

Signalized intersections are the most complex points in an urban roadway network. The main function of intersections is to provide a safe and efficient right of way for the conflicting traffic movements entering the intersection. The effectiveness of a signal at an intersection is commonly expressed by a measure of the delay that vehicles, on average, experience at the subject intersection. Volume to capacity ratio (v/c) may also be used and is related to delay and congestion.

Traffic congestion is defined as a condition of traffic delay in which the speed of vehicles is slower than reasonable speed and the number of vehicles trying to use the road exceeds the design capacity of the traffic network to handle them (1). Congestion has a significant effect on the economy, travel behavior, land use, and is a cause of discomfort for millions of motorists. The majority of the people in the United States choose to travel by their own automobile. According to ARTBA (American Road & Transportation Builders Association) (2), from 1982 to 2002 the US population grew by 19 percent and the number of registered motor vehicles has increased 36 percent and vehicle miles traveled (VMT) has increased 72 percent, whereas there was only a five percent increase in road capacity. The cost of this congestion is in billions of dollars. Recent studies by the Texas Transportation Institute (TTI) shows that congestion costs commuters 4.6 billion hours of delay, and amounts to almost $74 billion annually in time and fuel cost. Overall,

the annual cost ranges from $125 in small cities to over $1200 per eligible driver in larger metropolitan areas (3).

Traffic congestion becomes part of our daily commute in the USA, and majority of the researchers believe that it will stay and hence we have to live with it. Therefore attention needs to be given to make sure that the different analyses and models are appropriate for defining and quantifying congested conditions. Traditionally, it has been assumed that congestion occurs only when demand exceeds capacity ($v/c > 1$), but due to complex traffic operations, now congestion at signalized intersection network can occur due to bad offset, queue spillbacks from downstream intersections, short link spacing, and poor signal timing. While current delay models account for some forms of congested conditions, delay induced by downstream congestion such as long queues at a signalized downstream approaches are not captured by current delay models. There are many closely spaced intersections where this is an issue. Others not so closely-spaced intersections, but with heavy traffic flow, may be candidate sites where downstream congestion causes extra delay at upstream intersections.

When downstream disturbances, caused by queues or otherwise, induce additional delay at upstream intersections then the operational characteristics of such intersections cannot be observed or assessed autonomously. For the upstream intersection of such a system, models are needed to capture the part of the delay that is induced by the downstream disturbance. This research is part of an effort to study the operation of congested interrupted systems. The research proposes models to estimate the increased delay at a given intersection that is specifically caused by downstream disturbances.

1.2 Problem statement and motivation for study

Increased urbanization and lack of parallel roadway network for capacity additions in many areas of the United States causes congestion and increases the number of signalized intersection systems operating in saturated and over saturated modes. At the same time, all standard delay analysis procedures were developed for isolated under saturated conditions. They would generate deceptive and erroneous results if they were to be used to analyze congested closely spaced intersections. Optimal coordination and offsets between signalized intersections in networks are often difficult to obtain because of short intersection spacing, oversaturated conditions, uncertainty in traffic demand, and hardware limitations on the phasing and timing.

The level of service (LOS) of an intersection expresses the effectiveness of traffic controller at the signalized intersection. The LOS is based on control delay, as per current Highway Capacity Manual (HCM 2000) methodology. According to the HCM 2000 (4), control delay is a combination of three delays and the progression factor. The delays included in control delay are the uniform delay (d_1), incremental delay (d_2) and the initial queue delay (d_3), as shown in equation 1.1.

$$\text{Control delay} = (d_1) \times (PF) + d_2 + d_3 \qquad (1.1)$$

These delay terms depend upon factors like vehicle arrival type, green time ratio (g/c), percentage of vehicles arriving during green time, degree of saturation (v/c), capacity of lanes, length of analysis period and size of queue at the start of cycle. All of these factors are dependent on control parameters that are exclusively related to the intersection under consideration. Conditions at the downstream link and intersection are ignored. According to the HCM 2000 "The potential impact of downstream intersection on the upstream intersection are not taken into account." The HCM methodology is

intended for isolated or widely spaced intersections. For closely spaced intersections, where the downstream intersection has influence on the upstream one, we cannot calculate the control delay of upstream and downstream intersections independently. A more exhaustive look at the HCM 2000 delay methodology and limitations is presented in chapter 3.

Parameters like offsets, green time at downstream intersections, spacing between intersections, average speed of vehicles on the connecting link, queue lengths, queue spillbacks if applicable, and speed of mid block starting and stopping shockwaves should be included in calculating the delay of an upstream intersection. Depending on the exact values and interactions among these parameters, the upstream intersection may or may not incur added delay due to the downstream disturbance. If the intersections are closely spaced and/or the disturbance is significant, then the control parameters of the downstream intersection have a great impact on the operational characteristics of upstream intersection. Thus, delay should take into account the characteristics of a downstream intersection and the link between the two intersections. A fourth delay term may be needed to account for the influence of traffic of a downstream intersection on its upstream neighboring intersection.

1.3 Research objectives

As congestion becomes more prevalent in urban areas in the US and elsewhere, care must be taken to ensure that different analysis methods and models, particularly those for delay, are fit for those conditions. Given the lack of guidance in the current methods of the HCM 2000, the primary objectives of the research in this dissertation are:

1. Determine the conditions when downstream disturbance is affecting upstream intersection operations,
2. And if it is, quantifying the downstream induced delay on upstream-signalized intersection and propose a new delay term (call it d4) that will explicitly capture the effect of operations of a downstream intersection on the upstream intersection, and
3. Show the effect of geometric and operational factors such as intersection spacing, offsets and signal timing on delay through the proposed term d4.

1.4 Research contribution

The dissertation provides a systematical approach to analyze the traffic operation at two closely spaced signalized intersections. Analytical models to estimate the delay induced by downstream intersection on an upstream intersection are proposed, which can be included in as new delay term "d_4" in the HCM 2000 control delay formula. It is expected that the findings of this dissertation will have practical and methodological implications in traffic engineering. From this research, information is provided on the following:

- The conditions at which downstream disturbance induces delay on upstream intersections.
- The most influential geometric and traffic factors or parameters on traffic operations at closely spaced signalized intersections.
- The amount of additional delay experienced by vehicles at an upstream intersection due to downstream disturbances.

1.5 Research approach and layout

The dissertation initially presents a comprehensive review of all the work done earlier on the closely spaced or paired signalized intersection networks in chapter 2. Chapter 3 describes various methodologies to calculate delay at signalized intersections. More emphasis is given to the HCM 2000 methodology and its limitation.

Chapter 4 explains the research methodology to achieve the models, which can be used to quantify the delay induced by downstream disturbances on an upstream approach. Chapter 4 also provides the formulation and derivation of models, i.e., models for estimation of queue length between upstream and downstream intersections, models for average speed during each cycle at downstream link, and downstream induced-delay d_4 models. The impact of geometric, traffic flow and control parameters of both upstream and downstream intersections on downstream induced-delay d4 model are presented in chapter 5.

A microscopic simulation model was used to validate the d4 model. Brief introduction of the simulation model, methodology used for validation, and validation results are provided in chapter 6. Finally, the conclusions and recommendations for future studies are presented in chapter 7.

CHAPTER 2

Literature Review

Few researchers have investigated traffic operations at closely-spaced signalized systems in recent years. Rouphail and Akcelik (5) were the first to analyze paired signalized intersections. They developed a model for platoon arrivals and queue interactions for closely spaced signalized intersections. According to the authors, the interaction of vehicles coming from an upstream intersection with queue at the downstream approach depends upon the category of queue length. The Authors divided the queue length at a downstream approach into four categories, which are:

1. Interfering queue length: average queue size encountered by the front of a platoon arriving at the downstream approach.
2. Blocking queue length: maximum number of vehicles, which can be accommodated in the space between upstream and downstream intersection. This value can be estimated by dividing the link length by effective headway.
3. Critical queue length: longest queue length that allows a vehicle coming from upstream intersection to accelerate to a full departure speed and the decelerate to a stop again.
4. Maximum downstream queue length: maximum size of queue on the downstream approach during an average signal cycle.

Figure 2.1 shows the flow chart for the solution algorithm given by Rouphail and Akcelik to estimate the degree of saturation and system throughput when there is interaction between vehicles coming from the upstream intersection and vehicles queued at the

downstream approach. They concluded that existing tools and methodologies are not suitable for representing traffic performance of paired signalized intersections and queue interaction effect that may develop even when both intersections are operating below capacity.

The work of Rouphail and Akcelik has great importance in understanding the traffic operation in a closely spaced intersections system. However, they did not incorporate the impact of the downstream intersection on the operational characteristics of the upstream intersection. Rouphail and Akcelik's models did not take into account the delay caused by the interaction of queue passing well into the upstream intersection from downstream link and traffic at upstream intersection.

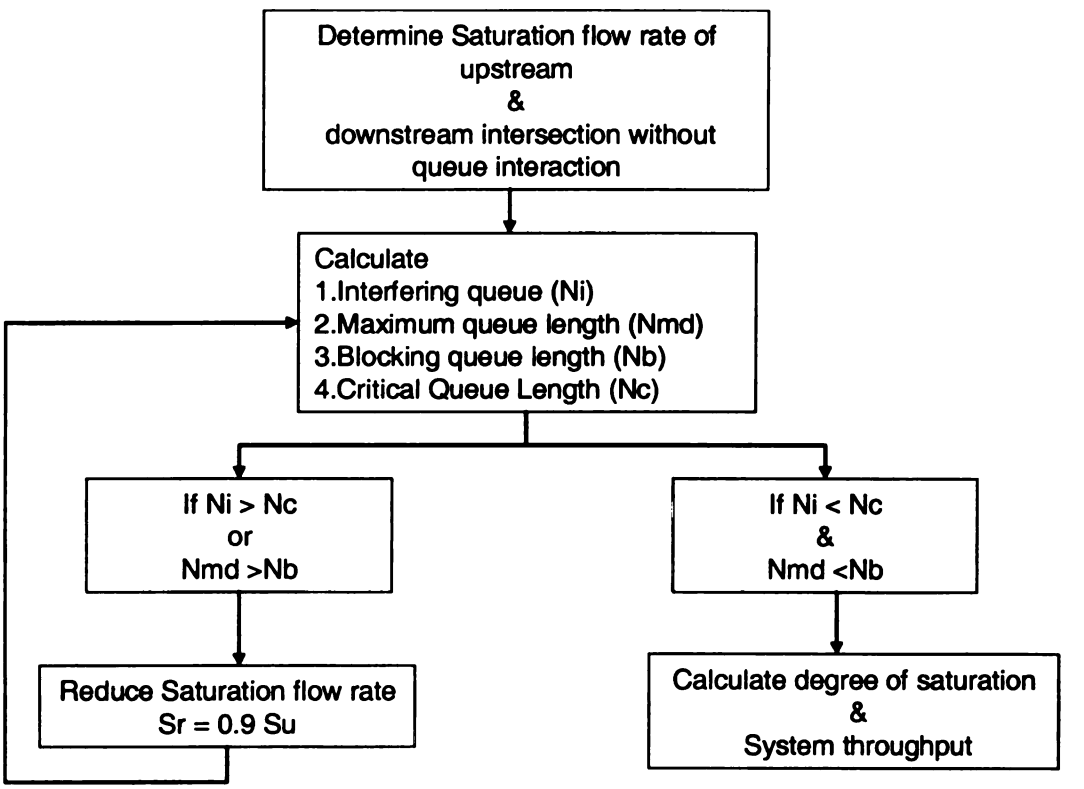

Figure 2.1 Flow chart to estimate degree of saturation and system throughput, Rouphail and Akcelik (5).

In another research effort, Prosser and Dunne (6) analyzed closely spaced paired signalized intersection by using a graphical technique to estimate the reduction in effective green time due to queue spillback. They also presented a methodology for estimating the capacities of movements at the upstream signal of paired intersection. They conducted a comparison based on a microscopic simulation model and also applied the procedure on staggered T-intersection in Sydney, Australia. The authors concluded that traffic passing through two closely spaced intersections can be blocked at the upstream signal by the queue propagating back from the downstream signal and that the queue interaction effect can significantly reduce the capacity of movements at the upstream intersection. Blockage only occurred when the downstream queue occupies the full length of the link between upstream and downstream intersection. The major drawback of the Prosser and Dunne model is that authors consider downstream queue interference only when the link between upstream and downstream intersections is completely full. In reality downstream disturbance can affect the operational characteristics of upstream intersection whether the downstream approach is fully filled by vehicles or not.

In 1998, Messer (7) further modified the Prosser and Dunne models for under and over saturated conditions. The results in the study showed that flow blockage due to queue spillback can occur not only during oversaturated conditions but also during undersaturated conditions given limited storage spacing, bad signal timing and offset. Messer used the TRAF-NETSIM microscopic simulation program to compare the output of the Prosser and Dunne model. Messer neither showed how the delay at the upstream intersection were affected by downstream intersection characteristics nor estimated the

volume of discharged traffic from the upstream intersection when the downstream disturbance was affecting the upstream approach.

In 1992, Johnson and Akcelik (8) reviewed the application of closely spaced signalized intersection in different analytical software's. The programs used for comparison are: PASSER II (Progression analysis and Signal System Evaluation Routine), SCATES (Computer Aided Traffic Engineering System), and TRANSYT-7F (Traffic Network Study Tool). The Measures of Effectiveness (MOE'S) studied were delay, queue length and stop rate by varying degree of saturation, cycle length, and offsets. The study concluded that the software packages have various limitations, in particular those related to queue interaction modeling, which restrict their applicability to paired signalized intersection analysis.

Abu-Lebdeh and Benekohal (9) presented models for estimating the capacities of oversaturated arterials as a function of the quality of signal coordination and physical capacities of individual approaches. They also derived expressions for estimating the volume of discharged traffic from an upstream intersection in the presence and absence of downstream disturbance. The results provided in the study showed that depending on the exact control and network characteristics, as much as 90 percent of the capacity can be lost in a given cycle if the control does not account for downstream conditions. The work of Abu-Lebdeh and Benekohal focused on the reduction in capacity of upstream intersection due to downstream disturbance. However they did not present any expression or model for estimate delay experienced by vehicles at the upstream intersection due to downstream disturbances.

A number of studies were conducted in relation to delays at signalized intersections. Brief introduction of some of these studies is presented below.

Early attention to signal control in oversaturated conditions was reported by Gazis (10) where he proposed a way (using graphic methods) to control two closely spaced and oversaturated intersections. This procedure, however, is of limited use unless constraints on queue length are taken explicitly. Longley (11) presented a procedure for control of congested computer-controlled networks. The basic premise of Longley's procedure is to manage queues so that a minimum number of secondary junctions are blocked. Singh and Tamura (12) used the dual function of a delay minimization function to obtain a two level hierarchical optimization strategy to control congested intersections. The control procedure presented was of the preventive type where constraints were used to control formation of queues. Michalopoulos and Stephanopoulos (13,14) used the Optimal Control Theory to devise control procedures that minimize delay of a system of oversaturated intersections subject to queue length constraints. As it turned out the solution to the problem may or may not exist if there is more than one constraint per intersection, and the optimal control becomes very complex and not possible if pre-timed signals are used. Vaughan and Hurdle (15) presented a theory for traffic flow for congested conditions in which the impact of origin-destination patterns on traffic dynamics and vice versa were explicitly modeled. However, the theory does not apply if congested intersections are close to each other. Gal-Tzur et al. (16) presented a control method based on metering traffic to the capacity of the critical intersection (the one to become congested first), and then used TRANSYT-7F (17) to design a coordination plan. This procedure may be useful only in limited situations. Hadi and Wallace (18) reported

that latest modifications in TRANSYT-7F enable the program to analyze and optimize signal timing plans under congested conditions. These enhancements include platoon progression diagram. Rathi (19) presented a control scheme based on cross street traffic spill-over avoidance. The scheme is applicable for recurrent congestion in steady state flow conditions. Shibata and Yamamoto (20) presented a methodology for control of congested urban road networks. This procedure, however, does not apply for closely spaced intersections where queue interference is present. There are number of other similar type of studies (21-29) done to estimated delay at signalized intersections.

Hence a lot of work is done to estimate delay and analysis vehicle operations at signalized intersections, but unfortunately none of these studies show the effect of downstream intersection operations on upstream intersection delay.

The following points summarize the previous work done on closely-spaced signalized intersections:

1. Modeling of interactions of queued vehicles at a downstream approach and vehicles coming from the upstream intersection.
2. Categorization of queue lengths at downstream approaches on the basis of the effect on the upstream intersection.
3. Estimation of traffic arrival pattern at the downstream intersection in paired signalized intersection system.
4. Estimation of reduction in effective green time at upstream intersections due to queue spillback.
5. Evaluation of different simulation models for closely space signalized intersection systems.

6. Calculation of capacity loss at upstream intersections due to downstream disturbance.

The research presented in this dissertation is in line with the work done by Rouphail, Akcelik, Prosser, Messer, Abu-Lebdeh and Benekohal on closely-spaced signalized intersection as all dealt with the same phenomenon but each group addressed a different side of the problem. The work in this dissertation aims at developing models to estimate the additional delay caused by downstream disturbance on upstream-signalized intersections and identifying the most influential geometric and traffic parameters for traffic operations at closely-spaced signalized intersection systems.

CHAPTER 3

Delay at Signalized Intersections

3.1 Introduction

Transportation system is defined as a system consisting of fixed facilities, the flow entities, and the control system that permit people and goods to overcome the friction of geographical space efficiently in order to participate in a timely manner in some desired activity (30). Fixed facilities are the physical components of the system, e.g., roadway, railway track, etc., whereas flow entities are the units which use the fixed facilities, e.g., cars, trucks, container units etc. The control system consists of two components; vehicular control, which refers to the technological way in which individual vehicles are guided on the fixed facilities, and flow control, which includes the means that permit the efficient and smooth operation of streams of vehicle and reduction of conflicts between vehicles e.g., traffic signals and pavement marking. Traffic flow on transportation facilities can be classified into two types: uninterrupted flow and interrupted flow.

3.2 Uninterrupted flow

A condition in which vehicles traveling in a traffic stream do not have to stop or slow down for reasons other than those caused by the presence of other vehicles in that stream is known as uninterrupted flow conditions. In this condition flow is regulated by vehicle-vehicle interactions and interactions between vehicle and roadways. The examples of uninterrupted flow are freeways, multilane highways, and two-lane highways.

3.3 Interrupted flow

In this flow condition, flow is regulated by external means e.g. traffic signals, stop signs etc. These devices cause traffic to stop periodically irrespective of how much traffic exists. Table 3.1 provides the types of facilities under the categories of uninterrupted and interrupted flow.

Table 3.1 Classification of transportation facilities by flow types (31)

Flow Type	Transportation Facility
Uninterrupted Flow	Freeways
	Multilane highway
	Two-Lane highway
Interrupted Flow	Signalized streets
	Unsignalized Streets with stop signs
	Arterial
	Transit
	Pedestrian Walkways
	Bicycle Paths

The flow type only describes the facility, not the quality of flow. For example, a freeway operating at jam density is still considered as uninterrupted flow. The research presented in this dissertation is limited to interrupted flow and more specifically to interrupted flow at signalized intersections.

3.4 Signalized intersection

An at-grade road intersection is a complicated and complex part of the highway system. At a typical intersection of two-way streets, there are twelve potential vehicular movements and four pedestrian crossing movements. The conflicts points between these sixteen movements are shown in figure 3.1. The main task of a traffic engineer is to

control and manage these conflicts in a manner that ensures safety and provides efficient movement through the intersection for both motorists and pedestrians.

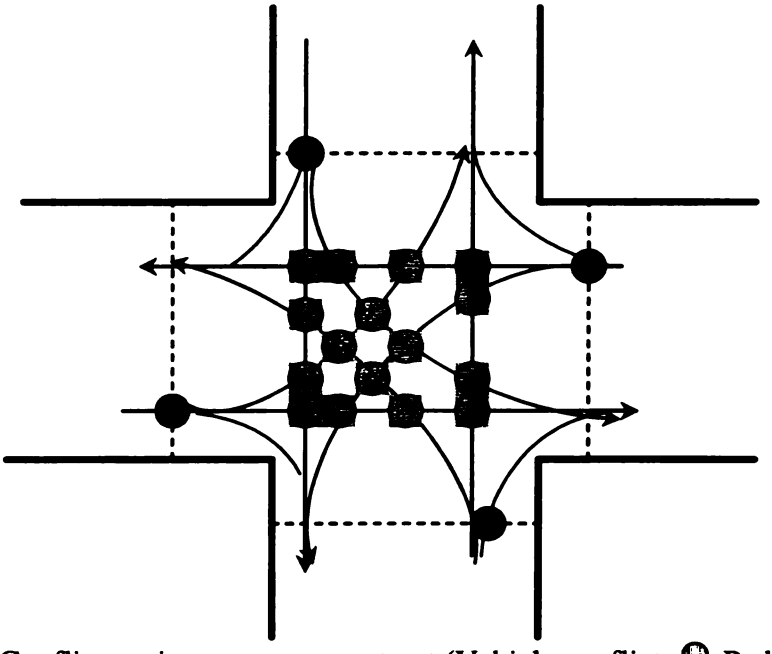

Figure 3.1 Conflicts points at two-way street (Vehicle conflicts ●, Pedestrian conflicts●)

There are different measures which can be used to control traffic and eliminate, or at least reduce the number of conflicts at an at-grade intersection (e.g., yield or stop sign, traffic signals).

Signalized intersections are the ultimate form of at-grade intersection control. It assigns right of way to specific movements to reduce the conflict movements. According to the HCM 2000 (4), signalized intersection operations can be analyzed by using four modules. Figure 3.2 shows each module's contents and the sequence of their occurrence (each box in figure 3.2 represent one module).

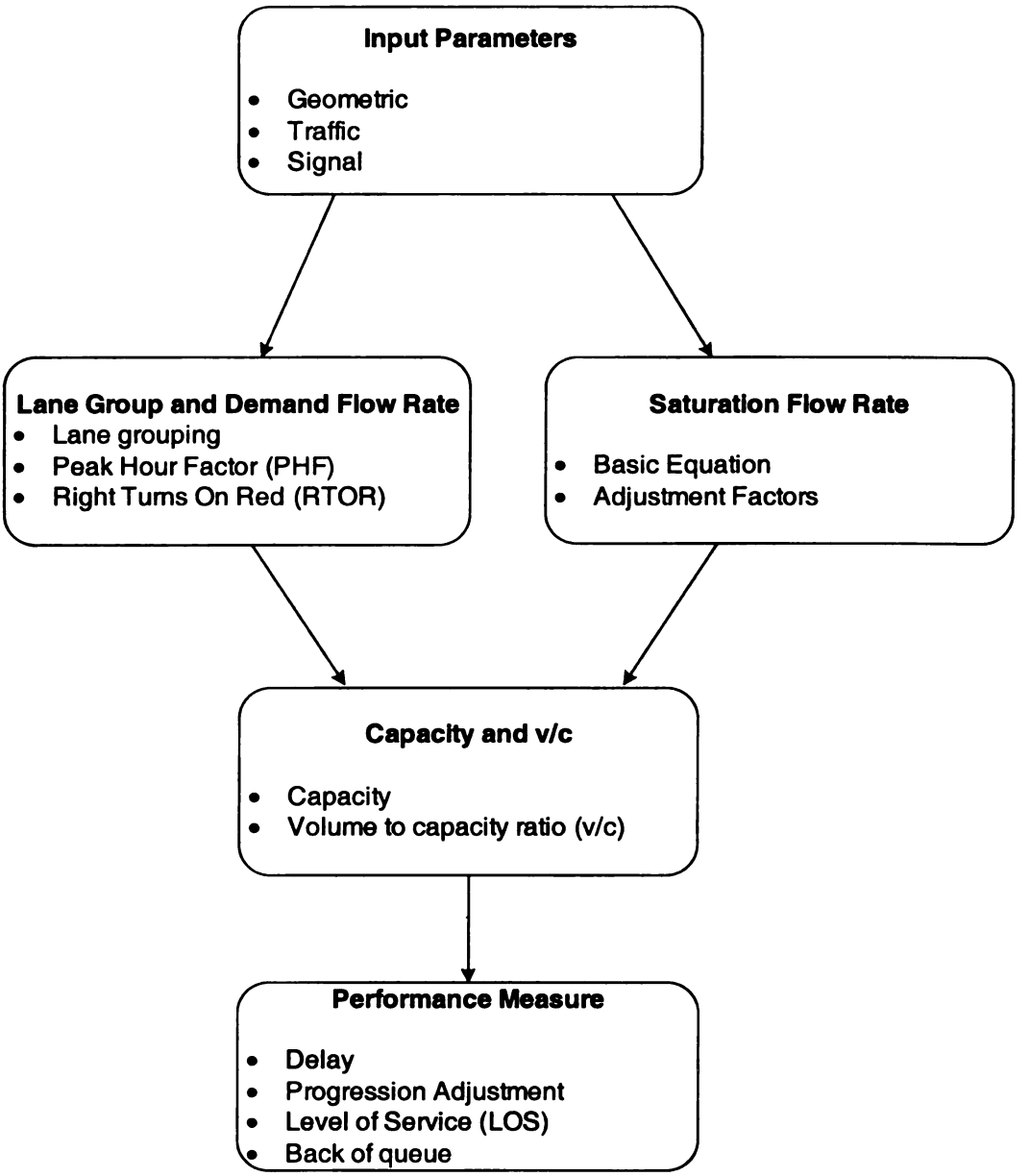

Figure 3.2 Flow chart to analysis operations at signalized intersection, according to HCM

There are various measures of performance for signalized intersections such as delay, level of service, progression for intersection etc. All performance measures are interrelated. Delay is one of the primary measures used to estimate the effectiveness of signalized intersection. Delay can be of different types, and various methods can be used to estimate it, as explained in the following sections.

3.5 Delay as measure of effectiveness

Delay is defined as the difference in travel time when a vehicle is unaffected by the controlled intersection and when it is affected by the controlled intersection (32).

3.5.1 Types of delay

Delay can be quantified in different ways. The most frequently used forms of delay are: 1) Stopped-time delay, 2) Approach delay, 3) Time-in-queue delay, 4) Travel time delay, and 5) Control delay.

3.5.1.1 Stopped-time delay

This is the time during which a vehicle is stopped in queue while waiting to pass through the intersection (see figure 3.3).

3.5.1.2 Approach delay

Approach delay is the time loss due to deceleration from the approach speed to a stop and the time loss due to reacceleration to the desire speed plus the stopped time delay, as shown in figure 3.3.

3.5.1.3 Time –in –queue delay

Time in queue delay is defined as the total time from a vehicle joining an intersection queue to its discharge across the stop line.

3.5.1.4 Travel time delay

Travel time delay is the difference between the drivers' expected travel time through the system (without interruption) and the actual travel time. Figure 3.3 shows the profile of a vehicle and the different types of delay it could experience while passing through a signalized intersection.

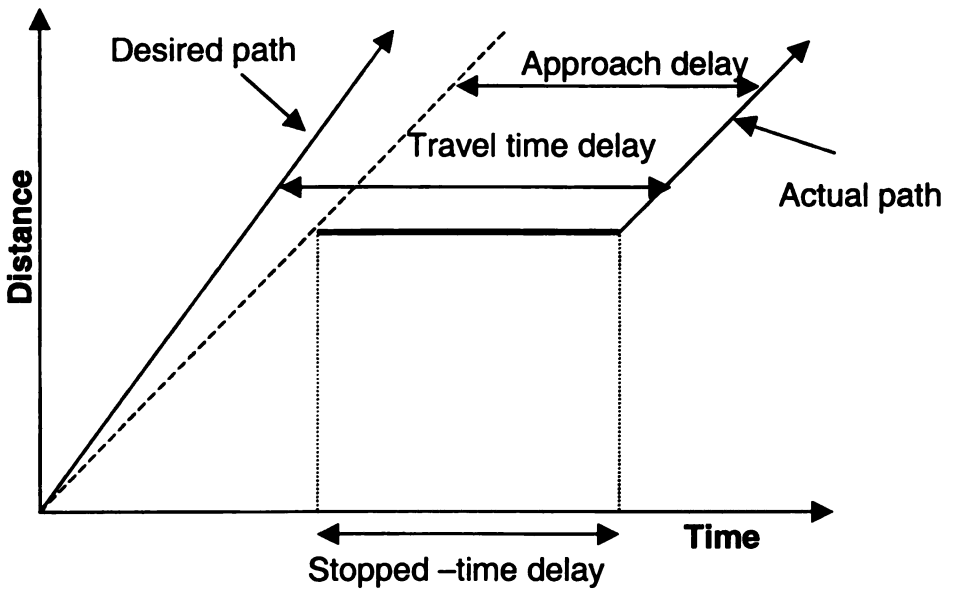

Figure 3.3 Different types of delay at signalized intersection

3.5.1.5 Control delay

Control delay is the most commonly used delay type. It is the delay caused by control devices, either a traffic signal or a stop sign. The concept of control delay was first introduced in the 1994 Highway Capacity Manual and is still used in the HCM 2000 (4). The level of service (LOS), which expresses the quality of operations and effectiveness of control at signalized intersections, is based on control delay. Each component of the control delay is illustrated later in this chapter.

3.6 Estimation of delay at signalized intersections

There are different types of methodologies used to estimate delay at signalized intersection. Some of these methods used are deterministic, and others used stochastic approaches. The commonly used methods are (35):

- Delay estimation using vertical queuing analysis
- Delay estimation using shockwave analysis

- Delay estimation using microscopic simulation

3.6.1 Delay estimation using vertical queuing analysis

Queues are formed when demand exceeds capacity of specific locations such as signalized intersections and toll plazas, in any transportation system. Queue may be stopped or moving in the form of platoon depending upon the type of service provided. On the basis of arrival patterns two types of queue analysis can be done; Deterministic queue analysis and stochastic queue analysis. In both approaches it is assumed that vehicle queue vertically i.e., occupies no space while queued, and that the vehicles accelerate and decelerated instantaneously (35).

3.6.1.1 Deterministic queuing analysis

In deterministic queue analysis, vehicle arrivals are assumed to follow a uniform pattern, with constant headway. This analysis can be undertaken at two different levels of details; macroscopic and microscopic levels. At the macroscopic level, arrivals and service rates are considered to be continuous and high, whereas in microscopic level, arrivals and service rates are considered to be discrete and low. Common example of deterministic macroscopic analysis is signalized intersections (32), although signalized intersection can also be analyzed by microscopic and stochastic analyses.

Figure 3.4 shows a plot of cumulative vehicles arriving and departing versus time at a given signal location. The vehicles are assumed to arrive at a uniform rate of flow. The shaded area is the total delay experienced by the vehicles at that typical intersection, as shown in figure 3.4.

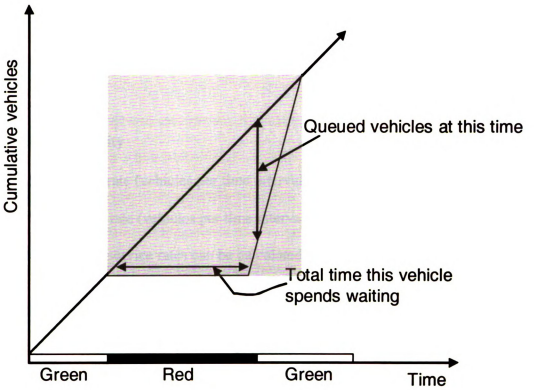

Figure 3.4 vehicles arrival and departure verse time at signalized intersection (shaded area = total delay)

3.6.1.2 Stochastic queuing analysis

Accurate estimation of vehicle delay at signalized intersections using stochastic analysis is difficult because of the randomness of the traffic flow process and the uncertainty associated with various factors affecting intersection capacity. Therefore, the mathematical models that are used to predict delay of a stochastic process usually use several simplifications. For traffic systems, the following assumptions are typically made: 1) Vehicle arrivals follow the Poisson distribution, and 2) Mean arrival flow rate is constant throughout the period of analysis. In stochastic queuing analysis, arrival and service distributions are probabilistic. To use stochastic queuing analysis, the traffic intensity (ρ) must be less that 1. Traffic intensity is given by equation 3.1.

$$\rho = \frac{\lambda}{u} \tag{3.1}$$

Where

ρ = Traffic intensity

λ = Mean arrival rate (vehicles per time interval)

u = Mean service rate (vehicles per time interval)

Mean arrival and service rates can be calculated by using the following equations 3.2 and 3.3

$$\lambda = \frac{3600}{\bar{h}} \tag{3.2}$$

$$u = \frac{3600}{\bar{s}} \tag{3.3}$$

Where

$\bar{h}$ = Mean arrival time (seconds per vehicle)

$\bar{s}$ = Mean service time (seconds per vehicle)

There are many types of probability distributions that can be used to model the arrival and discharge processes of vehicles at a transportation facility. A classification scheme based on the more commonly used distribution is shown in Table 3.2 (32).

Table 3.2 Classification of probability distribution used in stochastic queuing analysis

Arrival Distribution	Service Distribution			
	Constant (D)	**Random (M)**	**Erlang (E)**	**Generalized (G)**
Constant (D)	Deterministic	D/M	D/E	D/G
Random (M)	M/D	M/M	M/E	M/G
Erlang (E)	E/D	E/M	E/E	E/G
Generalized	G/D	G/M	G/E	G/G

Source: May, A.D., Traffic *Flow Fundamentals (32)*

Figure 3.5 shows a flow chart for determining appropriate queue analysis and delay estimation approaches to use. If the intensity is greater than 1 there is no mathematical solution for the problem. To estimate the delay incurred by motorists, the only possible solution is to convert the queuing process to a deterministic queuing problem or to introduce multi time slice by varying mean arrival rates and mean service rate and then solve each time slice using microscopic simulation techniques.

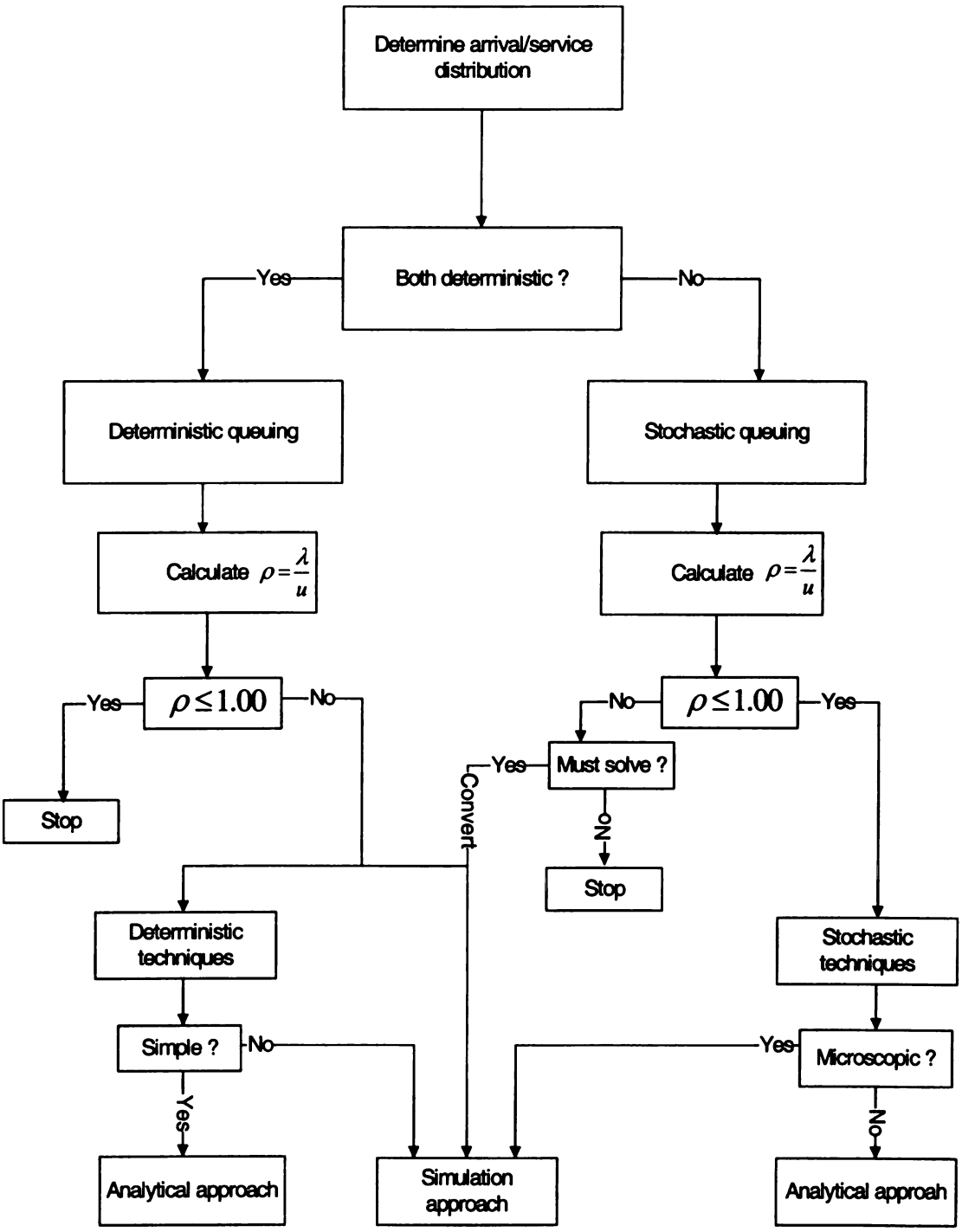

Figure 3.5 Flowchart of queuing analysis and delay estimation approaches (32)

3.6.2 Delay estimation using microscopic simulation models

Delay can also be estimated using microscopic simulation. Simulation is a numerical technique for conducting experiments on a digital computer, which may include stochastic characteristics, be microscopic or macroscopic in nature. Microscopic simulation also involves mathematical models that describe the behavior of a transportation system over extended periods of real time (32). Microscopic simulation models are commonly used to evaluate alternative traffic-improvement projects prior to their field implementation. A key factor in the use of a simulation tool is its validity or consistency with standard traffic flow theory.

Microscopic traffic simulation models have the ability to track individual vehicle movements within simulated street networks (33). Vehicle behavior is usually modeled utilizing car-following, lane-changing, and gap-acceptance logic. This allows such models, among other things, to consider virtually any traffic conditions, ranging from highly under-saturated to highly over-saturated conditions. Because of their ability to track the movements of individual vehicles, microscopic simulation models can determine the delay incurred by any individual vehicle while traveling a network of links with different characteristics by comparing simulated and ideal travel times. By constraining the vehicle deceleration and acceleration capabilities, microscopic simulation models can capture the deceleration and acceleration components of the delay. Some commonly used microscopic simulation models are CORSIM, AIMSUN 2, and VISSIM. Microscopic simulation is becoming common in every field of life because of its economic and valuable outputs. The success of the microscopic simulation depends upon the logic of the model.

3.6.3 Delay estimation using shockwave

Shockwave analysis can also be used to estimate delay at signalized intersections. Shockwaves are defined as boundary conditions in the time-space domain that demark a discontinuity in flow density conditions (32). In some situations the shockwave can be very mild, like a platoon of high speed vehicles catching up to a slightly slow moving vehicle, and in other situations the shockwave can be very significant like high-speed vehicles approaching a queue of stopped vehicles. Whenever there is a bottleneck, shockwaves are generated. This bottleneck situation can be produced by different conditions such as a slow moving truck that is followed by a platoon of vehicles on an upgrade, a three-lane freeway that is reduced to a two-lane freeway.

The use of shockwave analysis at signalized intersections is a common practice because of the concern for the length of queues interfering with upstream flow movement. Shockwaves at signalized intersection can be analyzed if a flow-density relationship is known for the approach to the signalized intersection and if the flow state of the approaching traffic is specified. Figure 3.6 shows occurrence of shockwaves at single-lane approach of a signalized intersection. There will be a discontinuity as vehicles join the rear of the standing queue, and as vehicles are discharged from the front of the standing queue when the signal turns green. Due to these discontinuities in flow, two shockwaves are generated; backward forming and recovery shockwaves. Both shockwaves are moving backward because overtime the discontinuity is propagating upstream in the opposite direction of moving traffic. There is also a frontal stationary shockwave at the stop line during the red phase. Frontal means it is downstream of the congestion, and the term stationary is used because it remains at the same position in space. Figure 3.6 shows that the last vehicle in queue starts moving when backward

forming and recovery shockwaves intersects each other. The total delay experienced by vehicles due to controller can be estimated by determining the area of shaded portion in figure 3.6.

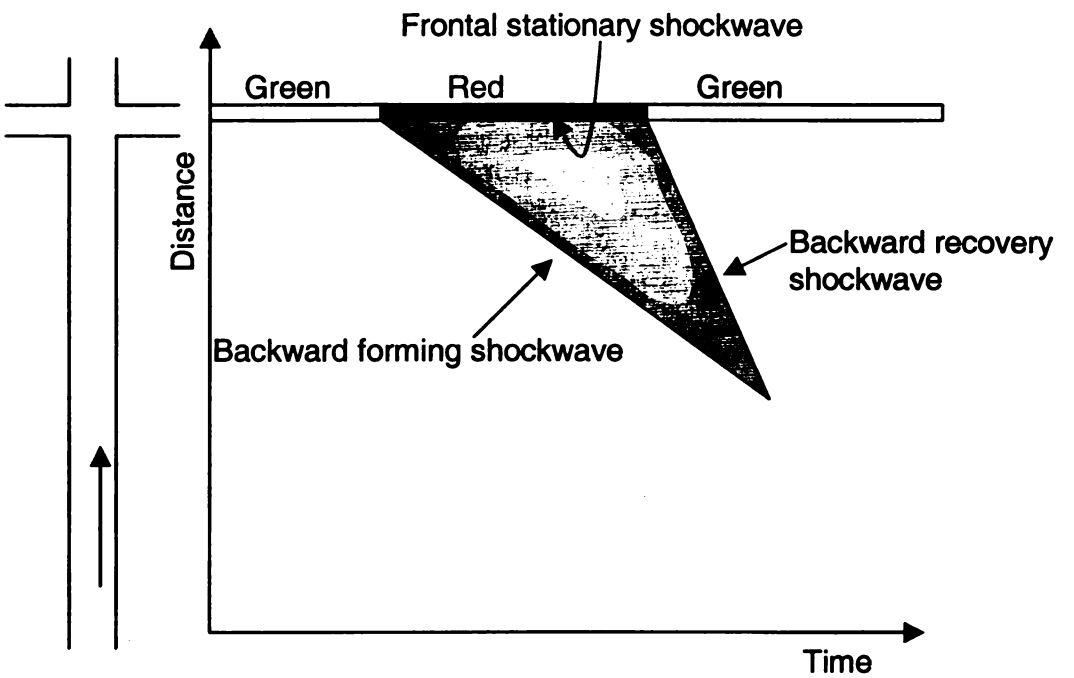

Figure 3.6 shockwaves occurrence at signalized intersection

3.7 Delay estimation methods defined by different capacity guides

The accurate estimation of delay is a major concern among transportation engineers and highway authorities. That's why delay models have been incorporated into a number of capacity guides, such as Canadian Capacity Guide (34) and Australian Signalised intersection capacity guide. In America, Highway Capacity Manual (HCM 2000) (4) is considered the standard by almost all States' departments of transportation.

3.8 Delay models of the 2000 Highway Capacity Manual (HCM 2000)

According to the HCM 2000, the level of service (LOS) for signalized intersections is defined in terms of control delay, which is a measure of driver discomfort, frustration, fuel consumption, and increase in travel time. LOS is directly related to the control delay values as given in table 3.3.

Table 3.3 Level of service criteria for signalized intersection

Level of Service	Control Delay (sec/veh)
A	≤ 10
B	>10-20
C	>20-35
D	>35-55
E	>55-80
F	>80

3.8.1 Control delay

As already discussed in section 3.5.1, control delay is delay caused by control devices either by a traffic signal or a stop sign. The average control delay is estimated for each lane group and aggregated for each approach and for the intersection as whole. According to HCM 2000, average control delay per vehicle for a given lane group is given by equation 3.4.

$$d = d_1(PF) + d_2 + d_3 \qquad (3.4)$$

Where

d = Control delay per vehicle (sec/veh)

d_1 = uniform control delay

PF = Uniform delay progression adjustment factor

d_2 = Incremental delay

d_3 = Initial queue delay

3.8.1.1 Uniform control delay (d_1)

The uniform control delay gives an estimation of delay assuming uniform arrivals, stable flow and no initial queue. It is obtained using Webster's uniform delay equation in the form given in equation 3.5

$$d_1 = \frac{0.5C(1-g/c)^2}{1-[\min(1,X)\times g/c]} \qquad (3.5)$$

Where

d_1 = uniform control delay assuming uniform arrivals

C = cycle length

g = effective green time

X = degree of saturation for lane group

3.8.1.2 Progression adjustment factor (PF)

Good or bad signal progression depends upon the proportion of vehicles arriving on the green; if this proportion is high then progression is good, otherwise it is poor. According to HCM 2000 (4) "The progression adjustment factor applies to all coordinated lane groups including both pre-timed control and non-actuated lane groups in semi actuated control system." Progression primarily affects uniform delay and thus the adjustment factor is applied only to d1. PF is calculated by using equation 3.6.

$$PF = \frac{(1-P)f_{pA}}{1-\left(\frac{g}{c}\right)} \qquad (3.6)$$

Where

PF = Progression adjustment factor

P = Proportion of vehicles arriving on green (estimated from arrival type)

g/c = Ratio of the effective green time of a phase to the cycle length

f_{pA} = Supplemental adjustment factor for platoon arriving during green

The value of P may be measured in the field or estimated from the arrival type. HCM 2000 (4) categories vehicles arriving at a point or uniform segment of lane or roadway for determining the quality of progression, this categorization is known as Arrival type. The approximate ranges of platoon ratio (Rp) are related to arrival type as shown in table 3.4.

Table 3.4 Relationship between arrival type and platoon ratio (4)

Arrival Type	**Range of platoon Ratio (Rp)**	**Default Value (Rp)**	**Progression Quality**
1	≤ 0.50	0.333	Very Poor
2	>0.50-0.85	0.667	Unfavorable
3	>0.85-1.15	1.000	Random arrivals
4	>1.15-1.50	1.333	Favorable
5	>1.50-2.00	1.667	Highly favorable
6	>2.00	2.000	Exceptional

Source: HCM 2000 *(4)*

Table 3.5 may be used to determine PF in term of the arrival type. When progression is favorable, a larger g/c ratio is beneficial, and the adjustment factor decreases with the increase of g/c ratio. When progression is unfavorable, the factor increases with increasing g/c ratio.

Table 3.5 Progression adjustment factors for uniform delay calculation (4)

Green Ratio (g/c)	**Arrival Type (AT)**					
	AT 1	**AT 2**	**AT 3**	**AT 4**	**AT 5**	**AT 6**
0.20	1.167	1.007	1.00	1.00	0.833	0.750
0.30	1.286	1.063	1.00	0.986	0.714	0.571
0.40	1.445	1.136	1.00	0.895	0.555	0.333
0.50	1.667	1.240	1.00	0.767	0.333	0.00
0.60	2.001	1.395	1.00	0.576	0.000	0.00
0.70	2.556	1.653	1.00	0.256	0.000	0.00
f_{pA}	1.00	0.93	1.00	1.15	1.00	1.00
Default Rp	0.333	0.667	1.00	1.333	1.667	2.00

3.8.1.3 Incremental delay (d_2)

Incremental delay is caused by non-uniform arrivals, temporary cycle failure and delay caused by temporary periods of over saturation. Incremental delay consists of components which depend upon:

- Arrival type
- Over saturation queues
- Type of signal control
- Duration of analysis period

This delay component assumes that there is no initial queue for the lane group at the start of the analysis period. Equation 3.7 shows the expression used to calculate the incremental delay

$$d_2 = 900T\left[(X-1)+\sqrt{(X-1)^2+\frac{8KIX}{CT}}\right] \qquad (3.7)$$

Where

d_2 = incremental delay

T = duration of analysis period (h), typically taken to be 15 minutes

K = incremental delay factor that is dependent on controller setting

(For pre timed signals, k = 0.5)

I = upstream filtering /metering adjustment (I = 1.0, for isolated intersection)

C = lane group capacity (veh/h)

X = lane group v/c ration or degree of saturation

3.8.1.4 Initial queue delay (d_3)

Initial queue delay occurs when a residual queue from a previous time period causing an initial queue to occur at the start of the analysis period (T). If traffic demand is satisfied by each time period and there is no residual queue from a previous time period, then d_3 = 0. When X or v/c > 1.0 for 15- minutes period, the following period begins with an initial queue. When the initial queue (Q_b) ≠ 0, vehicles arriving during the analysis period will experience an additional delay, known as d_3. d_3 depends mainly on

- Size of initial queue
- Length of analysis period
- V/c ratio during the analysis period

3.9 Summary of delay estimation models

All the delay estimation methodologies and models, except the microscopic simulation technique which estimate delay for each vehicle separately, depends upon the following characteristics of signalized intersection.

- Traffic arrival pattern
- Signal timing (e.g. g/c ratio)
- Intersection capacity
- Saturation flow rate
- Arrival volume

All these factors are related to the subject intersection for which delay is to be estimated, so these methodologies are only valid for isolated signalized intersection and paired signalized intersections system where downstream traffic operations is not affecting upstream intersection. These limitations of existing delay models, and particularly of the HCM 2000 delay model, are illustrated in the following section.

3.10 Limitation of HCM 2000 delay methodology

According to the HCM 2000 "The potential impacts of downstream intersection on the upstream intersection are not taken into account." The HCM 2000 methodology is intended for isolated or widely spaced intersections. To demonstrate this limitation, consider an experimental setup of paired signalized intersection system, shown in figure 3.7. In closely spaced signalized intersection system, the spacing between intersections, traffic volume, and signal timing (offset and green time) plays an important role in traffic operations at both signalized intersections. For example, if traffic on the downstream link is affecting traffic operations at the upstream intersection, then, by decreasing the link

length between the two intersections, this effect should be increased. For this experiment the control delay at the eastbound approach of the upstream intersection is observed by varying link length, and offset. Note that the traffic volume, geometric characteristics are kept constant throughout the experiment.

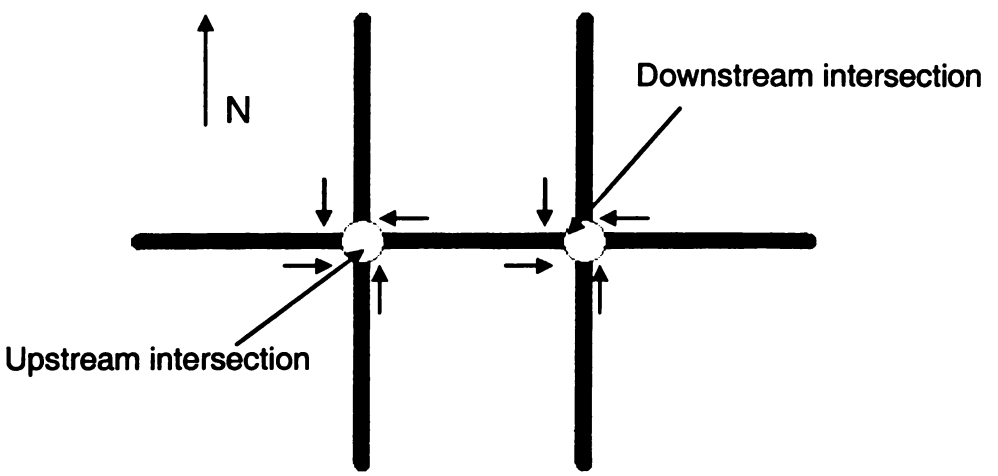

Figure 3.7 Paired signalized intersection system

For the first experiment, control delay at the eastbound approach of the upstream intersection was observed by varying the link length between upstream and downstream signalized intersections, from 100 ft to 500ft at increments of 100ft. Table 3.6 shows the results of the experiment. The LOS and control delay values remain the same regardless of the link length. In the second experiment, control delay was observed by varying offset from –15 to 15sec with increments of 5 sec. Table 3.7 shows the results for the second experiment. It is clear from the results of both experiments that the control delay at upstream intersection is insensitive to offset and link length.

Table 3.6 Control delay for upstream EB approach by varying link length (Cycle length = 120 sec and 0.67 g/c for both intersection, offset 0 sec)

Link Length (ft)	Control delay, sec/veh (Upstream intersection EB approach)	Level of service
500	26.1	C
400	26.1	C
300	26.1	C
200	26.1	C
100	26.1	C

Table 3.7 Control delay for upstream EB approach by offset (Cycle length = 120 sec and 0.67 g/c for both intersection, link length = 400 ft)

Offset (secs)	Control delay, sec/veh (Upstream intersection EB approach)	Level of service
-15	26.1	C
-10	26.1	C
-5	26.1	C
0	26.1	C
5	26.1	C
10	26.1	C
15	26.1	C

Note that varying link length and offset should not necessarily increase the downstream disturbance and hence delay at the upstream intersection approach, therefore both experiments were also simulated in the microscopic simulation program CORSIM, to check whether downstream disturbance is occurring or not. There is no queue spillback when link length is 500 m and for all other cases there is a queue spillback from downstream link and wasted green time on the eastbound approach of the upstream intersection. One case is shown in figure 3.8.

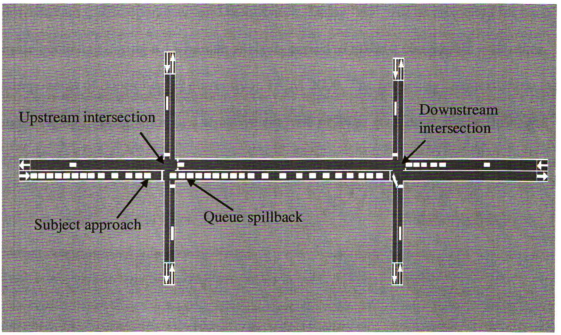

Figure 3.8 Queue spillback from downstream link to the upstream intersection (snap shot of the microscopic simulation experiment)

So the existing control delay model of the HCM 2000 is only valid for isolated or paired intersection where downstream disturbance is not causing any effect on the upstream intersection. New models or improvement in existing delay models are needed which can capture the downstream effect and estimate the delay induced by downstream disturbances. Following are the parameters on which the new model should depend:

- Effective green time or g/c ratio of both upstream and downstream intersection
- Offset
- Queue length at downstream link
- Average speed of downstream link
- Spacing between both intersection

In this dissertation, a new delay term "d4" is proposed. It will represent the additional delay experienced by vehicles at the upstream-signalized approach due to downstream traffic operations and disturbance. Delay "d4" will be estimated for each cycle occurring during a 15-minute analysis period to make it compatible with other components of control delay currently in HCM 2000. The following chapters show the methodology, formulation and sensitive analysis of d4 to geometric, traffic flow, and control parameters.

CHAPTER 4

Formulation and Derivations of Downstream Induced-delay d4 Model

4.1 Introduction

This chapter presents the derivation of the formulae used to calculate the length of delay induced by the downstream approach traffic on the upstream approach. The general term "traffic disturbance" is used to denote significant traffic presence on the downstream link. Traffic disturbances can occur when an upstream approach discharges a large enough volume of traffic onto the downstream link to oversaturate the downstream approach and to cause queue spillback into the upstream approach. A graphical technique is utilized to analyze closely spaced paired intersections. Figure 4.1 shows a system that consists of four signalized intersections. The system is divided into subsystems each composed of two neighboring intersections.

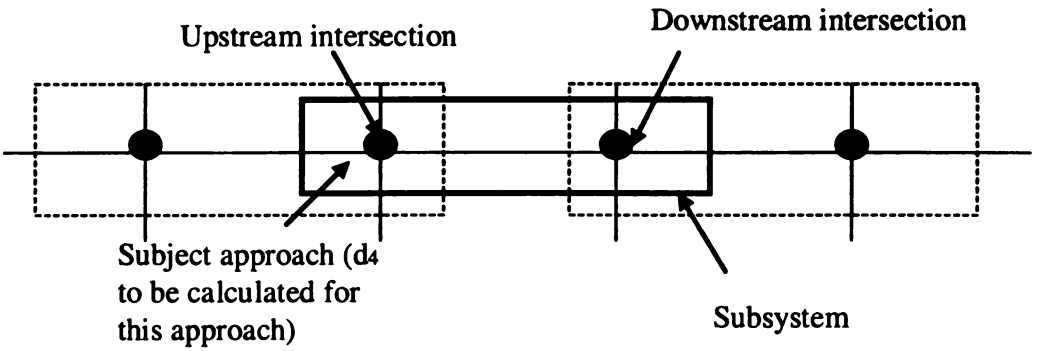

Figure 4.1 Paired-Intersection system setup

Figure 4.1 also shows the subject approach for which delay induced by downstream disturbance (d4) is to be calculated. Note that if delay d4 is to be calculated for intersection 0, then intersections 0 and 1 will become the upstream and downstream intersections, respectively. The models derived in the following section are applicable to any system size; the system would be divided into subsystems each consists of two paired signalized intersections.

Downstream induced-delay on upstream approach, d_4, depends on the geometric and traffic characteristics of both the upstream and downstream signalized intersections. Shockwave analysis is used to determine whether the disturbance produced by the downstream approach is significant enough to cause any additional delay at the upstream approach. If the answer is positive then the delay d_4 is quantified based on the operational characteristics of the upstream and downstream intersections and the average speed on the downstream link. The following steps describe the process used to quantify d4 (for the cases where d4 is non-zero).

1) Derive equations for mid block shockwaves produced by blockage at the downstream approach. These equations will provide the speed of shockwaves in terms of traffic parameters of upstream and downstream intersections. Use these equations to locate the spatial-temporal coordinates of the point of intersection of mid-block starting and stopping waves. The purpose of calculating the coordinates of the point of intersection of the shockwaves is to determine whether or not there is delay due to disturbance from downstream intersection traffic (i.e., d4>0 ?).

2) Estimate the parameters needed to quantify d4. These parameters include offset, effective green time at upstream and downstream approaches, link length, queue length,

and average speed at downstream link. Among these parameters the unknown values are (i.e., these are values that are not readily available and hence have to be estimated based on other known parameters/variables):

a) Queue length at downstream link at start of each cycle

b) Average speed at downstream link during each cycle.

The downstream queue length directly impacts the magnitude of d_4. In this step, a model for estimating the queue length downstream of the upstream intersection will be developed. The queue length model will be a function of the offset, incoming volume from the upstream approach, speed of mid block starting and stopping shockwaves, effective green time at upstream and downstream approaches, and link length.

3) Estimate the average speed of traffic on the link between the upstream and downstream intersections during each cycle. Average speed is another important parameter needed to estimate the downstream induced-delay, d4, on the upstream approach. The average speed will be a function of space not occupied by queue at the downstream approach.

4) Derive an expression to calculate the length of delay d_4. d_4 will be a function of queue length, average speed and signal timing of upstream and downstream approaches. This model will quantify the impact of a downstream disturbance on the upstream approach in terms of delay. Initially delay d4 will be estimated for one cycle.

5) Extend delay calculation for multiple cycles so that it can be estimated for a 15-minute time period. This will make it compatible with the other delay terms (d_1, d_2, d_3) currently in the HCM 2000 control delay formula.

All of these steps are explained in the following sections. First, necessary notations and symbols are presented below:

L = Length of the link between upstream and downstream intersections (meters, m)

g_1= Effective green time at the upstream approach (seconds, s)

g_2= Effective green time at the downstream approach (s)

R_1 = Red phase at the upstream approach (s)

R_2 = Red phase at the downstream approach (s)

off = Offset (s)

L_1= Queue length measured from the downstream approach stop line to the tail of the queue (m)

L_2= Remaining space on the downstream approach (not occupied by vehicles) (m)

h_v= Effective space headway (m)

λ_1= Speed of the mid block stopping shockwave (meter/seconds, m/s)

v_1= Speed of the mid block starting shockwave (m/s)

λ_2= Speed of the stopping shockwave at the downstream approach (m/s)

v_2= Speed of the starting wave at the downstream approach (m/s)

V_f = Free flow speed (m/s)

Va = Average link speed (m/s)

S_1 = Saturation flow rate at the upstream approach (vehicles/ hour of green, vphg)

S_2 = Saturation flow rate at the downstream approach (vphg)

4.2 Formation of shockwaves due to a downstream traffic disturbance

As discussed earlier, traffic disturbance at a downstream intersection can cause interruption in flow on the link between two intersections. Due to this disturbance and discontinuity of flow, a number of shock waves will be generated. Only stopping and starting shock waves, generated at downstream approach, are considered because other shockwaves have not significant speed hence little or no impact on traffic flow at closely spaced signalized intersections. Experiments using the microscopic simulation model CORSIM (CORridor SIMulation Model) (36) were conducted, to check the speed of other shockwaves. These experiments found that shockwaves (i.e., shockwaves generated due to diverse car following behaviors and various acceleration/deceleration rates) other than those generated at mid block and on approaches have no significant speed and effect on traffic operation. Mid-block is considered as any location between the upstream and downstream intersection, not necessarily the middle of the link. The shockwaves considered here are:

- Mid-block starting shockwave (ν_1)
- Mid-block Stopping shockwave (λ_1)
- Starting shockwave (ν_2) at the downstream approach
- Stopping shockwave (λ_2) at the downstream approach

Figure 4.2 shows the location and speed of each of those four shockwaves. The point of intersection of the mid-block stopping and starting shockwaves within the time-space domain is critical for the calculation of d4. The location of the intersection point

determines whether or not there is downstream-induced delay, d4. If the shockwaves intersect upstream of the upstream approach, then there is a value for delay d4, as shown in figure 4.3.

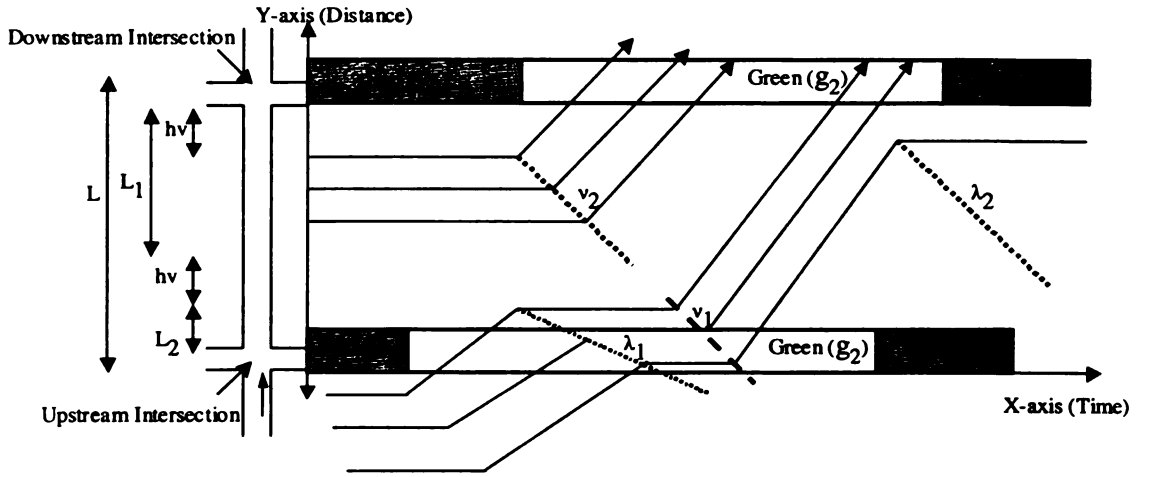

Figure 4.2 Location and speed of four shockwaves

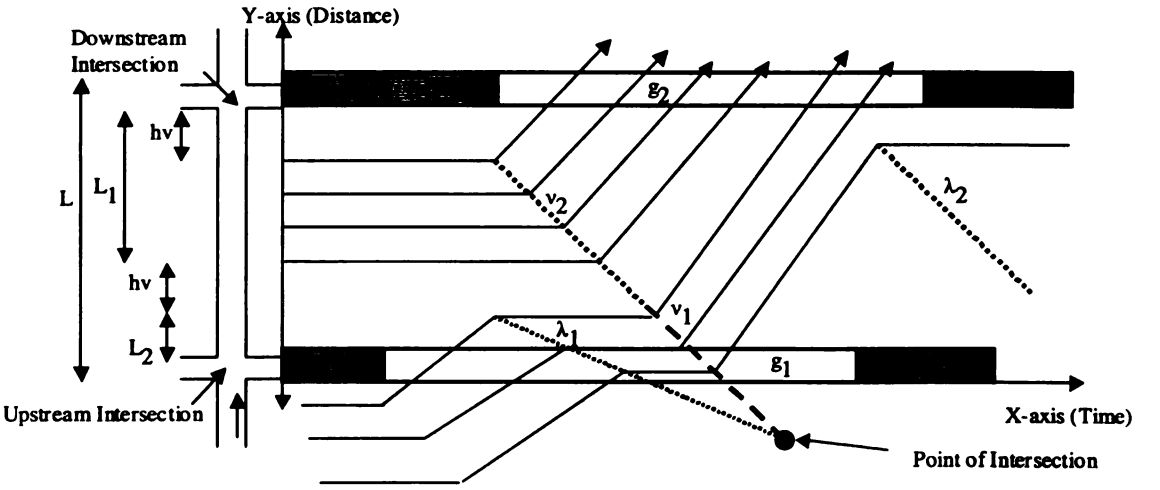

Figure 4.3 Shockwaves intersecting upstream of the upstream intersection (d_4>0 in this case)

If the intersection point of the shockwaves is located anywhere between the two intersections, then there is no downstream-induced delay ($d_4 = 0$), as shown in figure 4.4.

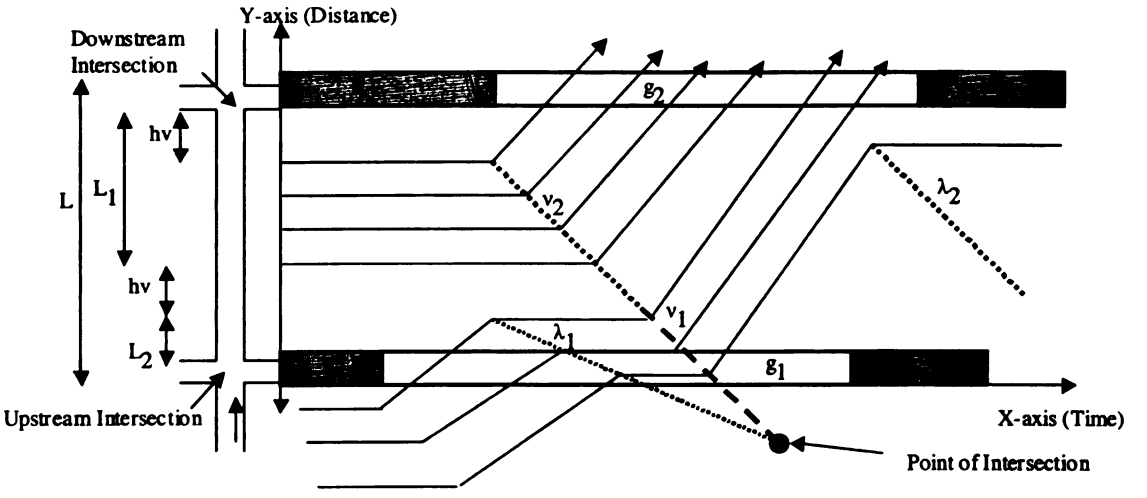

Figure 4.4 Point of intersection located downstream of the upstream intersection ($d_4 = 0$ in this case)

Hence the location of the point of intersection of mid block shockwaves decides whether the delay d4 occurs or not .To find the location (coordinates) of the point of a intersection of the shockwaves, an equation for each of the shock waves in terms of the signal system attributes (i.e., signal timing, link geometry, and traffic flow characteristics) is needed.

4.2.1 Mid-block stopping shock wave (MBW1)

The MBW1 starts from the point where the first vehicle from the upstream approach stops on the link due to the presence of queued vehicles on the downstream link. This starting point is shown as point 1 in figure 4.5. In addition to point 1, points 2, 3 and 4 are important in determining the value of d4. The coordinates of these points are:

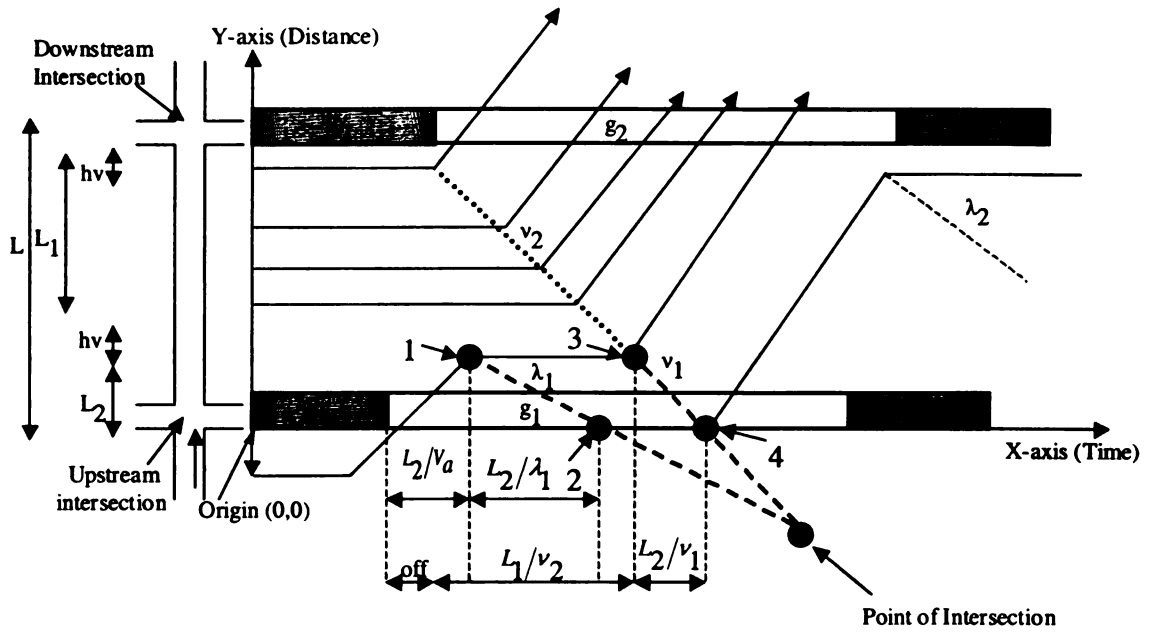

Figure 4.5 Important coordinates of the mid block starting and stopping shockwaves

Coordinates of point 1 are $(R_1 + \frac{L_2}{V_a}, L_2)$

Coordinates of point 2 are $(R_1 + \frac{L_2}{V_a} + \frac{L_2}{\lambda_1}, 0)$

Coordinates of point 3 are $(R_1 + \frac{L_1}{v_2} + off, L_2)$

Coordinates of point 4 are $(R_1 + \frac{L_1}{v_2} + \frac{L_2}{v_1} + off, 0)$

The x-coordinate of point 1 is the summation of the red time, R1, at the upstream approach and the time taken by the first vehicle to travel from the upstream intersection to the back of the queue standing at the link. The y-coordinate of point 1 is the empty space at the downstream link, L2. Note that delay due to acceleration is ignored for departing vehicles from the upstream intersection. So, the coordinates of the point at which the mid-block stopping wave starts, point 1 in figure 4.5, are $\left(R_1 + \frac{L_2}{V_a}, L_2\right)$. Point 2 in figure 4.5 shows the coordinates of the point at which the mid-block stopping wave crosses the upstream approach stop line. The coordinates are $\left(R_1 + \frac{L_2}{V_a} + \frac{L_2}{\lambda_1}, 0\right)$. The x-coordinate is the summation of the red time R1 at the upstream approach, time taken by the first vehicle to travel from the upstream intersection to the back of the queue standing at the link, and the time taken by the mid block stopping shockwave to cover the distance equals to the empty space at the downstream link. The y-coordinate is zero because it is exactly located at the x-axis.

A general equation for the spatio-temporal location (coordinates) of shockwave can be obtained by using basic straight-line equations. For clarification, consider two points having coordinates (x1, y1) and (x2, y2) respectively in xy plane, as shown in figure 4.6.

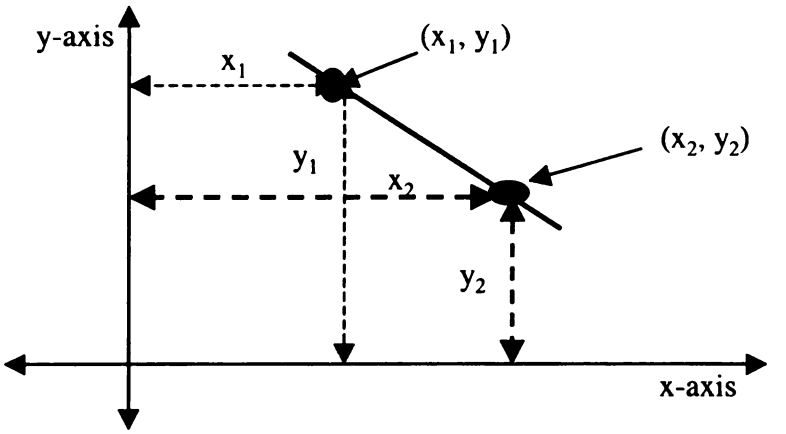

Figure 4.6 Two points (x_1, y_1) and (x_2, y_2) in xy plan.

Consider a line passing through distinct points (x_1, y_1) and (x_2, y_2) (see figure 4.6), its slope "m" is given by:

$$m = \frac{y_2 - y_1}{x_2 - x_1} \qquad (4.1\ a)$$

The equation of a line with slope "m" and passing through point (x_1, y_1) is:

$$y - y_1 = m(x - x_1) \qquad (4.1b)$$

Substituting the value of m from equation 4.1a in equation 4.1b, we have:

$$\frac{x - x_1}{x_2 - x_1} = \frac{y - y_1}{y_2 - y_1} \qquad (4.2)$$

In closely space signalized intersection system, instead of xy, there is time-space frame of reference, therefore

x = t (time), y = d (distance),

And instead of (x_1, y_1) and (x_2, y_2), MBW1 is passing through points having coordinates $\left(R_1 + \frac{L_2}{V_a}, L_2\right)$ and $\left(R_1 + \frac{L_2}{V_a} + \frac{L_2}{\lambda_1}, 0\right)$, as shown in figure 4.5. Therefore:

$$x_1 = \left(R_1 + \frac{L_2}{V_a}\right), x_2 = \left(R_1 + \frac{L_2}{V_a} + \frac{L_2}{\lambda_1}\right), \qquad y_1 = L_2 \text{ and } y_2 = 0$$

Substituting the above values in equation 4.2 and rearranging:

$$\lambda_1 t + d - \left[\lambda_1\left(R_1 + \frac{L_2}{V_a}\right) + L_2\right] = 0 \qquad (4.3)$$

"t" and "d" in the above equations represent the time and distance variables along the x and y axes, respectively. The MBW1 is expressed by equation 4.3, which shows the location of MBW1 in a time-distance coordinate system with the upstream intersection as the origin.

4.2.2 Mid-block starting shock wave (MBW2)

A MBW2 is generated when the first vehicle from the upstream approach starts moving after being stopped on the link due to a queue on the downstream link. The coordinates of the point at which the MBW2 starts, point 3 in figure 4.5, are $\left(R_1 + \frac{L_1}{v_2} + off, L_2\right)$, and the coordinates of the point where MBW2 crosses the upstream approach stop line, point 4 in figure 4.5, are $\left(R_1 + \frac{L_1}{v_2} + \frac{L_2}{v_1} + off, 0\right)$. Similar to equation 4.3 for MBW1, equation 4.4 below is the expression for MBW2 in a time-distance coordinate system with upstream intersection as an origin.

$$v_1 t + d - \left[v_1\left(R_1 + \frac{L_1}{v_2} + off\right) + L_2\right] = 0 \qquad (4.4)$$

Equations 4.3 and 4.4 for MBW1 and MBW2, respectively, will now be used to determine the location of their point of intersection. This is necessary to determine the value of d4.

4.2.3 Point of intersection of shock waves

The intersection point of the MBW1 and MBW2; whether d4 is zero or greater than zero. The coordinates of the point of intersection, in terms of traffic flow properties and control parameters, can be obtained by using MBW1 and MBW2 location equations.

For clarification, consider two lines represented by general line equations 4.5 and 4.6 as:

$$a_1 x_1 + b_1 y_1 + c_1 = 0 \qquad (4.5)$$

$$a_2 x_1 + b_2 y_1 + c_2 = 0 \qquad (4.6)$$

The coordinate of the point of intersection of the above two equations along the x-axis is:

$$\left(\frac{b_1 c_2 - b_2 c_1}{a_1 b_2 - a_2 b_1} \right) \qquad (4.7)$$

and the coordinate of the point of intersection along the y-axis is

$$\left(\frac{c_1 a_2 - c_2 a_1}{a_1 b_2 - a_2 b_1} \right) \qquad (4.8)$$

Similarly, consider two mid-block shockwaves represented by equations 4.3 and 4.4.

In this case the values of the constants in equations 4.7 and 4.8 that correspond to equations 4.3 and 4.4 are as follows:

$a_1 = \lambda_1 \qquad b_1 = 1 \qquad c_1 = -\lambda_1 \left(R_1 + \frac{L_2}{V_a} \right) - L_2$

$a_2 = \nu_1$ $\quad b_2 = 1$ $\quad c_2 = -\nu_1\left(R_1 + \frac{L_1}{\nu_2} + off\right) - L_2$

Substituting the above values in equation 4.7 and 4.8, we get:

$$[(\lambda_1)(R_1 + \frac{L_2}{V_a}) - (\nu_1)(R_1 + \frac{L_1}{\nu_2} + off)] \Big/ (\lambda_1 - \nu_1) \qquad (4.9)$$

$$[(\lambda_1)(\nu_1)(off - \frac{L_2}{V_a} + \frac{L_1}{\nu_2}) + L_2(\lambda_1 - \nu_1)] \Big/ (\lambda_1 - \nu_1) \qquad (4.10)$$

Equations 4.9 and 4.10 represent the coordinates of the point of intersection of the MBW1 and MBW2 in terms of signal timing, link geometry, and queue characteristics along the x and y axes respectively (See figure 4.7). If the value of equation 4.10 is less than zero that means there is an impact of the downstream intersection on upstream intersection (i.e., $d_4 > 0$).

The parameters needed to locate the point of intersection of MBW1 and MBW2, from equation 4.10, include queue length at the downstream link at the start of cycle of the upstream intersection and average the speed at the downstream link during the same cycle. The models for estimation of these parameters are explained in the following sections.

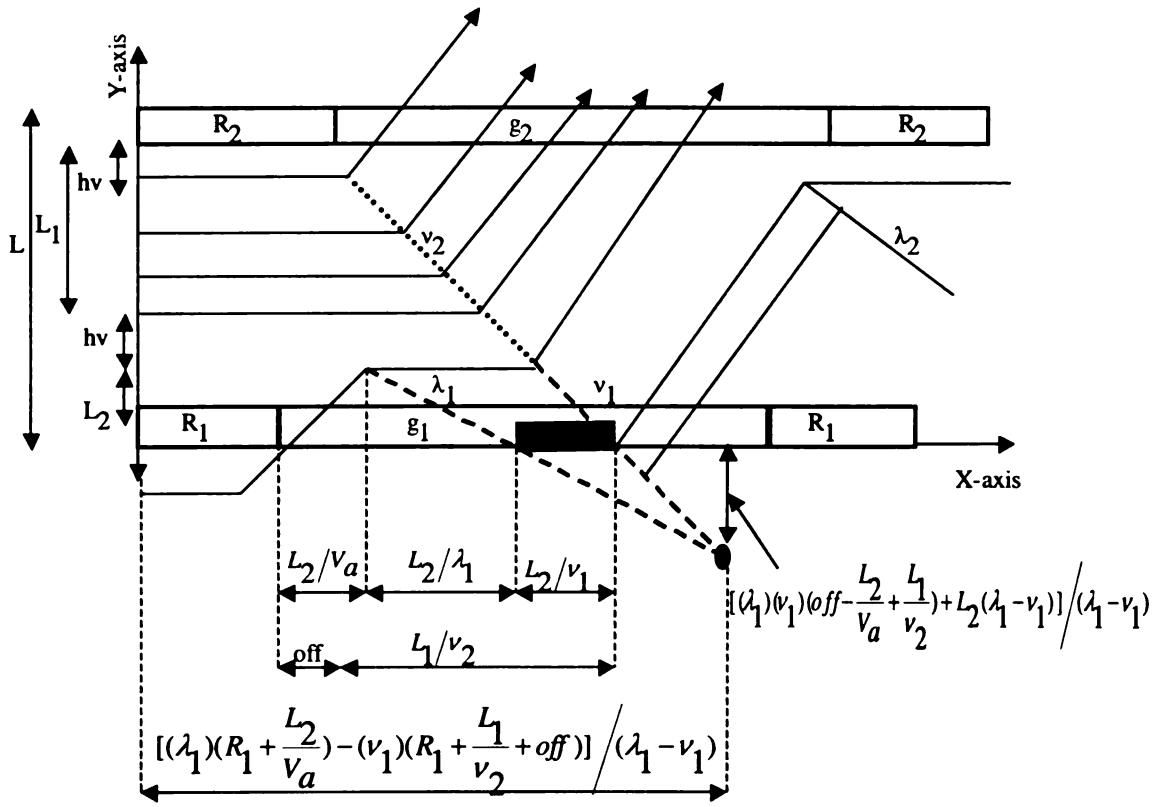

Figure 4.7 Coordinates of point of intersection of mid block stopping and starting shockwaves.

4.3 Estimation of queue length between upstream and downstream intersections

The downstream-induced delay, d4, depends on the length of the remaining space or the queue length on the downstream approach. The queue length at the downstream approach at the start of a cycle (i.e., cycle of the upstream intersection) depends upon the traffic output from the upstream and downstream approaches and the queue length at the downstream approach in the previous cycle. The traffic output is the number of vehicles discharged from the upstream or downstream approach during any specific cycle.

Equation 4.11 shows the expression to estimate queue length at the start of the i^{th} cycle.

$$L_{(1)i} = O_{(1)i-1} - \left(O_{(2)i-1} - L_{(1)i-1}\right) \qquad (4.11)$$

Where

$L_{(1)\,i}$ = queue length at downstream approach at start of i^{th} cycle of the upstream approach

$L_{(1)\,i-1}$ = queue length at downstream approach at start of $(i-1)^{th}$ cycle of the upstream approach

$O_{(1)\,i-1}$ = Traffic output from upstream approach during $(i-1)^{th}$ cycle of the upstream approach

$O_{(2)\,i-1}$ = Traffic output from downstream approach during $(i-1)^{th}$ cycle of the upstream approach

Traffic output from upstream and downstream approaches during a cycle depends on the following factors: offset, incoming volume from the upstream intersection, link average speed, effective green time at the downstream and upstream approaches and speed of the MBW1 and MBW2. Besides these factors, traffic output from both signalized approaches is also affected by the occurrence of following three conditions:

1. Wasted green time
2. Blockage due to downstream traffic
3. Passage of new traffic (after the standing queue clears) through downstream approach.

These conditions are explained one by one in the following section.

4.3.1 Wasted green

Wasted green refers to the unused portion of green time at the subject approach that occurs because of two scenarios. The first is when the green interval started too early that

the leading vehicle from the upstream approach reaches the downstream approach after the start of green (arrival at green) as shown in figure 4.8. The second is when there is a gap between the departure of the existing queue and the arrival of new traffic due to early start of green, as shown in figure 4.9.

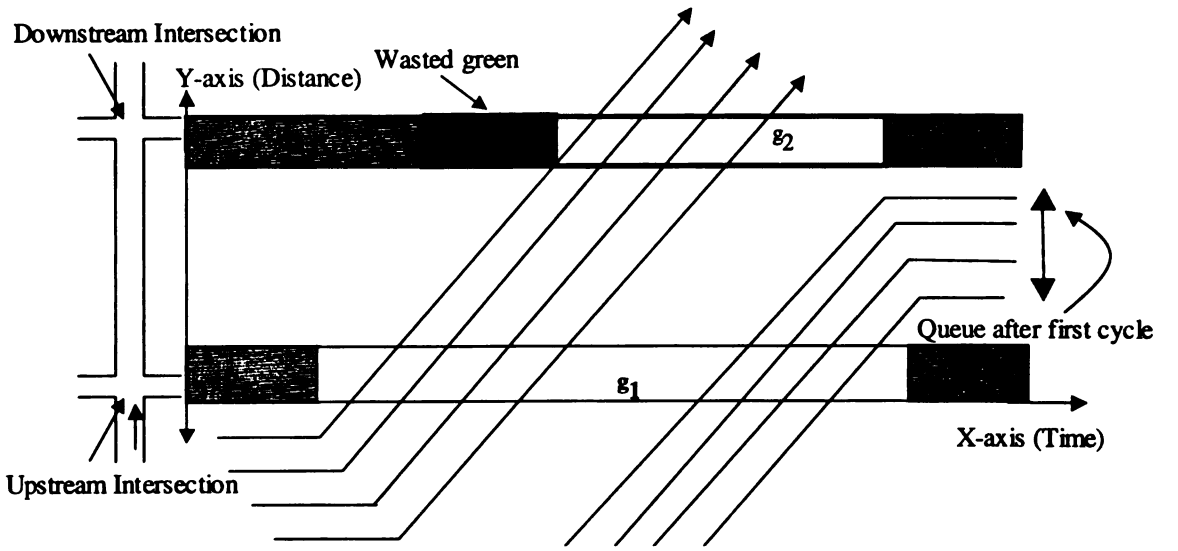

Figure 4.8 Wasted green due to late arrival at green of downstream approach

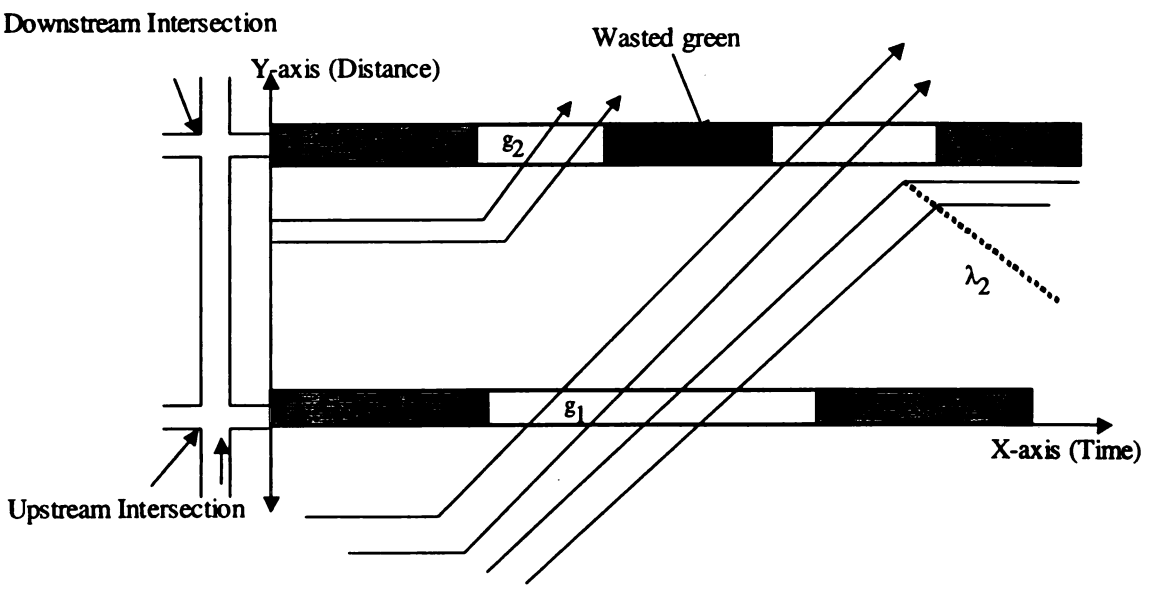

Figure 4.9 Wasted green due to gap between departure of existing queue and arrival of new traffic

There are two conditions which contribute to occurrence of wasted green. The equations for occurrence of these conditions have already been derived in previous study done by Abu-Lebdeh et.al (37), some modifications are made here to make them applicable to system setup shown in figure 4.1. Condition 1 occurs when the effective green time at the subject approach is larger than the summation of time to process the queue on the subject approach and one saturation headway. Equation 4.12 represents condition one:

$$\frac{L_{(1)i}}{S_2} + t_{hw} < g_2 \qquad (4.12)$$

Where:

t_{hw} = Saturation headway

Condition 2 occurs when the difference between the time taken by vehicles from the upstream approach to reach the downstream approach and the offset is more than the time needed to clear the queue at downstream approach.

$$\frac{L_{(1)i}}{S_2} + t_{hw} < \left(\frac{L}{Va} - offset\right) \qquad (4.13)$$

Both conditions must be satisfied for wasted green to occur. There is no wasted green for the upstream approach because it is assumed that continuous traffic demand is available at upstream approach. If there are gaps and disruption in traffic demand, then instead of continues demand, an appropriate statistical distribution can be used to analyze the arrival pattern of traffic at the upstream approach. The most frequently used distribution for traffic arrival in uncongested conditions is Poisson distribution and if demand is heavy uniform distribution is used.

4.3.2 Blockage

Blockage occurs when traffic at the subject approach cannot flow through the upstream intersection because the downstream link is full of traffic. Figure 4.3 and 4.4 show the scenarios for blockage and no blockage, respectively. Blockage occurs only at the upstream approach because it is assumed there is no downstream disturbance for the downstream intersection. In the case when there is a downstream disturbance for the downstream intersection, blockage conditions can be determined by considering the downstream intersection as the upstream intersection, i.e., considering another subsystem consisting of intersections 2 and 3, as shown in figure 4.1. The following condition should be satisfied for a blockage to occur at the upstream approach.

$$O_{(1)i} < (g_1 \times S_1) \qquad (4.14)$$

4.3.3 New traffic

New traffic is defined as traffic that goes through the downstream approach after the queue that had been waiting on the downstream approach, has already cleared the approach. New traffic starting from the upstream approach will be able to pass through downstream intersection if the following condition is satisfied:

$$g_2 > \left(\frac{L}{Va} - offset \right) \qquad (4.15)$$

Note that the occurrences of wasted green and blockage, and passage of new traffic from the downstream intersection, are independent from each other. The occurrence of one or more does not imply occurrence of the others.

4.3.4 Estimation of output from upstream and downstream approaches during a cycle

To determine the type of traffic flow and associated traffic output from upstream and downstream approaches that will result from any control plan for the two closely spaced signalized intersections, three questions need to be answered for every cycle: 1) does wasted green occur? 2) Does blockage occur? 3) Does new traffic pass through downstream intersection? Depending on the answer to these questions, eight possible traffic flow regimes ($2^3 = 8$) can occur, each of which having signal output value associated with it. Table 4.1 shows the eight possible flow regimes with different combination of conditions.

Table 4.1 Eight traffic flow regimes

Regime	Wasted green	Blockage	New traffic
1	Yes	No	No
2	Yes	Yes	No
3	No	Yes	Yes
4	No	No	Yes
5	*No*	*Yes*	*No*
6	Yes	Yes	Yes
7	Yes	No	Yes
8	**No**	**No**	**No**

Note: shaded cells represent regimes only applicable to downstream approach, cell with italic text are valid for upstream intersection whereas cell with bold text apply to both upstream and downstream intersections.

For the given setup and system (see figure 4.1), the no-wasted green and new-traffic conditions do not apply for the upstream approach as it is assumed there is continuous demand at the upstream approach. Therefore only regimes 5 and 8 are applicable for estimation of upstream approach traffic output. Whereas for the downstream approach, there is no blockage because it is assumed that there is no downstream disturbance at downstream approach. So, regimes 1, 4, 7, and 8 are applicable for downstream approach traffic output. Note that if there is an intersection upstream of the upstream approach or downstream of the downstream approach, then all eight traffic flow regimes will be applicable to the upstream and downstream approaches. The derivations of these regimes were first presented by Abu-Lebdeh et.al (37) and it is here modified to fit the context of this research.

4.3.4.1 Regime 1 (wasted green, no blockage, no new traffic)

Figure 4.10 shows the time space diagram for traffic flow regime 1. In this regime, vehicles from upstream approach cannot cross the downstream intersection during the green at downstream intersection so neither new traffic condition nor downstream disturbance occur. This type of flow regime can occur when the offset is not optimal or there is large spacing between upstream and downstream intersection. For this regime, only the queued vehicle at the downstream approach will discharge from the downstream approach, as shown in equation 4.16:

$$O_{(2)i} = \frac{L_{(1)i}}{hv} \qquad (4.16)$$

Where

$O_{(2)i}$ = Output from downstream approach during i^{th} cycle (vehicles)

$L_{(1)i}$ = Queue length at downstream approach at start of cycle (meter)

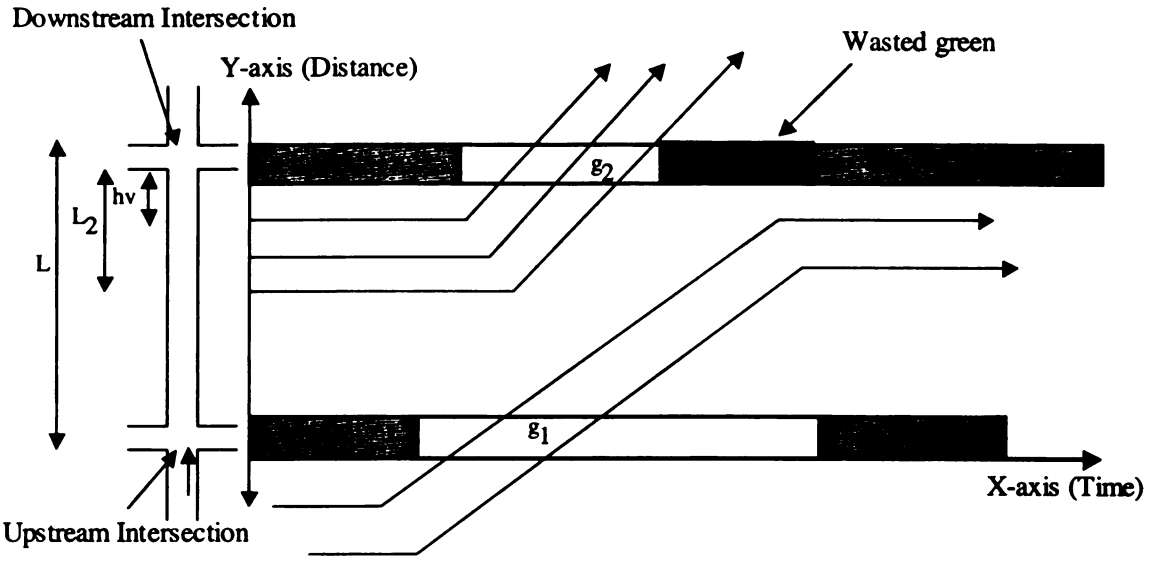

Figure 4.10 Flow regime with wasted green, no blockage, and no new traffic (Regime 1)

4.3.4.2 Regime 4 (no wasted green, no blockage, new traffic)

Figure 4.11 shows vehicle profiles for regime 4. In this case there is no wasted green, no blockage, and new traffic from upstream approach passes through the downstream approach during the i^{th} cycle at the downstream intersection. The traffic output for this regime, is the sum of queued vehicles at the downstream approach and the new traffic that arrives from the upstream approach during the i^{th} cycle. The expression for output for this regime is:

$$O_{(2)i} = \frac{L_{(1)i}}{hv} + \left\{ g_2 - \frac{1}{S_2}\left(\frac{L_{(1)i}}{hv} + 1 \right) \right\} \times S_2 \qquad (4.17)$$

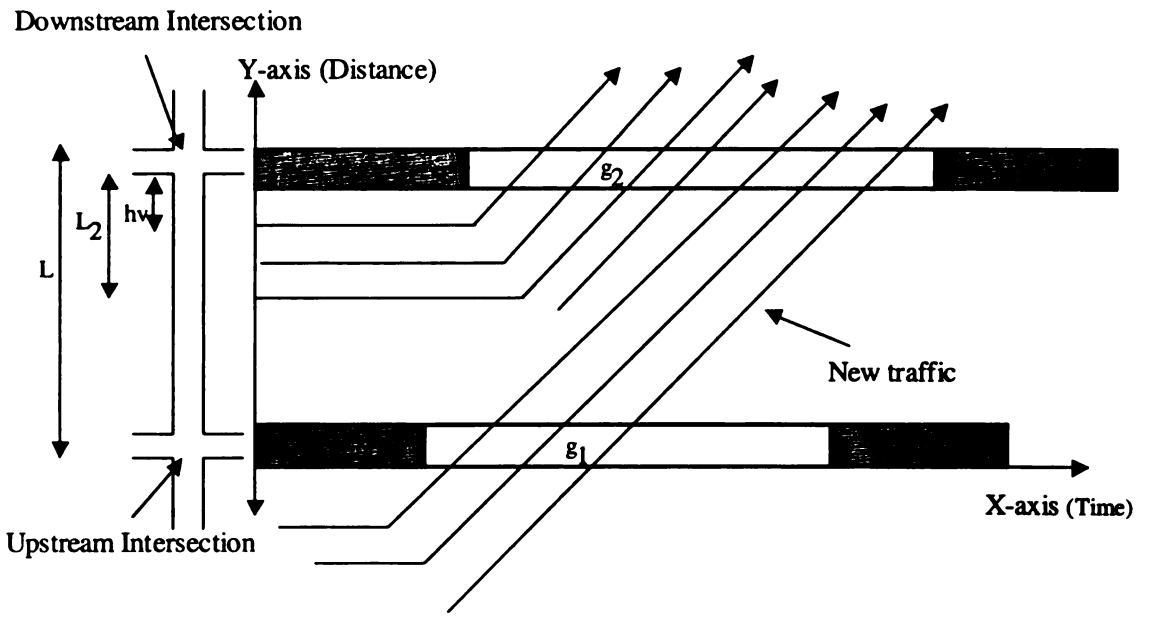

Figure 4.11 Flow regime with new traffic, no wasted green and no blockage (Regime 4)

4.3.4.3 Regime 5 (no wasted green, blockage, no new traffic)

Blockage occurs at the upstream approach due to the downstream disturbance (i.e., long queues). Traffic output depends upon the duration of the blockage time. Figure 4.12 shows the time space diagram for regime 5. The output expression is;

$$O_{(1)i} = \left(g_1 - d_{(4)1} - \frac{1}{S_1} \right) \times S_1 \qquad (4.18)$$

Where

$d_{(4)1}$ = Downstream-induced delay experienced by the first vehicle at the upstream approach

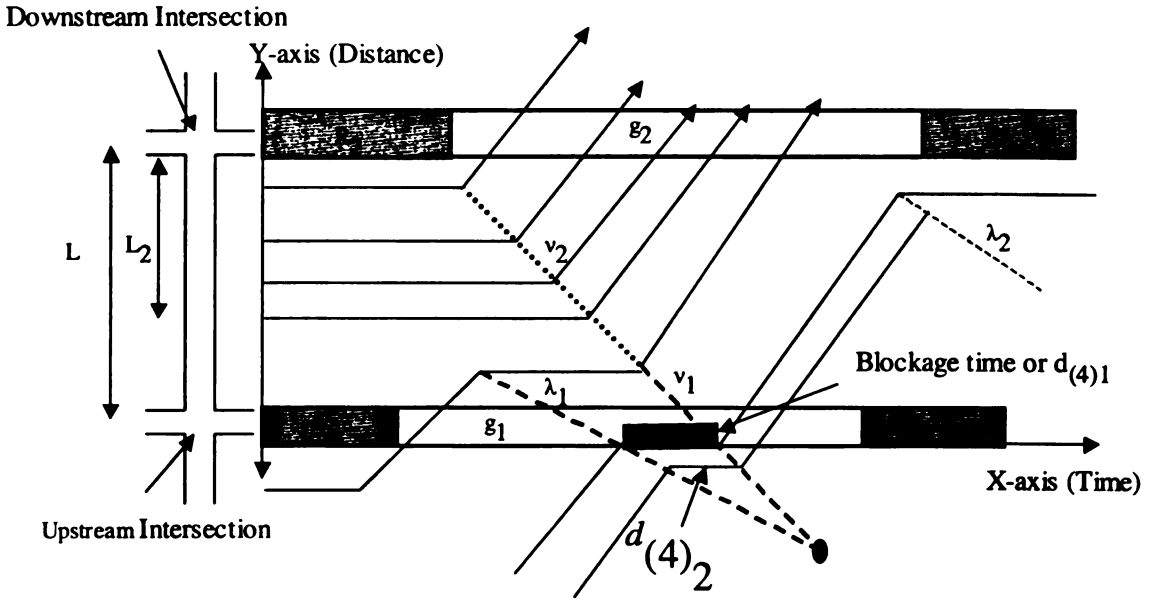

Figure 4.12 Flow regime for upstream intersection with blockage (Regime 5)

4.3.4.4 Regime 7 (wasted green, no blockage, new traffic)

Figure 4.13 shows the vehicles' profile for regime 7. The traffic output from the downstream approach depends on the duration of wasted green and queue length on the downstream approach at start of cycle. The equation for regime 7 is:

$$O_{(2)i} = \frac{L_{(1)i}}{hv} + \left(g_2 - \frac{L}{Va} + offset \right) \times S_2 \qquad (4.19)$$

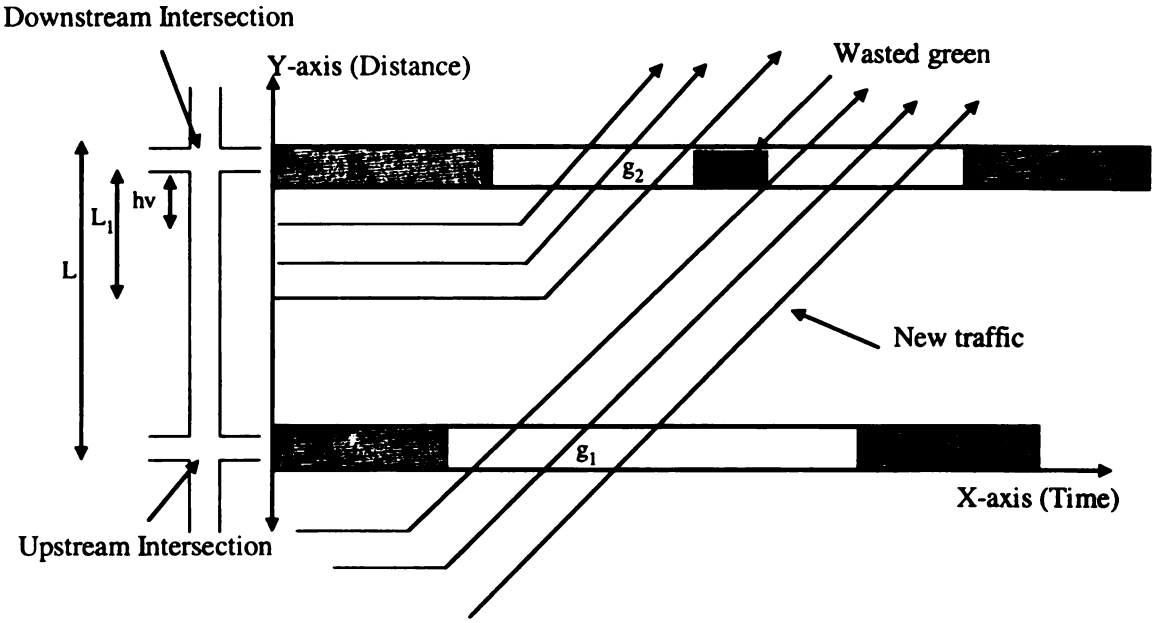

Figure 4.13 Flow regime for downstream intersection with wasted green and new traffic (Regime 7)

4.3.4.5. Regime 8 (no wasted green, no blockage, no new traffic)

This is the only regime that can occur at both upstream and downstream approaches, for the given system setup. In this case, there is no wasted green, no blockage, and no new traffic passes the downstream approach. Figures 4.14 and 4.15 show the profile of vehicles for regime 8 for downstream and upstream approaches, respectively. Following are the expressions for calculating the traffic output from downstream and upstream approaches for regime 8.

Downstream approach traffic output:

$$O_{(2)i} = \left(g_2 - \frac{1}{S_2} \right) \times S_2 \qquad (4.20)$$

Upstream approach traffic output:

$$O_{(1)i} = \left(g_1 - \frac{1}{S_1} \right) \times S_1 \qquad (4.21)$$

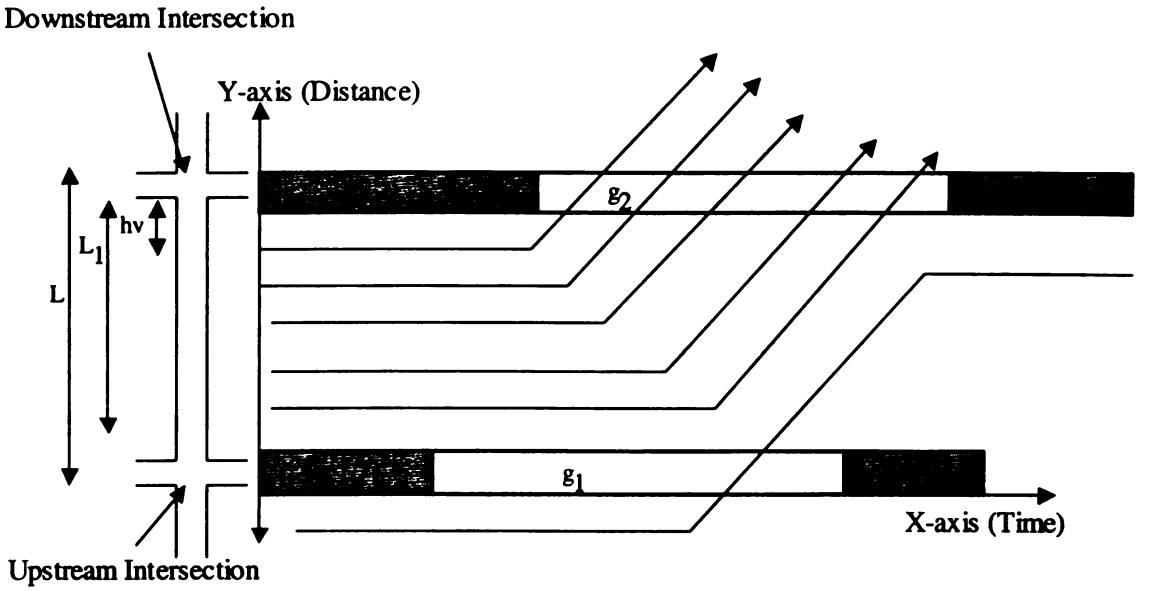

Figure 4.14 Flow regime for downstream approach for Regime 8

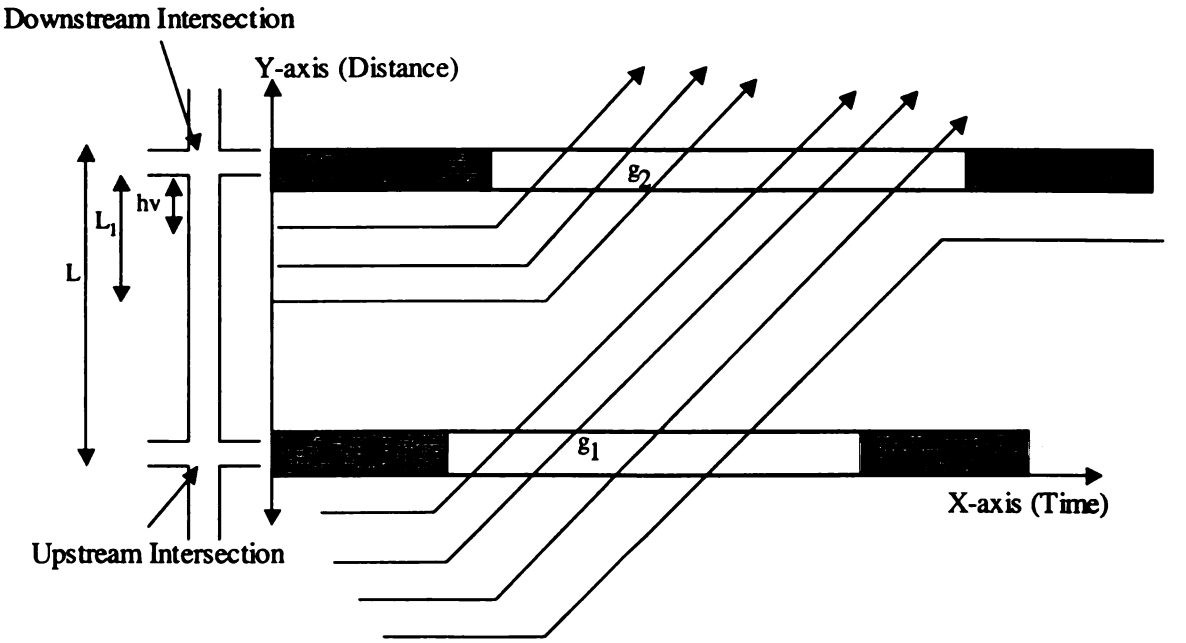

Figure 4.15 Flow regime for upstream approach for Regime 8

Traffic outputs from upstream and downstream approaches, associated with each regime are used in equation 4.11 to estimate the queue length at the downstream approach during each cycle. The assumptions used to estimate queue length at downstream approach are given in the following section.

4.3.5 Assumptions for queue estimation at downstream approach

The following assumptions were used in formulating the queue length models for the downstream approach:

1. Arrivals at the downstream approach occur in platoons. Platoon length depends on upstream signal timings and demand at the upstream approach,
2. Platoons maintain their headway due to the short link length, i.e., dispersion is assumed negligible,
3. Mid block traffic generation is considered non-existent, i.e., no traffic sink or source exists between upstream and downstream intersections,
4. Finite queuing space exists at the downstream approach. Infinite space is available at the upstream approach,
5. Continuous is demand present at the subject approach at the upstream intersection, and
6. Volumes of Left and right turning vehicles are considered non-existent in the model.

The basic structure of the model to estimated queue length at the downstream approach at the start of each cycle for closely spaced signalized intersections system is presented in this research. The limitations noted above can be addressed by refining or modifying the models presented. For example, vehicles from left and right turns at the

upstream intersection and from upstream mid-block sources, if known, can be easily accommodated by adding appropriate terms to equation 4.11. This, however, will not fundamentally change the models of this research.

4.4. Expression for link average speed (Va)

Link average speed, Va, is defined as the average speed at which vehicles from upstream approach travel on downstream link. As discuss earlier, downstream-induced delay d_4 depends on Va of the downstream link during a given cycle, beside other factors. Va depends on the queue length on the downstream approach, or, in other words, the unoccupied space available for vehicles arriving from the upstream approach. To estimate the average speed on the link between upstream and downstream intersections, two cases were considered. The derivations of these cases were first presented by Abu-Lebdeh et.al (9) and it is here modified to fit the context of this research. Both cases are explained below.

1. The remaining space (L_2) on the link is long enough for vehicles from the upstream approach to reach free flow speed and cruise before they start decelerating.
2. The remaining space (L_2) is not long enough for vehicles from the upstream approach to cruise at free flow speed. In this case vehicles will accelerate at an assumed rate of a_1 for the first half of the remaining space and decelerate at a rate of a_2 for the second half. Note that the assumption of half of the distance for acceleration and the other half for deceleration can be different (e.g., one-third distance for acceleration and two-third distance for deceleration). That will not substantially affect the average speed estimation model.

4.4.1 Case 1: Vehicle accelerate to free flow speed, cruise, and finally decelerate

In this condition, vehicles from the upstream intersection have enough space to perform the following three maneuvers.

1. Accelerate to free flow speed,
2. Cruise at free flow speed,
3. Decelerate to a stop

Figure 4.16 shows the speed profile of a vehicle for Case 1. D1 is the distance travel by a vehicle to reach free flow speed and D2 is the distance covered by the vehicle to decelerate to a stop from free flow speed.

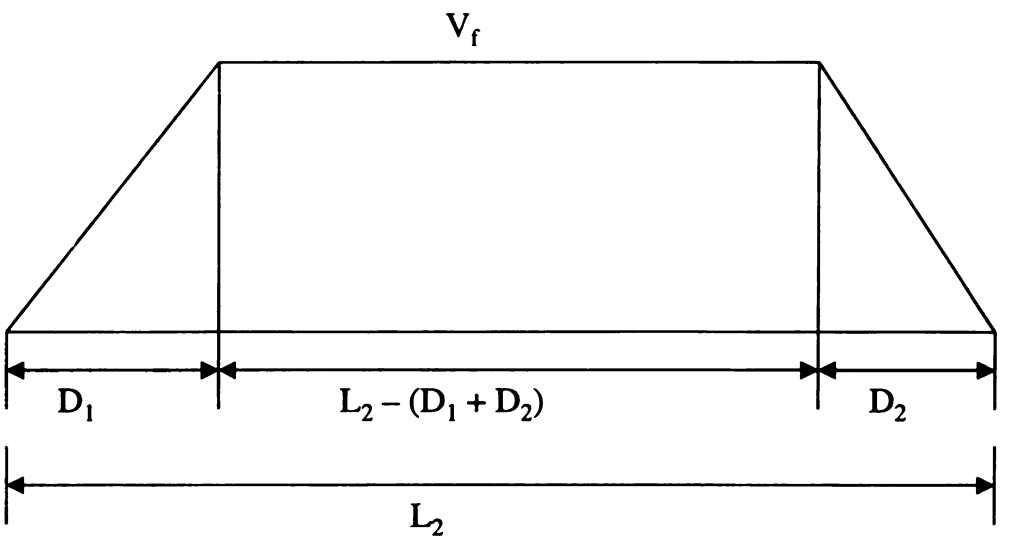

Figure 4.16 Speed profile for a vehicle that accelerates to free-flow speed, cruises and then decelerates to a stop (Case 1)

According to Newton second equation of motion, the distance (S) covered by a body during a time interval (t) is given by equation 4.22.

$$S = Ut + \frac{1}{2}at^2 \qquad (4.22)$$

Where

S = Distance (m)

U = Initial speed (m/s)

a = acceleration (m/s^2)

t = time taken to cover distance S

For the given system as shown in figure 4.16, when a vehicle accelerates to free flow speed:

$S = D_1$ = Distance covered during accelerating from stop to free flow speed

U = 0 = Vehicle starts from the stop line of upstream intersection

$t = t_1$ = Time spent to cover distance D_1

$a = a_1$ = Acceleration rate of a vehicle coming from upstream intersection

Substituting the above values in equation 4.22, we have:

$$D_1 = \frac{1}{2} \times a_1 \times t_1^{\,2} \qquad (4.23)$$

Rearranging equation 4.23:

$$t_1 = \sqrt{\frac{2D_1}{a_1}} \qquad (4.24)$$

From Figure 4.16, the distance traveled at free flow speed is $L_2 - (D_1 + D_2)$, so the time (t_3) taken to complete this distance is:

$$t_3 = \frac{L_2 - (D_1 + D_2)}{v_f} \qquad (4.25)$$

Similarly the time (t_2) to travel D_2, which is the distance traveled by the vehicle while decelerating from free flow speed to a stop is:

$$t_2 = \sqrt{\frac{2D_2}{a_2}} \qquad (4.26)$$

Where

a_2 = deceleration rate (m/s^2)

Hence the average speed (Va) over the link is

$$V_a = \frac{\text{Remaining Space}}{\text{Total Time}} = \frac{L_2}{t_1 + t_3 + t_2} \qquad (4.27)$$

Substituting the values of t_1, t_3 and t_2 from equation 4.24, 4.25 and 4.26 respectively in equation 4.27, Va can be estimated as follows:

$$V_a = \frac{L_2}{\sqrt{\frac{2D_1}{a_1}} + \frac{L_2 - (D_1 + D_2)}{v_f} + \sqrt{\frac{2D_2}{a_2}}} \qquad (4.28)$$

4.4.2. Case 2: Vehicle accelerate for half of distance and then decelerates for other half

For Case 2, due to the limited unoccupied space on the link between the upstream and downstream intersection to reach free flow speed, it is assume that the vehicle will accelerate for half of the distance and then decelerate for the other half. Vehicles coming from the upstream approach can perform only two maneuvers, which are:

1. Accelerated for the half of available distance
2. Decelerate for other half

Figure 4.17 shows the speed profile of a vehicle from the upstream approach. If D_a and D_d are the distances traveled during acceleration and deceleration, respectively, then equation 4.28 becomes:

$$V_a = \frac{D_3 + D_4}{\sqrt{\frac{2D_3}{a_3}} + \sqrt{\frac{2D_4}{a_4}}} \qquad (4.29)$$

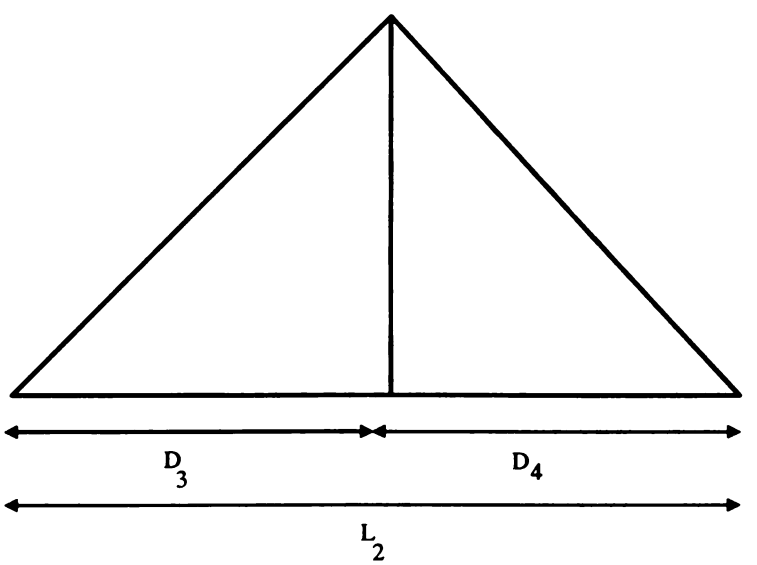

Figure 4.17 Speed profile for vehicle that accelerates to half of distance and then decelerates to a stop (Case 2)

4.5 Length of delay d_4 at the upstream intersection due to downstream traffic disturbance

The length of d4 that is experience by the upstream approach vehicles depends upon the location of the intersecting point of the mid-block starting and stopping shock waves, as discuss and explained in section 4.2. The proportion of d4 incurred by the first vehicle at

the upstream approach is equal to the "distance" (in time units) between the points where the mid-block starting and stopping wave cross the upstream intersection. The portion of d4 incurred by the first vehicle at the upstream intersection, therefore, is:

$$d_{(4)1} = (\frac{L_1}{v_2} + \frac{L_2}{v_1} + off - \frac{L_2}{V_a} - \frac{L_2}{\lambda_1}) \qquad (4.30)$$

Where

$d_{(4)1}$ = Portion of d4 incurred by the first vehicle at the upstream approach (see figure 4.18 below)

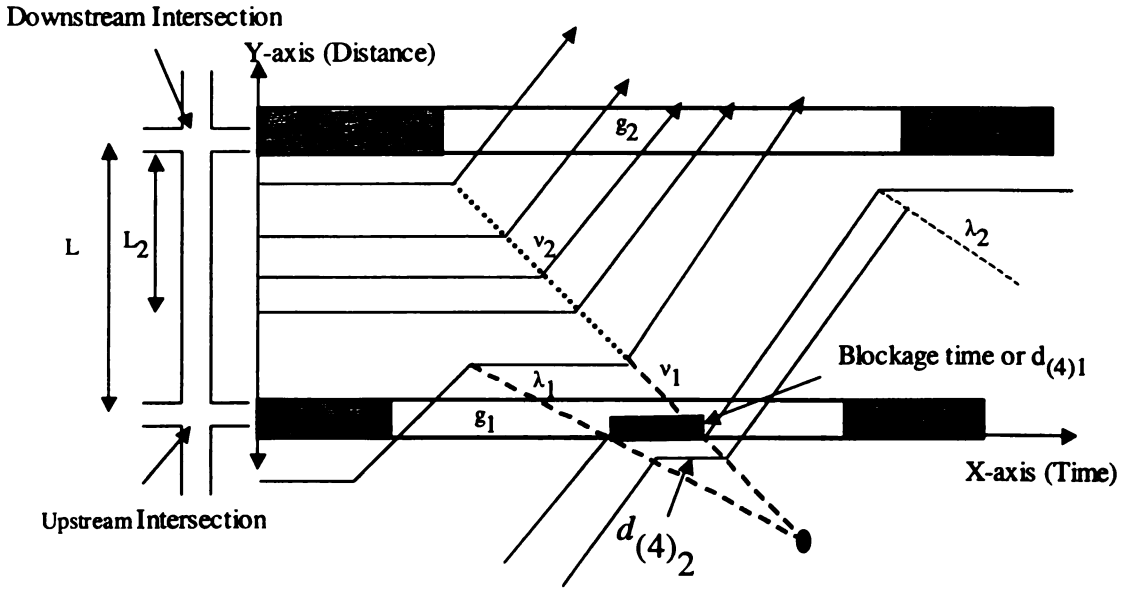

Figure 4.18 Additional delay observed by first and second vehicle at upstream approach

The portion of d_4 incurred by the second vehicle at the upstream approach is:

$$d_{(4)2} = d_{(4)1} + \frac{h_v}{v_1} - \frac{h_v}{\lambda_1} \qquad (4.31)$$

Rearranging equation 4.31, we have:

$$d_{(4)2} = d_{(4)1} + h_v\left(\frac{1}{v_1} - \frac{1}{\lambda_1}\right) \qquad (4.32)$$

Note that the length of $d_{(4)1}$ will always be larger than $d_{(4)2}$, because v_1 is always greater than λ_1 as shown in figure 4.19. The portion of d4 for the nth vehicle at the upstream approach is:

$$d_{(4)_2} = d_{(4)_1} + nh_v\left(\frac{1}{v_1} - \frac{1}{\lambda_1}\right) \qquad (4.33)$$

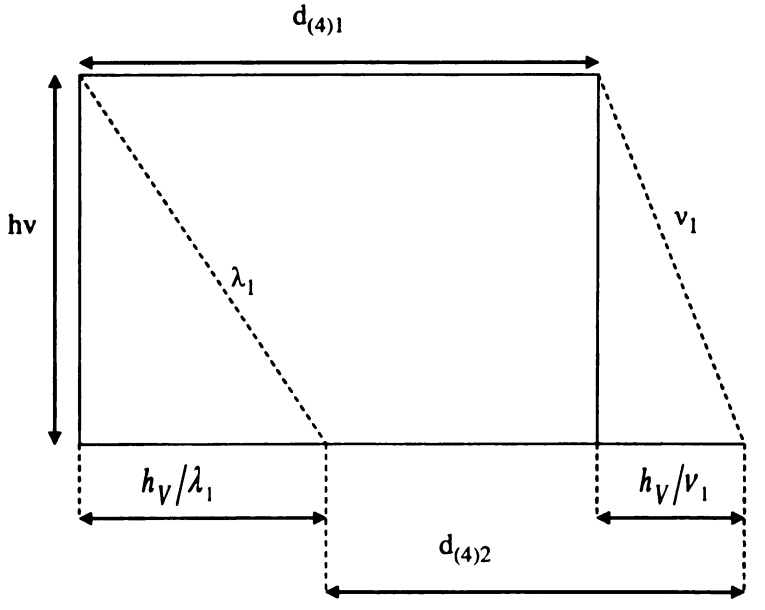

Figure 4.19 Reduction of delay "d4" for the second vehicle at upstream approach

The value of the delay term d4 for all affected vehicles at the upstream approach is comparable to the arithmetic progression. In general the arithmetic progression is known as an arithmetic sequence of "n" numbers such that the differences between successive terms is a constant. The equation 4.34 shows the general form of arithmetic progression

$$\{a_0, a_0 + d, a_0 + 2d, ..., a_0 + nd\} \qquad (4.34)$$

Where

a_0 = First value of sequence

d = Common or constant difference

In term of delay, we have

$a_0 = d_{(4)_1}$ = Delay d_4 observed by first vehicle

d = Common difference of delay between neighboring vehicles, equals to

$$d = h_v\left(\frac{1}{\nu_1} - \frac{1}{\lambda_1}\right) \qquad (4.35)$$

Substituting values of d, a_0 in equation 4.34, the arithmetic sequence becomes

$$\left\{d_{(4)_1}, d_{(4)_1} + h_v\left(\frac{1}{\nu_1} - \frac{1}{\lambda_1}\right), d_{(4)_1} + 2h_v\left(\frac{1}{\nu_1} - \frac{1}{\lambda_1}\right), \ldots\ldots, d_{(4)_1} + nh_v\left(\frac{1}{\nu_1} - \frac{1}{\lambda_1}\right)\right\} \qquad (4.36)$$

Using the formula for the sum of a series for arithmetic progression, the total value of d4 for the upstream approach is

$$d_4 = \frac{n}{2}\left[2d_{(4)1} + (n-1)h_v\left(\frac{1}{\nu_1} - \frac{1}{\lambda_1}\right)\right] \qquad (4.37)$$

Where

n = Total number of the vehicles at the upstream approach.

4.6. Estimation of delay for multiple cycles

The downstream-induced delay d_4 may be added to the three already existing delay terms of HCM 2000 control delay formula. Therefore the unit of analysis for d_4 should be comparable to that of the HCM 2000. Control delay and its components were already explained in chapter 3. The analysis period for the calculation of control delay is 15

minutes according to HCM 2000 methodology. So the delay d4 should be calculated for each cycle occurred during 15-minute time interval. The number of cycles needed in the analysis can be obtained by the following expression

$$C_t = \frac{900}{CL} + 1 \qquad (4.38)$$

Where

C_t = Total number of cycles to be analyzed

CL = Cycle Length (seconds)

Note that one is added for the initial cycle where it is assumed that the network is empty and which will not be considered in the 15-minute analysis period. The initial cycle starts with the green of the upstream approach and finish with end of red at the upstream approach. The purpose of using an initial cycle is to estimate the queue length at the start of cycle 1.

Figure 4.20 shows the flow diagram for the analysis of multiple cycles. The same procedure will be repeated for each cycle for the 15-minute analysis period. At the end we have d_4 for each cycle. Delay d_4 for the subject approach of upstream intersection will be

$$d_4 \text{ for the subject approach } = \frac{d_{(4)c_1} + d_{(4)c_2} + d_{(4)c_3} + \ldots\ldots + d_{(4)c_n}}{C_n} \qquad (4.39)$$

Where

$d_{(4)c1}$ = d4 for all vehicle at the upstream approach during cycle 1

$d_{(4)cn}$ = d4 for the n^{th} cycle

C_n = Total number of cycles during 15-min interval

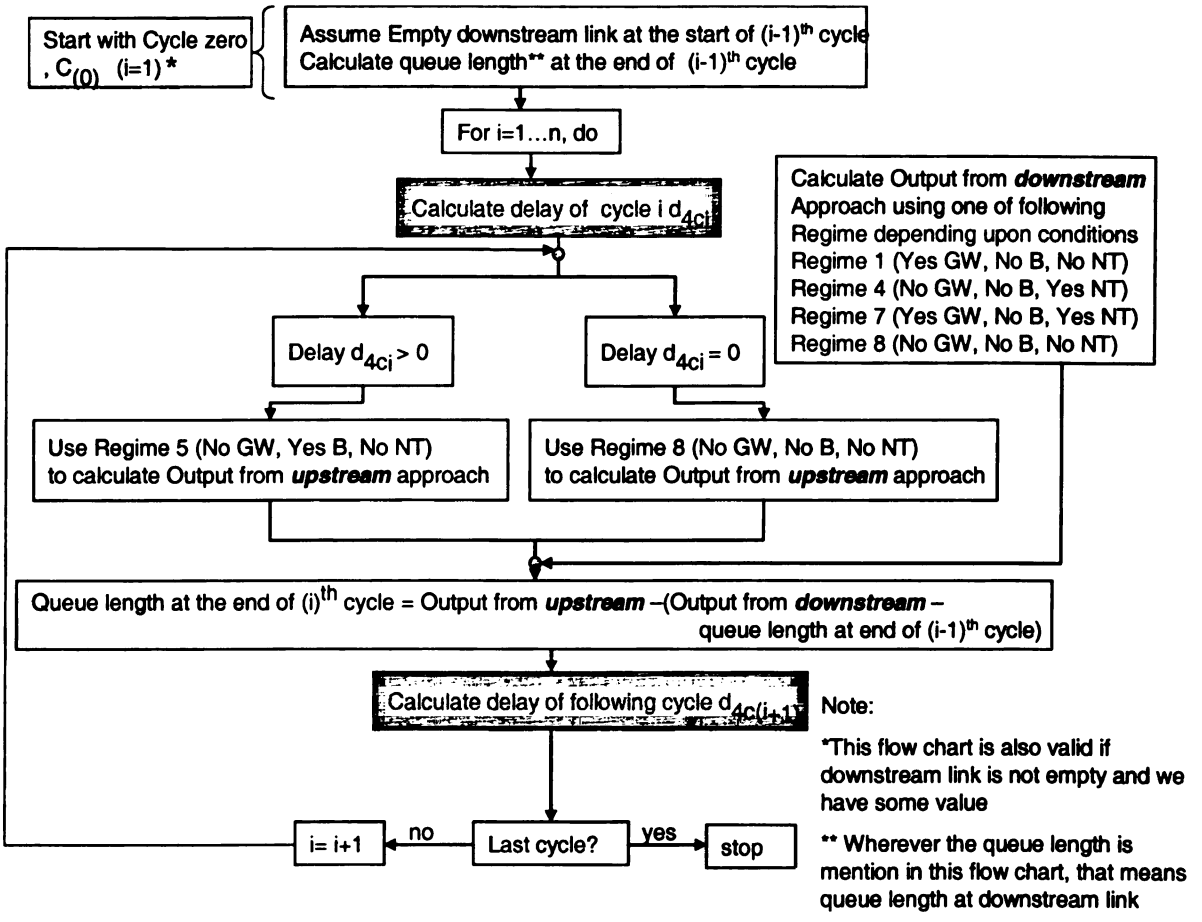

Figure 4.20 Flow chart for the estimation of delay d_4 for multiple cycles

CHAPTER 5

Results and Sensitivity Analysis of Downstream-Induced Delay

5.1. Introduction

Chapter 4 presented the formulation of three models, which can be used to quantify the following:

- Queue length at the start of each cycle on the downstream approach
- Average speed at the downstream link
- Downstream induced delay, d_4, at the upstream approach

The model to determine the downstream-induced delay, d4, is the most pertinent of the three models. The outputs of the other two models are essential inputs to the d4 model. This chapter presents the sensitivity of the d4 model vis-à-vis geometric, traffic flow, and control traffic parameters of the upstream and downstream intersections and the link connecting the two intersections.

The d4-model provides the amount of additional delay induced by the downstream intersection on the upstream signalized approach. To study the outputs of the d4-model, two types of analysis are used: cycle-by-cycle analysis and average of 15-minute interval analysis. In the cycle-by-cycle analysis, d4 is estimated for individual cycles, whereas in the 15-minute average analysis, the average value of d4 is calculated for all cycles within the 15-minute time interval. There are two reasons for doing these analyses: one is to see how the d4 changes from cycle to cycle, and the second is to make the analysis period for d4 compatible with the current HCM methodology (where the analysis period for delay calculations is 15-minutes).

5.2. Example application of the d4-model

A hypothetical system is used to demonstrate how traffic flow, geometry, and control characteristics interact and influence the values of d4. Figure 5.1 shows the system layout of two closely spaced signalized intersections. The following are the geometric, traffic and control parameters of the system:

Saturation flow rate, S1 = 1800 vph,

Speed of stopping shockwave, $\lambda 1$& $\lambda 2$ = 4 m/s

Speed of starting shockwave, v1 & v2 = 5.5 m/s

Effective headway, hv = 6.5 m

Number of lanes = 1

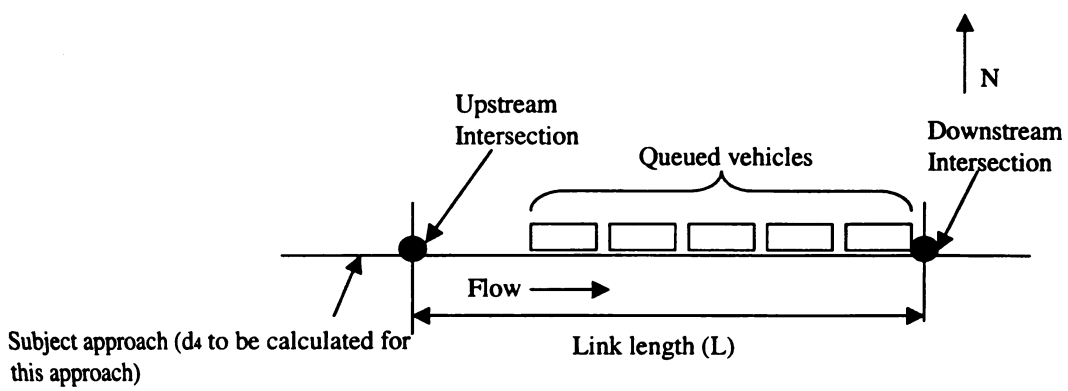

Figure 5.1 Upstream and downstream intersection location

5.3. Cycle-by-Cycle analysis

The length of d4 experienced by vehicles at the subject approach of the upstream intersection during each cycle depends upon:

- g/c of the upstream and downstream approaches
- Average link speed
- Offset

- Queue length and remaining empty space at the downstream link at the start of each cycle of the upstream approach

The above mentioned parameters depend upon the traffic flow conditions during the current and preceding cycles except for the offset and g/c for both intersections, which are fixed for all cycles. Note that if the traffic signal is adaptive, i.e., has the capability to change in signal timings according to the traffic demand, then the offset and g/c ratio will vary cycle by cycle and this type of controller can be accommodated by adding the appropriate parameters in the d4-model. For example for flow regime 7 (see figure 4.13), when there is a wasted green and new traffic but no blockage, the output from the downstream is estimated by equation:

$$O_{(2)i} = \frac{L_{(1)i}}{hv} + \left(g_2 - \frac{L}{Va} + offset \right) \times S_2$$

If offset and the green at the downstream approach is changing cycle by cycle then the above equation becomes

$$O_{(2)i} = \frac{L_{(1)i}}{hv} + \left(g_{(2)i} - \frac{L}{Va} + (offset)_i \right) \times S_2$$

Where $g_{(2)i}$ and $(offset)_i$ are green and offset at the downstream approach and offset, respectively, during the i^{th} cycle of the upstream intersection.

The d_4 can eventually be add to the three already existing delay terms in the HCM 2000 control delay formula, which are based on a 15-minute analysis period. Therefore all cycles during a 15-minute time interval should be analyzed for d_4 calculations. In the following sections, first, values of d4 during each cycle and queue length at the start of

each cycle are observed, and then the sensitivity of d4 is evaluated versus link length, offset, and g/c of upstream and downstream approaches.

5.3.1 Variation of d4 and queue length during each cycle

Figures 5.2 and 5.3 show a cycle-by-cycle variation of d4 for the subject approach, and the queue length at the downstream approach for different cycles and g/c values. System parameters for the scenario, shown in figure 5.2, are: cycle length of 150 sec, distance between upstream and downstream intersection is 300 m, offset is 20 sec with the upstream eastbound approach (see figure 5.1) as a reference phase, and g/c of 0.8 and 0.6 for the upstream and downstream approaches, respectively. Figure 5.3 shows the results for a scenario with the following system parameters: link length and offset similar to first scenario, cycle length is 120 sec, g/c ratio of 0.9 and 0.6 for the upstream and downstream approaches, respectively. The second scenario (results in figure 5.3) is more congested because of the higher g/c ratio at the upstream approach. By giving more green time at the upstream approach, more traffic is fed into the downstream link thus creating more congestion; this explain why there is higher d4 values and longer queue lengths at the downstream link for the second scenario (figure 5.3).

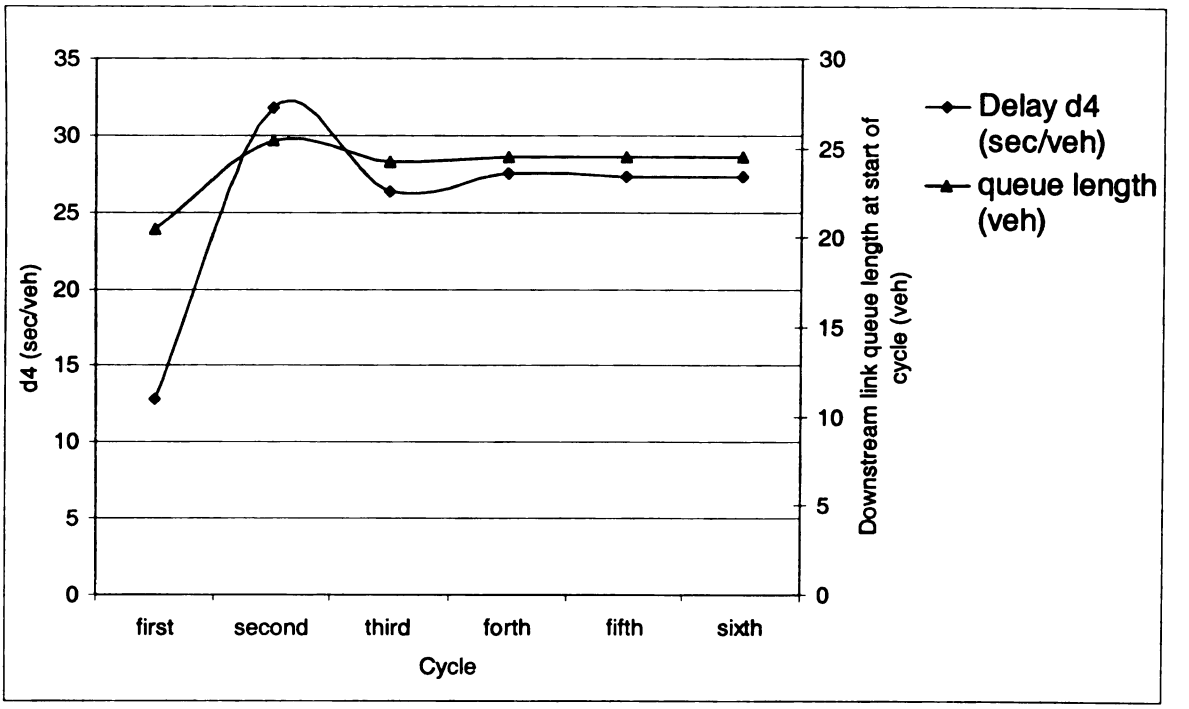

Figure 5.2 Variation of d4 at subject approach, and change of queue length at downstream link for each cycle. In this case g/c for upstream and downstream are 0.8 and 0.6, respectively; cycle length 150 sec, offset 20 sec, and link length 300 m.

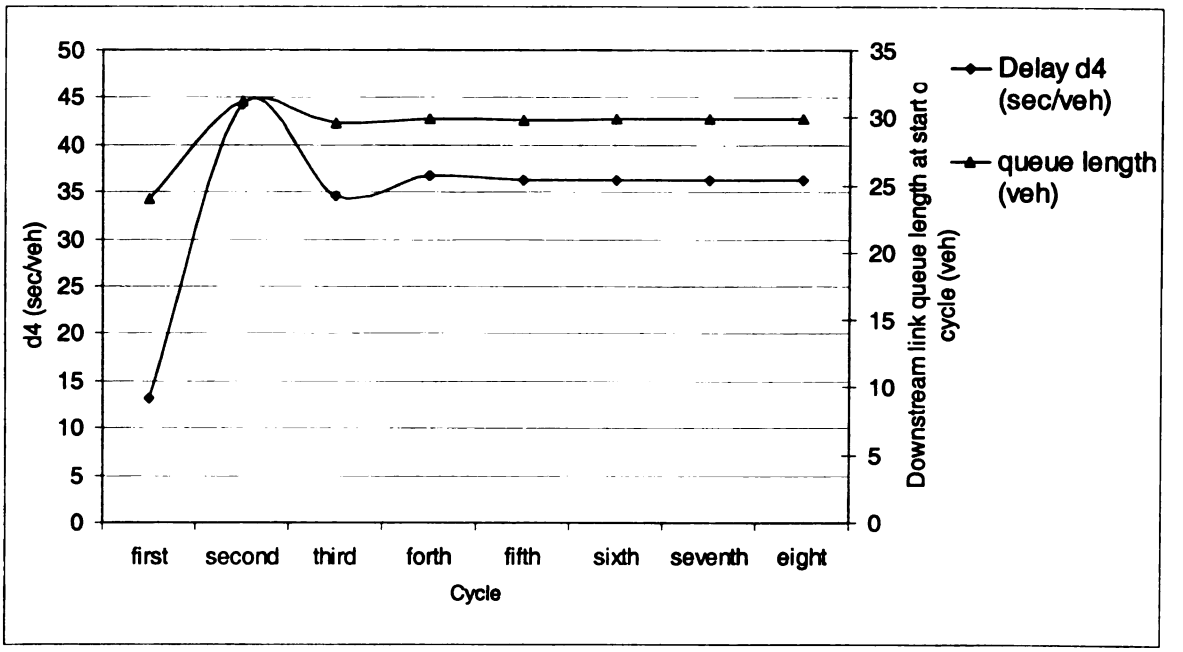

Figure 5.3 Variation d4 at subject approach, and change of queue length at downstream link for each cycle. In this case g/c for upstream and downstream are 0.9 and 0.6, respectively; cycle length 120 sec, offset 20 sec, and link length 300 m.

For the 15-minute interval analysis, six cycles were used when the cycle length at both upstream and downstream intersections were 150 seconds. Another analysis was conducted for eight cycles where the cycle length is 120 seconds (i.e. 900/120 = 8). The queue lengths shown in figures 5.2 and 5.3 represent the number vehicles present at the downstream link at the start of the cycle at the upstream intersection. This queue length is contributing to d4 during the cycle besides other factors like the offset, average speed, link length, and g/c ratios at the upstream and downstream approaches. The general trends depicted in figures 5.2 and 5.3 agree with expectations. The positive correlation between the queue on the downstream link and the d4 values makes sense. The increase of queue length on the downstream link at the start of a cycle reduces the space for vehicles arriving from the subject approach. Arriving vehicles reach the back of the queue quickly, increasing the probability of blockage at the upstream intersection and hence the value of d4 at the upstream approach.

The first cycle in both scenarios, shown in figures 5.2 and 5.3, has the lowest d4 value as compared to other cycles. This makes sense because the network is assumed to be empty at the beginning of the initial cycle (cycle 0), which immediately precede the cycle in question. After two or three cycles the system reaches equilibrium for the given conditions. Both d_4 and queue length thus remain the same for each cycle during the remaining cycles. Since the traffic demand and signal timing at the upstream intersection remain the same throughout the cycles, the value of d4 for each cycle thus assumes steady values as soon as the queue length at the downstream link starts repeating itself during subsequent cycles. If the offset or cycle length were dynamic, i.e., change with demand, then the delay d4 would fluctuate more during subsequent cycles.

5.3.1.1 Impact of link length on d4

Figures 5.4 to 5.9 show the variation of d4 with link length for different g/c ratios, and offset values. The cycle length is 150 seconds at both upstream and downstream intersection. Different scenarios are generated by varying the offset and g/c ratios for both the upstream and downstream approaches. d4 experienced by vehicles at the upstream approach during the first cycle is the lowest among all cycles, and decreases with the increase of link length for each scenario. As noted earlier, during cycle zero the network is empty, i.e., there is no queue at the downstream approach, therefore the first cycle is the least congested and hence expected to have the least delay during the 15-minute analysis period. The assumption of an empty network prior to first cycle is only used to get some starting point for estimation of queue length. The d4 model will work equally well if the queue was greater than zero for the cycles before the first one. For example if the first two cycles are ignored and the analysis period begins with the third cycle then in this scenario the system already reached equilibrium and the d4 remain the same for all the cycles, as shown in figure 5.4a.

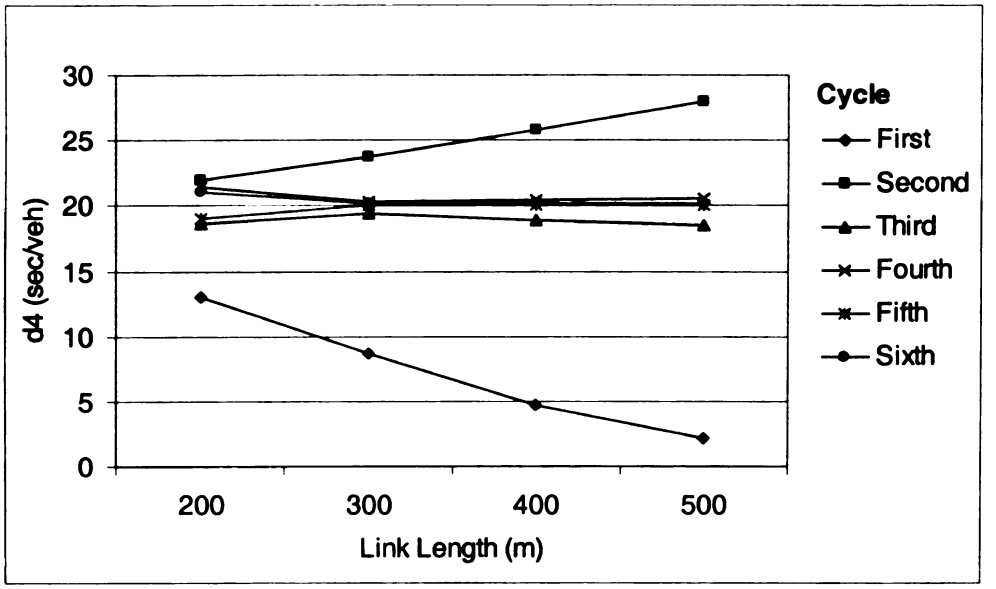

Figure 5.4 Variation of d4 with link length (g/c for upstream and downstream are 0.8 and 0.6, respectively; offset 0 seconds; and cycle length is 150 sec)

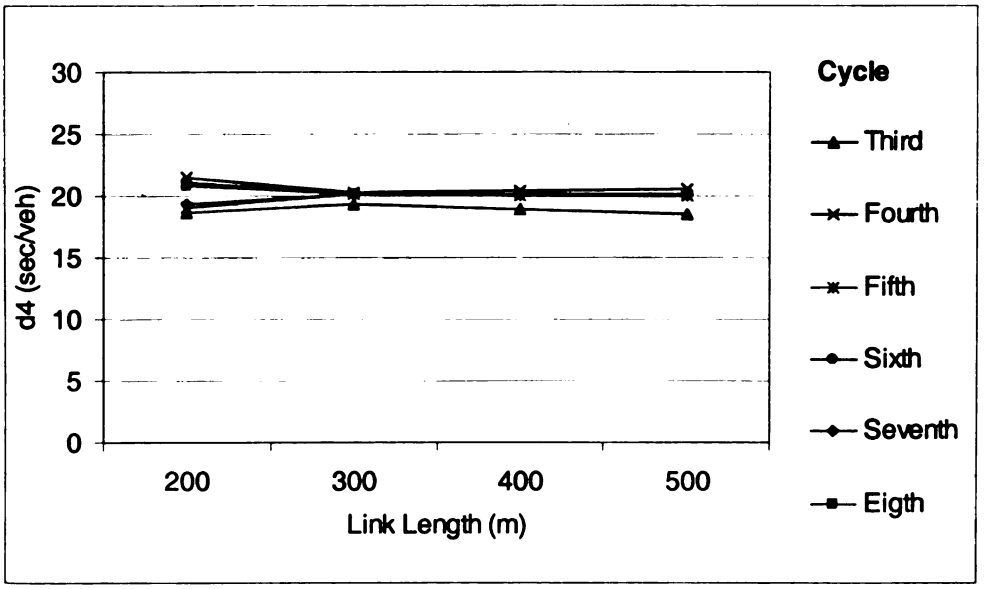

Figure 5.4a Variation of d4 with link length (g/c for upstream and downstream are 0.8 and 0.6, respectively; offset 0 seconds; and cycle length is 150 sec) (Analysis period starts at third cycle)

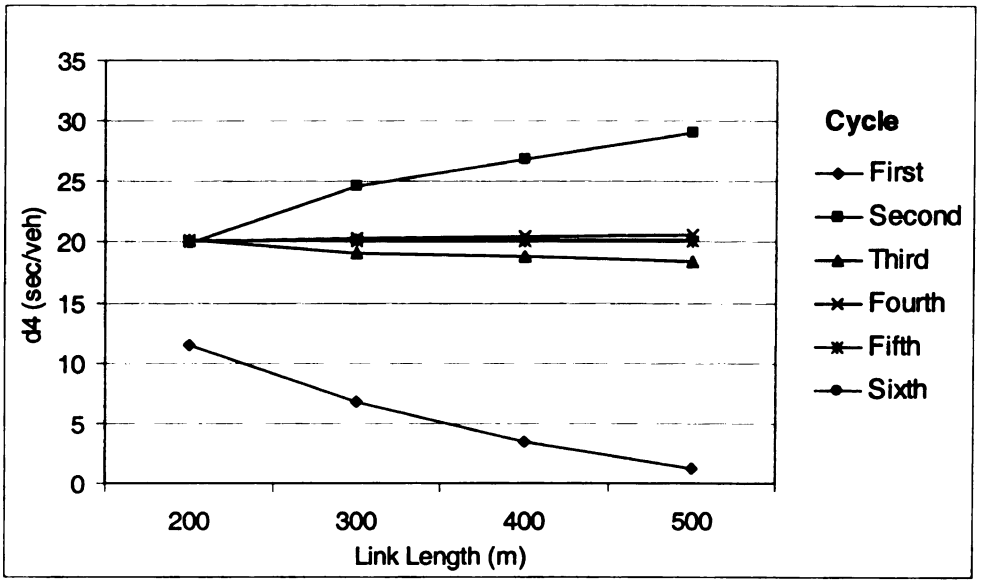

Figure 5.5 Variation of d4 with link length (g/c for upstream and downstream are 0.8 and 0.6, respectively; offset 10 seconds; and cycle length is 150 sec)

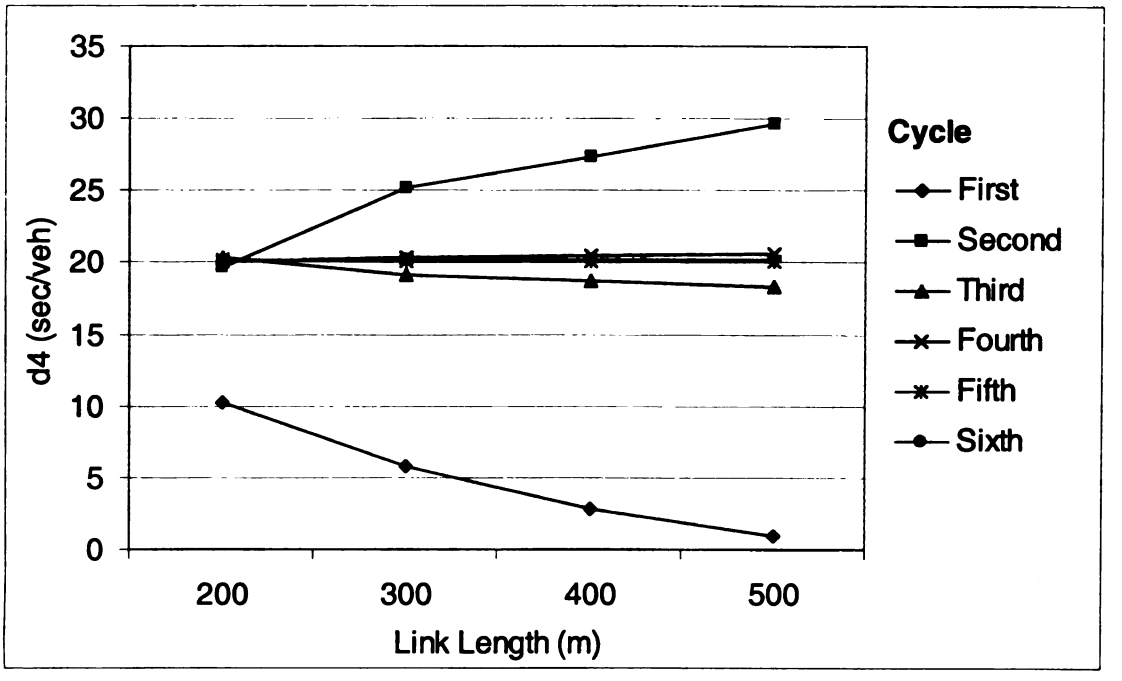

Figure 5.6 Variation of d4 with link length (g/c for upstream and downstream is 0.8 and 0.6, respectively; offset 15 seconds; and cycle length is 150 sec)

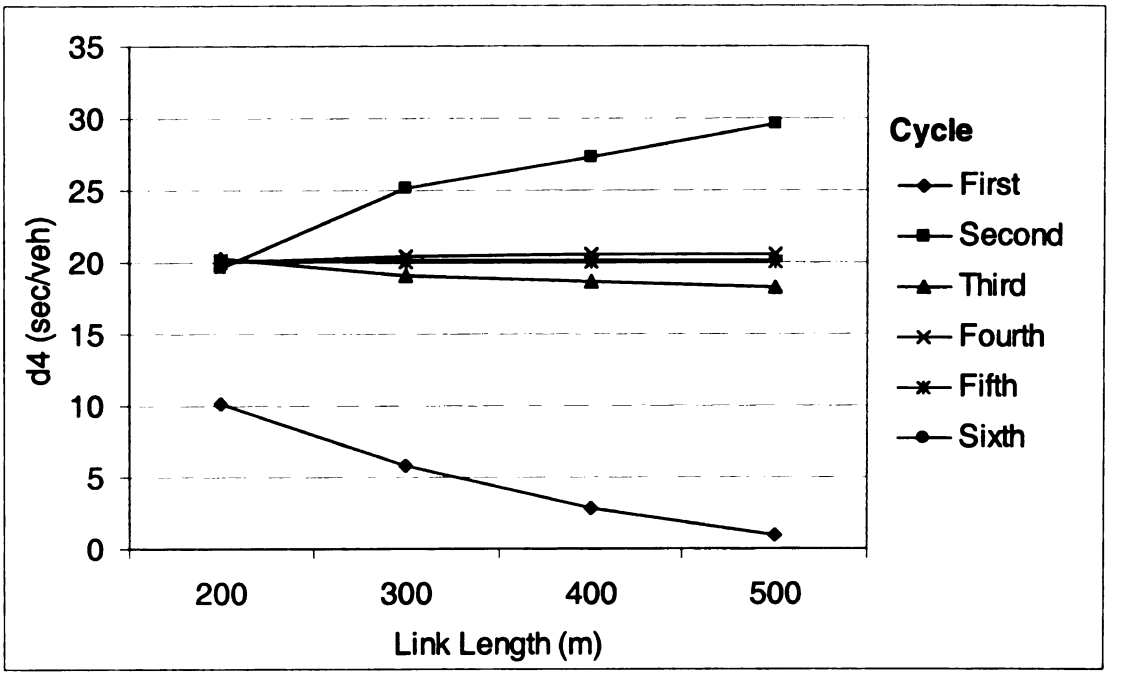

Figure 5.7 Variation of d4 with link length (g/c for upstream and downstream are 0.8 and 0.6, respectively; offset 20 seconds; and cycle length is 150 sec)

An increase in link length provides more space at the downstream link for vehicles arriving from the upstream approach during the first cycle, which increases the throughput from the upstream approach and decreases d4 value. Trends of d4 values during first cycle and second cycle are opposite of each other; the second cycle delay increases with increase in link lengths while the delay of first cycle decrease. The reason for this is that the second cycle in each scenario has the maximum queue length at the downstream approach (see figures5.2 and 5.3). The queue is maximum at the beginning of cycle 2 because of a high discharged volume from the upstream approach during the fist cycle. This leads to the second cycle being the most congested cycle for the 15-minute analysis period. Therefore, during the second cycle, vehicles at the upstream approach experienced highest d4 value as compared to other cycles. Note that the results for the first and second cycles are only valid for the given system and conditions

assumed. If cycle zero is not considered empty and we know the length of queue at downstream approach, then first and second cycle will behave similar to the other cycles. As noted earlier, starting with an empty link (0 queue length) at the beginning of cycle one was just one of many other possible starting conditions.

For cycles three and beyond, the system reaches equilibrium and the value of d4 does not change significantly with the increase of link length. Figures 5.4 through 5.7 show the results for scenario 1 when the g/c ratios are 0.8 and 0.6 for upstream and downstream approaches, respectively, whereas figures 5.8 and 5.9 show the results for the scenario 2 when the g/c ratio are 0.9 and 0.6 for the upstream and downstream approaches, respectively, (this is a more congested conditions). As observed, there are some differences in the trends of d4 with link length between these scenarios. In general, increasing the g/c ratios of the upstream approach allows more vehicles to enter downstream link, while reducing or maintaining a constant g/c ratio at the downstream approach contribute to the increase of congestion at the downstream link. Due to comparatively higher congested conditions, d4 values are higher for each cycle of scenario 2 (figures 5.8 and 5.9) when compared to those for scenario 1 (figures 5.4 through 5.7). Also, for both scenarios, the trends of d4 values for the first and second cycle are similar. However, the d4 values for cycles three and beyond show different trends for both scenarios, as explained next.

In the first scenario, cycles three and beyond are insensitive to the link length and the d4 values for those cycles remains relatively stable for different link lengths. Whereas in the second scenario, the d4 values in cycles three and beyond are sensitive to link length up till some link length (400 m in this case). Beyond this link length, the d4 values

of cycles three and beyond remain relatively stable while the d4 values of cycle keep increasing with higher link lengths and those of cycle 1 keep decreasing with link length.

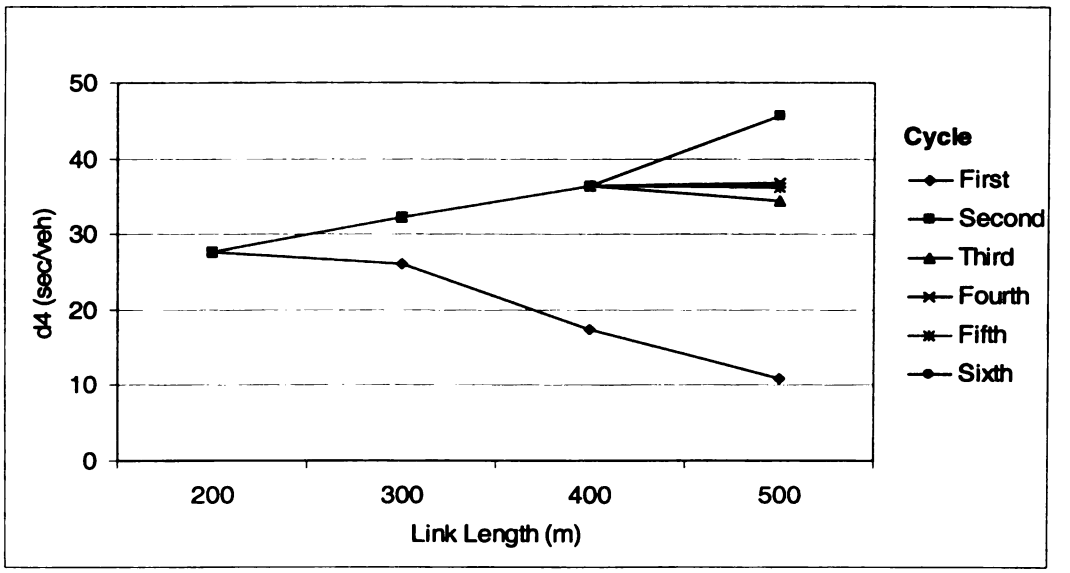

Figure 5.8 Variation of d4 with link length (g/c for upstream and downstream are 0.9 and 0.6, respectively; offset –15 seconds, and cycle length is 150 sec)

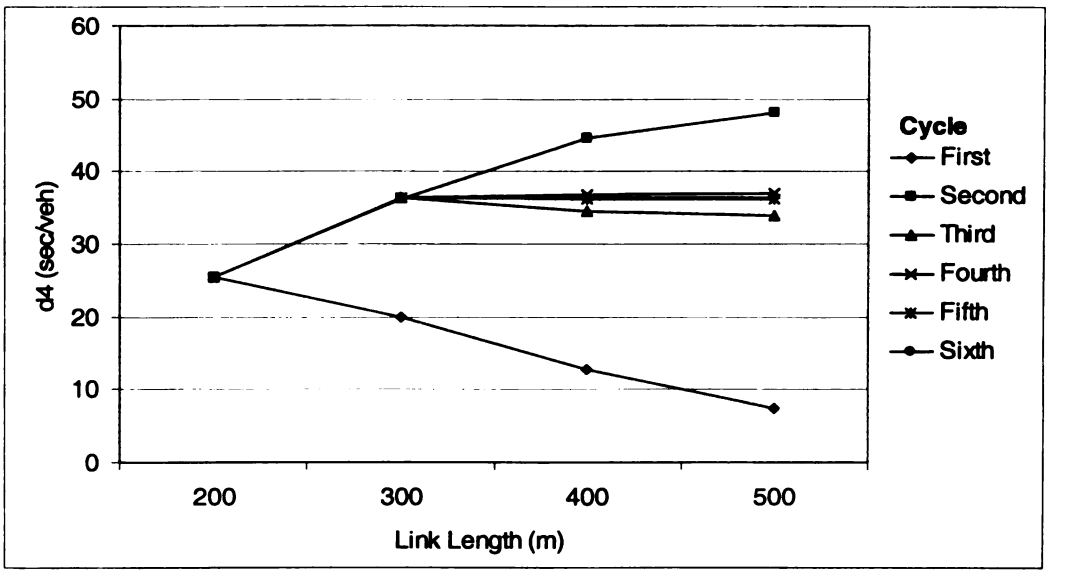

Figure 5.9 Variation of d4 with link length (g/c for upstream and downstream are 0.9 and 0.6, respectively; offset 0 seconds, and cycle length is 150 sec)

5.3.1.2 Impact of offset on d4

Figures 5.10 to 5.13 show the variation of each cycle's d4 with the offset for various link lengths, and different g/c ratios at upstream and downstream approaches. The first cycle has minimum value of d4 for all offsets. The reason for this is already given in the previous section, i.e., the network is assumed to be empty for the cycle that precedes first one (cycle zero). Figures 5.10 through 5.12 show that d4 for the first cycle decreases with the increase in offset for the range –10 to 25 seconds and then starts increasing.

Shorter offsets mean that the upstream green starts after or soon before the downstream green. For these offsets, there is higher probability of wasted green at the downstream approach during the first cycle. Wasted green time at the downstream approach will reduce the traffic output from the downstream approach, which means longer queues at the end of the cycle and hence higher chance of blockage at the upstream approach. Note that this trend is true only for the first cycle, since the preceding cycle had no queue at the downstream approach. An opposite trend is observed for the second cycle. Here, there are already queued vehicles on the downstream link, so shorter offsets perform better than longer ones. In this case, shorter offsets will give more chance for the downstream queued traffic to clear the downstream approach before new traffic starts arriving from the upstream subject approach. Therefore, the d4 increases with increase in offset up to a certain limit.

For offsets greater than 25 sec for the scenarios shown in figures 5.10 to 5.12, vehicles arriving from the upstream approach reach the downstream approach during the red of the first cycle at the downstream approach. This causes an increase in the queue length and a decrease in the average speed at the downstream approach. These factors

contribute to the increase of d4 at the upstream approach during the first cycle. The trend, however, will reverse for higher offsets as more vehicles start arriving on green.

Figure 5.13 shows the results for the condition for which the spacing between upstream and downstream intersections is 500m, whereas for the previous scenarios the link lengths were 300 m (figures 5.10-5.11) and 400 m (figure 5.12). Figure 5.13 shows that d4 keeps on decreasing for the first cycle with the increase of offset because vehicles arriving from the upstream approach still reach at green due to the higher value of link length. So for the first cycle the combination of higher offsets and long link length creates a favorable condition for queues not to form on the downstream link and hence there are fewer prospects for d4 to occur. An opposite trend is observed for the second cycle, and that is because of the higher discharged volume during cycle one.

For third and higher cycles, the system has reached an equilibrium state and conditions at the downstream approach started replicating. With fixed signal timing at both approaches and continuous traffic demand at the upstream approach, d4 during the last four cycles became insensitive to offset. However, reaching an equilibrium state, under certain combination of link length and g/c ratios, will occur at different offsets. And before this equilibrium state is reached the values of d4 will be oscillating up and down between successive cycles (see for example figure 5.10 for offsets below -10 sec, and figure 5.11 for offsets below zero sec). This oscillation is a consequence of the cyclic increase and decrease of discharged traffic from the upstream approach.

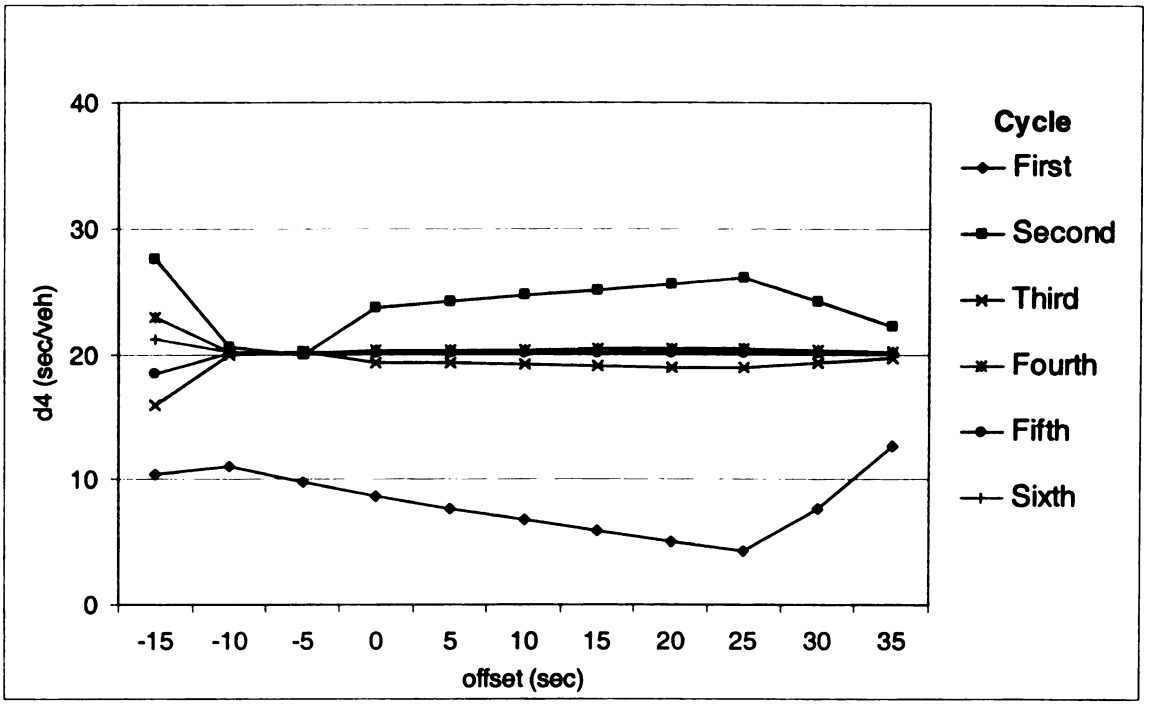

Figure 5.10 Variation of d4 with offset for different cycles (g/c for upstream and downstream are 0.8 and 0.6, respectively; and link length is 300m)

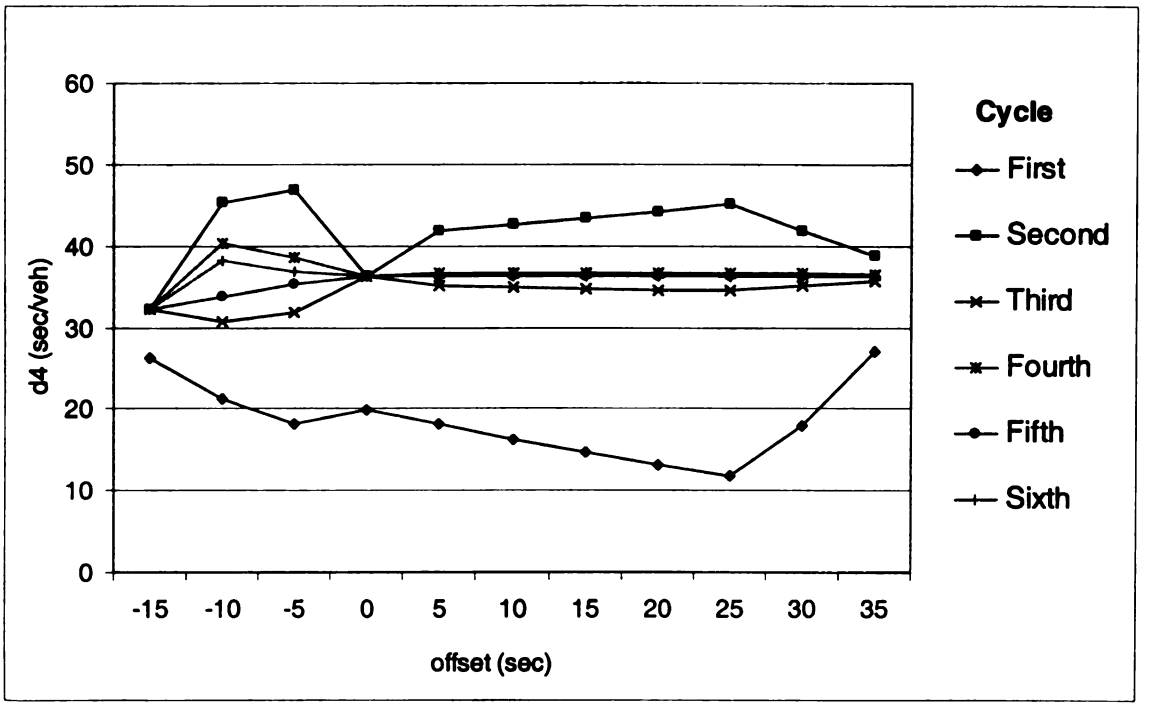

Figure 5.11 Variation of d4 with offset for different cycles (g/c for upstream and downstream are 0.9 and 0.6, respectively; and link length is 300m)

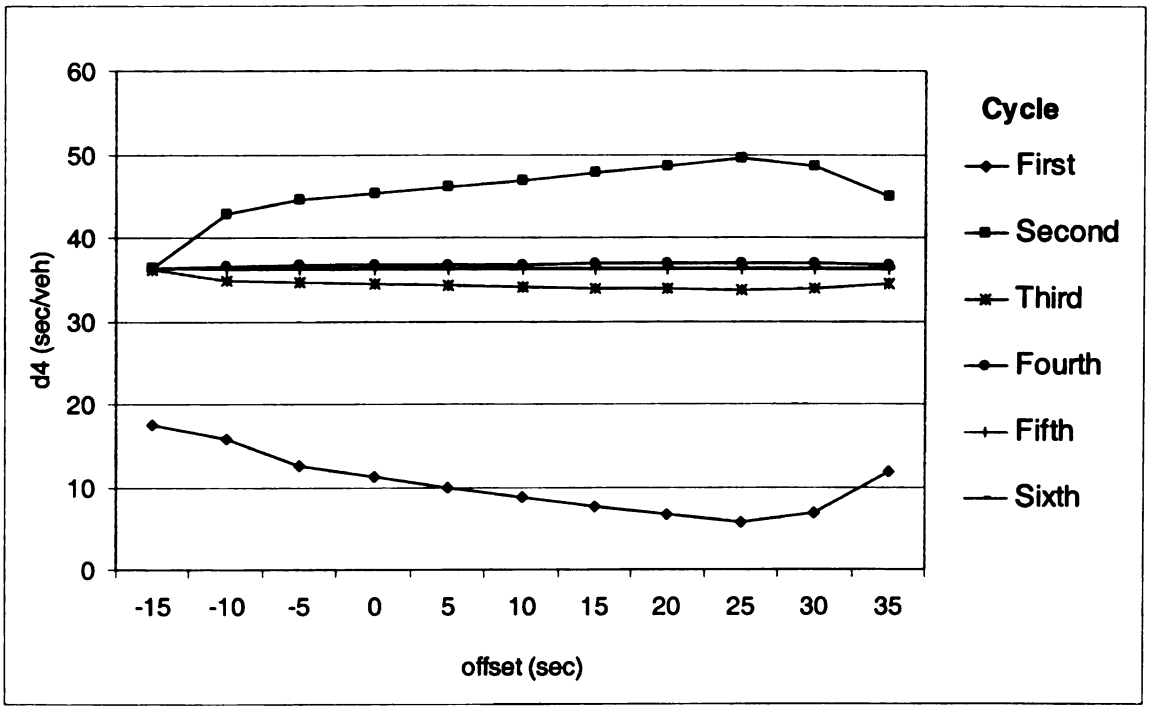

Figure 5.12 Variation of d4 with offset for different cycles (g/c for upstream and downstream are 0.9 and 0.6, respectively; and link length is 400m)

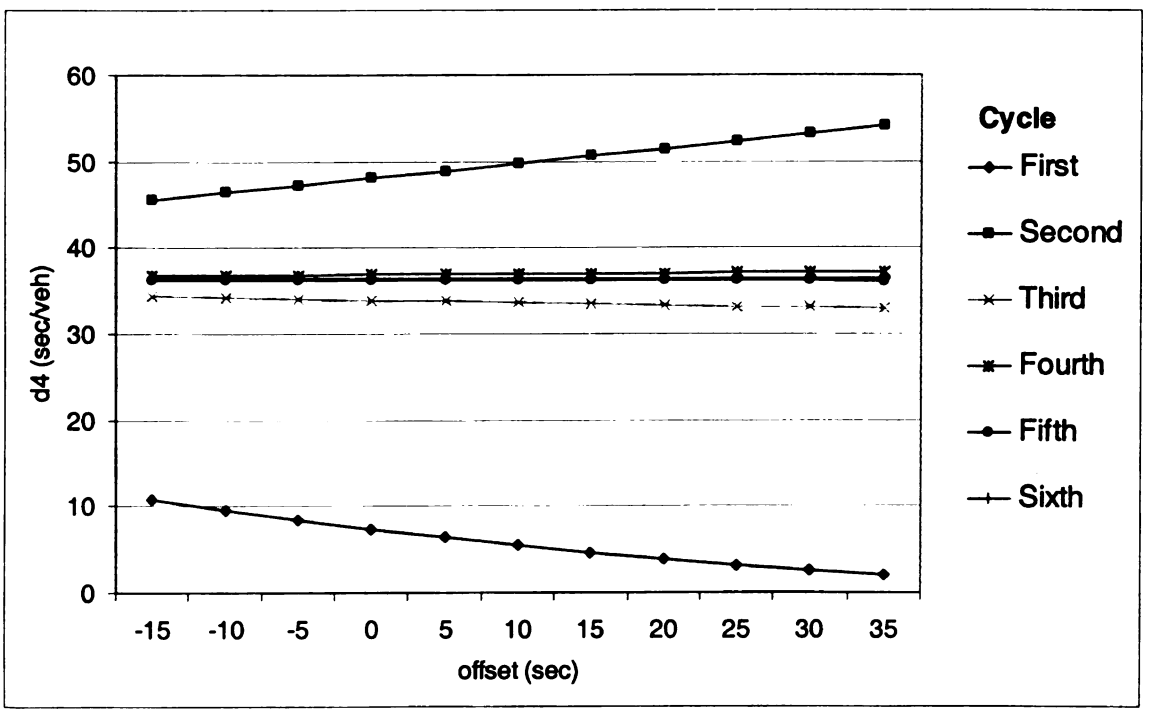

Figure 5.13 Variation of d4 with offset for different cycles (g/c for upstream and downstream are 0.9 and 0.6, respectively; and link length is 500m)

5.3.1.3 Impact of g/c ratio of upstream and downstream approaches on d4

Figures 5.14 through 5.18 show d4 for each cycle as it changes with change in g/c for the upstream and downstream approaches. As the g/c ratio of upstream approach increases and that of the downstream approach decreases, the value of d4 increases for each cycle. This trend is as expected. By increasing the g/c of upstream approach, more vehicles are fed into the downstream link and at the same time a decrease of g/c for the downstream approach reduces the traffic output from downstream approach. All of these factors contribute to the increase of congestion at the downstream link which then leads to an increase in d4 at the upstream approach. Higher g/c values for the upstream approach are used as compared to the downstream approach because that inequality creates congested conditions at the downstream link and leads to higher probability of getting a high d4 value. For uncongested scenarios, for example, when the upstream approach g/c ratio is 0.73 and the downstream approach g/c ratio is 0.67, d4 is almost negligible.

The trends of each cycle are consistent with the previous results. The least amount of d4 is observed by vehicles at the upstream approach during the first cycle, whereas d4 is maximum during the second cycle. Contrary to the impact of offset and link length, d4 experienced by vehicles during the last three or four cycles is sensitive to the g/c ratio of the upstream and downstream approaches. As compared to the impact offset and link length, the g/c ratios of the upstream and downstream approaches have greater impact on the downstream link congestion. Therefore, d4 varies significantly with change in g/c ratios of the upstream and downstream approaches.

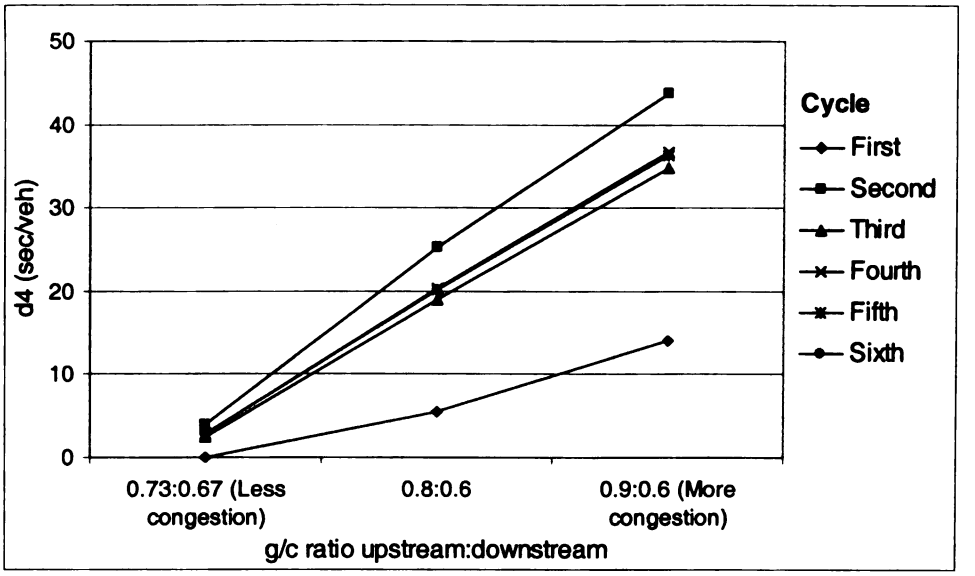

Figure 5.14 Variation of d_4 with g/c ratios of upstream and downstream (link length 400m and offset –5 sec)

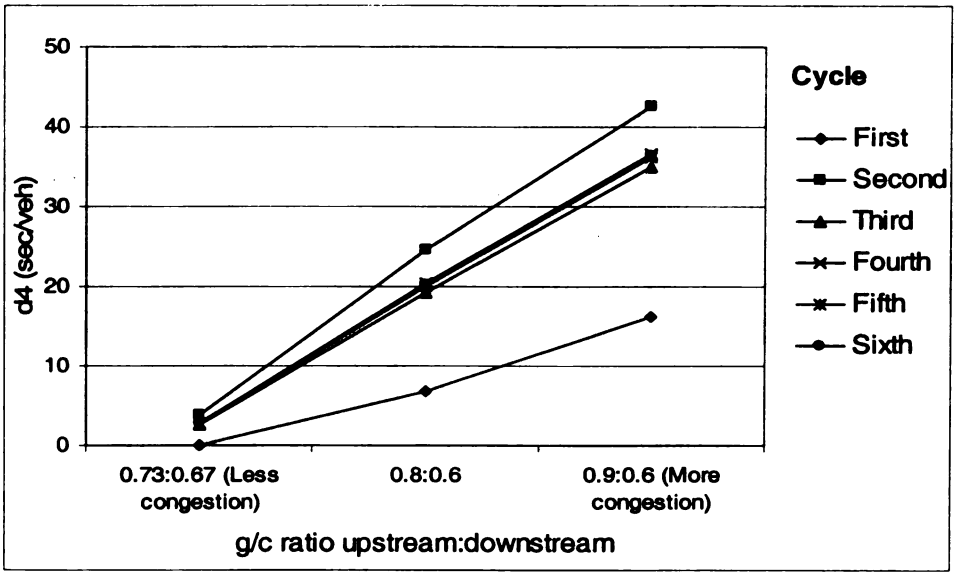

Figure 5.15 Variation of d_4 with g/c ratios of upstream and downstream approaches (link length 300m and offset 10 sec)

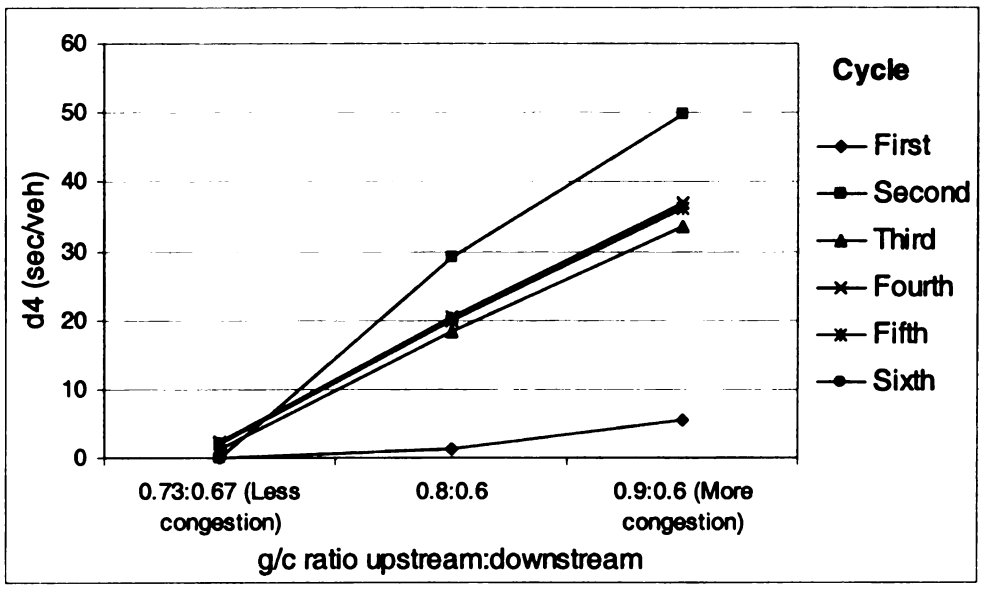

Figure 5.16 Variation of d_4 with g/c ratios of upstream and downstream (link length 500m and offset 10 sec)

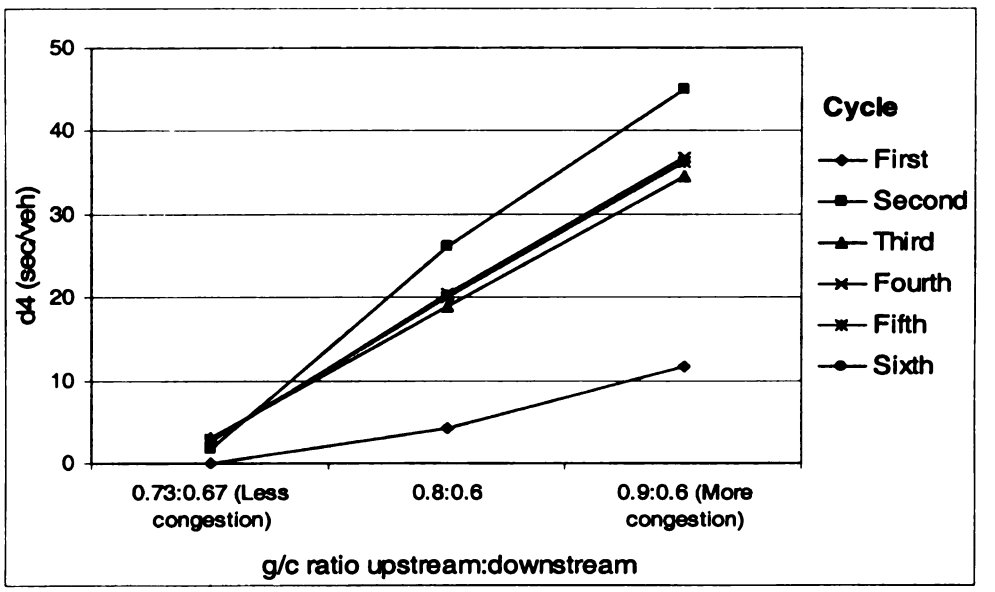

Figure 5.17 Variation of d_4 with g/c ratios of upstream and downstream (link length 300m and offset 25 sec)

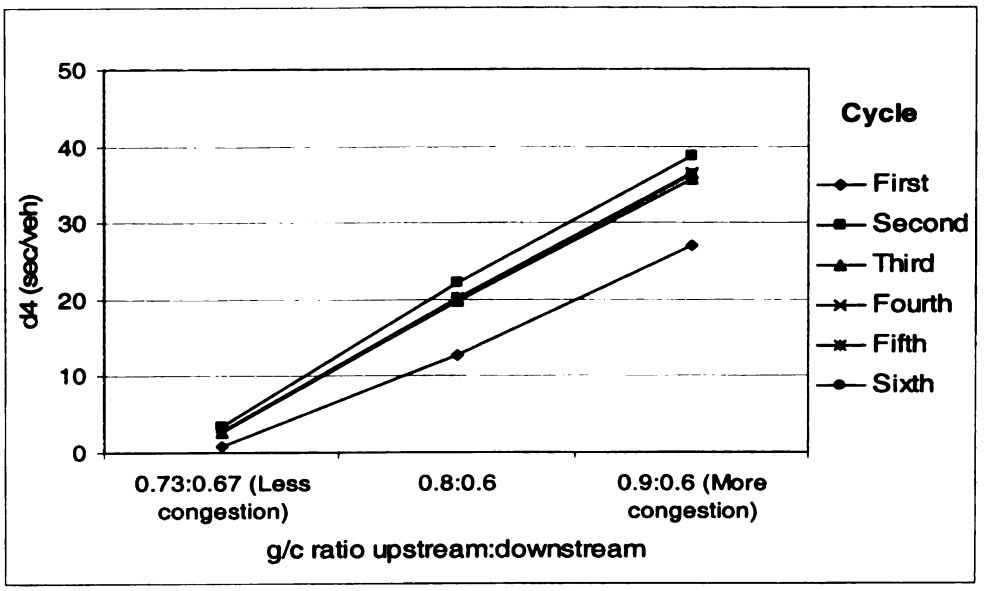

Figure 5.18 Variation of d_4 with upstream and downstream approaches g/c ratios (link length 300m and offset 35 sec)

For the lowest g/c ratio difference, the difference in d4 between different cycles is negligible. This is so because for this condition the arriving traffic from the upstream approach is not enough to cause congestion and blockage (hence small d4 values). However, for the larger g/c ratio difference, the number of vehicles fed into the downstream link from the upstream approach is higher and hence we expect relatively higher values of d4. In addition to that there is an oscillation between higher volumes fed into the downstream link followed by lower volumes. This leads to parallel oscillation in the queue length, which in turn leads to higher oscillating d4 values.

In figure 5.16, d4 for the first cycle is increasing with the increase in the value of the g/c ratios but at a gentler rate than other scenarios. This is due to the longer link length which tends to reduce the impact of the queue. This result is consistent with the trend shown in figure 5.13 for cycle 1.

5.4 Average value of d4 for 15-minute analysis period

Section 5.3 presented the results and sensitivities of d4 on a cycle-by-cycle basis. Here, the average value of d4 from all cycles in a 15-minute period is evaluated. The 15-minute analysis period is used to make the d4 value compatible to HCM 2000 methodology to estimate control delay. The downstream-induced delay and incurred by the upstream approach, d_4, is calculated for each cycle that occurs during 15-minute time interval and is then averaged using equation 5.1.

$$\text{Average } d_4 \text{ for the subject approach} = \frac{d_{(4)c_1} + d_{(4)c_2} + d_{(4)c_3} + \ldots\ldots\ldots + d_{(4)c_n}}{C_n} \quad (5.1)$$

Where

$d_{(4)c1}$ = d4 experienced by vehicles at the upstream approach during the first cycle

$d_{(4)cn}$ = d4 experienced by vehicles at the upstream approach during the n^{th} cycle

C_n = Total number of cycles in a15-minute time interval

The following sections present the impact of geometric, traffic flow characteristics, and control parameters of upstream and downstream approaches on the average value of d_4 based on a 15-minute analysis period.

5.4.1 Impact of link length on average d4 value

Figures 5.19 and 5.20 show the variation of the ratio of queue length to link length and the average d4 versus link length. The downstream-induced delay, d4, depends on the length of the queue at the downstream link as well as on the remaining space on the downstream link; therefore the ratio of the queue length to the link length is used to account for both. The queue length to link length ratio (L_1/L) varies from 0 to 1. One means the whole link is filled with vehicles and there is no remaining space; 0 means the

link is empty. Higher values of this ratio indicate more congestion on the downstream link.

The downstream-induced delay, d4, decreases with increase of link length for the same conditions, as shown in figures 5.19 and 5.20 (i.e. all other parameters were kept constant, e.g. offset, g/c ratio at upstream and downstream approaches). The decrease in average d4 value is not dramatic for longer link length as shown in figures 5.19 and 5.20. For example figure 5.19 shows that the average d4 value changes from 35sec/veh to 33sec/veh for 300 m link length change (i.e., from 200m to 500 m). It is obvious that longer link length means more empty space is available for vehicles arriving from the upstream approach and hence there is less probability of getting a completely filled downstream link, which is the main cause for d4 at the upstream approach. But for this case we are assuming there is continuous traffic demand at the upstream approach, so by increasing link length, we are providing more space for vehicle arriving from the upstream approach which in turns increase the discharge volume from the upstream approach and leads to more congested downstream link. If the discharged volume from the upstream approach is kept constant then longer link length will significantly reduce the average d4 value for at the upstream approach. This statement is also verified by the results of microscopic simulation presented in chapter 6. Figure 5.19 shows higher values of d4 at the upstream approach as compared to figure 5.20, for same link length, because the difference between the g/c ratios of the upstream and downstream approaches is greater for the scenario shown in figure 5.19.

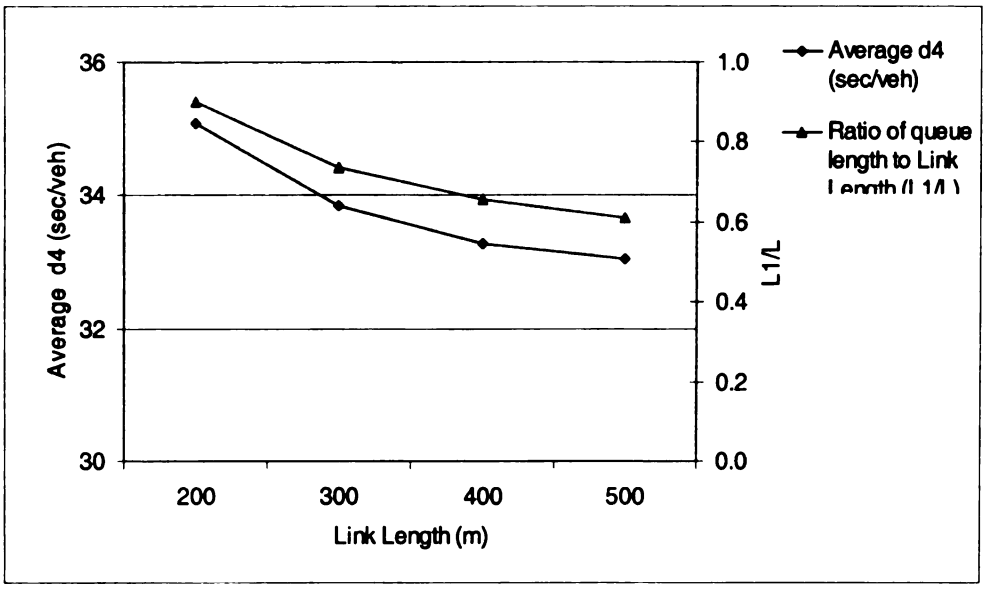

Figure 5.19 Variation of ratio of queue length to link length and average d_4 with link length (g/c for upstream and downstream are 0.9 and 0.6, respectively; offset 10sec, and cycle length 150 sec)

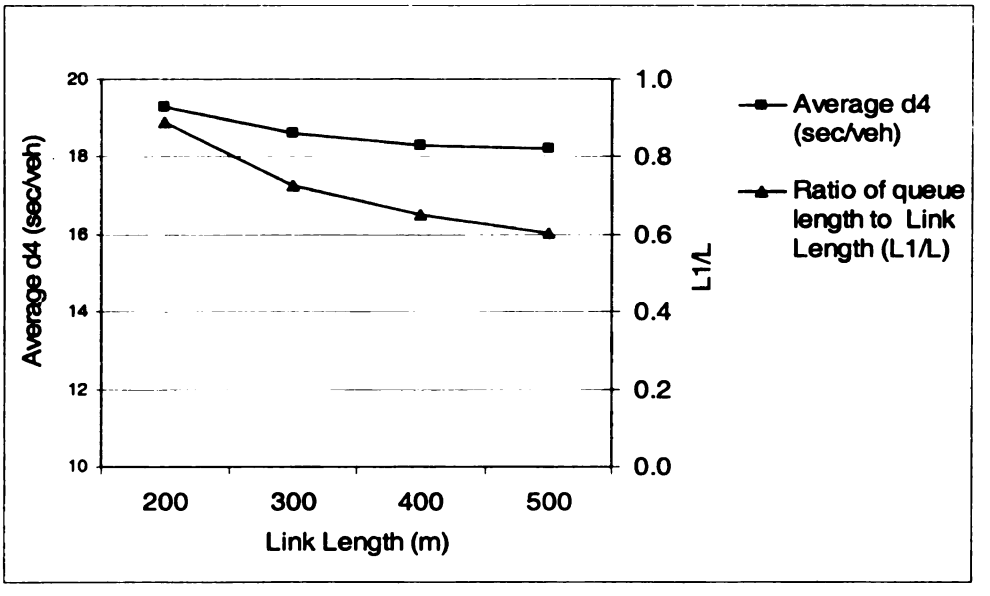

Figure 5.20 Variation of ratio of queue length to link length and average d_4 with link length (g/c for upstream and downstream are 0.8 and 0.6, respectively; offset 5sec, and cycle length 150 sec)

5.4.2 Impact of g/c ratio of upstream and downstream approaches on average value of d4

Figures 5.21 and 5.22 show the effect of the g/c ratios of the upstream and downstream approaches on d4 and the queue length to link length ratio to the downstream link for two scenarios. All other control parameters were kept the same. For the first scenario, shown in figure 5.21, the distance between the upstream and downstream intersections is 300m, cycle length is 150 sec, and the offset is -10 sec whereas for the second scenario the link length is 200 m, the offset is 20 sec and the cycle length is the same as the first scenario, i.e., 150 sec.

Three combinations of upstream and downstream approaches g/c ratio are used to demonstrate trends in the downstream-induced delay, d4, for congested and uncongested conditions. A g/c ratio combination of 0.73:0.67 creates uncongested condition whereas a g/c combination of 0.8:0.6 and 0.9:0.6 both create congested conditions. It is assumed that there is continuous traffic demand waiting at the upstream approach.

The values of d4 and L_l/L ratio are directly proportional to the difference between the g/c ratios of the upstream and downstream approaches. This trend is as expected. The increase of g/c at the upstream approach relative to the downstream approach allows more vehicles to enter the downstream link during each cycle, increases the probability of getting longer queues (and congestion) at the downstream link. This, in turn, leads to higher values of d4 for the subject approach at the upstream intersection.

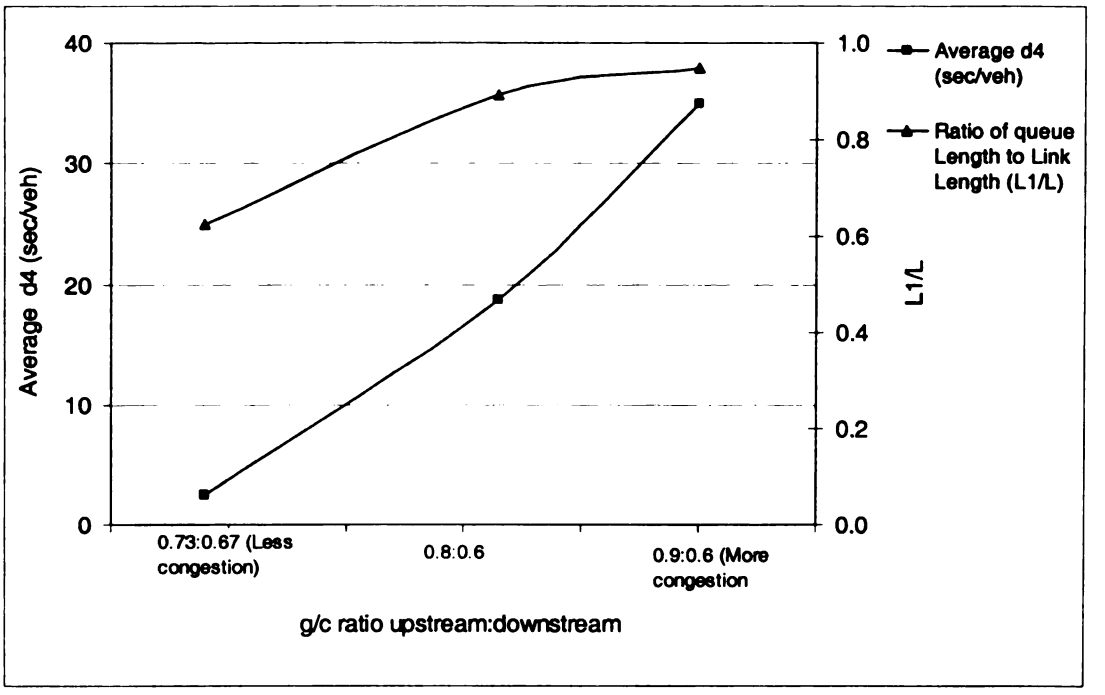

Figure 5.21 Variation of average d_4 with g/c ratios of upstream and downstream approaches (offset –10 sec, link length 300m, and cycle length is 150 sec)

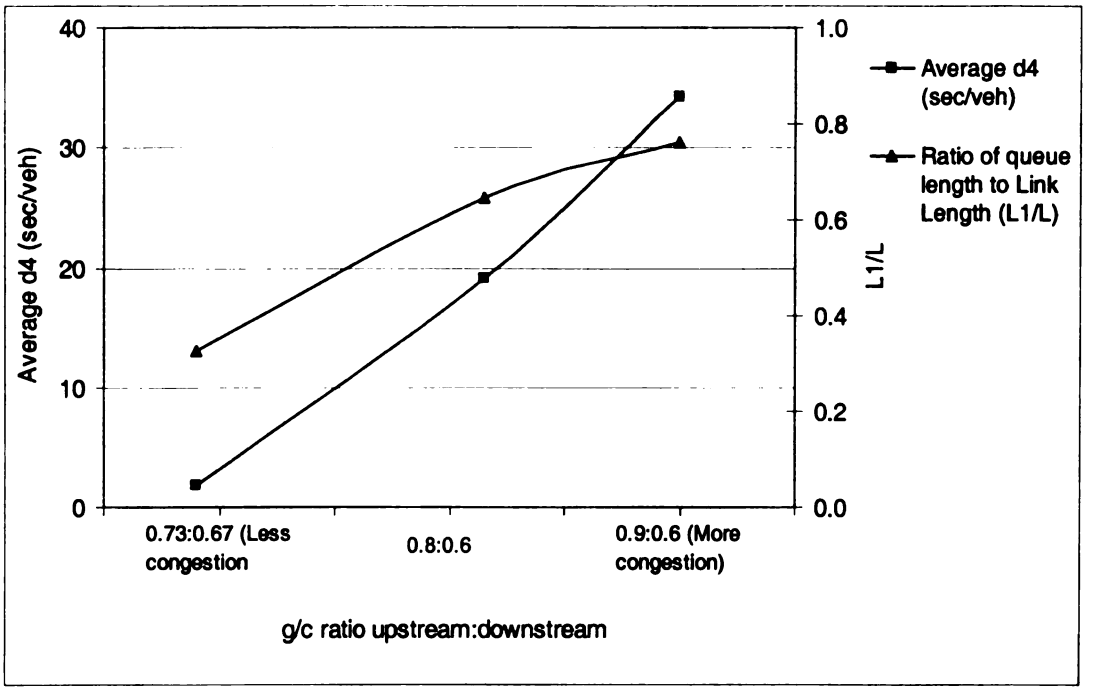

Figure 5.22 Variation of average d_4 with g/c ratios of upstream and downstream approaches (offset 20 sec, link length 200m, and cycle length is 150 sec)

5.4.3 Impact of offset on average value of d4

Figure 5.23 shows the impact of offset on the average values of d4 for three different conditions; First, an uncongested condition, when g/c ratios are 0.73 and 0.67 for the upstream and downstream approaches, respectively. For this scenario, the average value of d4 is insensitive to the offset. The reason for that is there is not enough traffic arriving from the upstream approach into the downstream link to create blockage at the upstream approach. In this case, it does not matter what the offset value is if there is not enough incoming traffic to make the downstream link congested. The second and third conditions are congested, where g/c ratios for the upstream approach are 0.8 for both conditions and the g/c ratio for the downstream approach are 0.6 and 0.5 for second and third conditions respectively. In these two cases, the value of the average d4 at the upstream approach increase with increase in offset, but the magnitude of change is different for the two g/c ratio combinations. The reason is that reducing the g/c ratio at the downstream approach (from 0.6 to 0.5) creates more congestion on the downstream link and, therefore there is a higher probability of getting higher d4 values for the upstream approach.

The rate of change of d4 versus offset and the point where d4 becomes insensitive to the offset are not the same for the two congested conditions. For the most congested conditions the value of d4 keeps increasing up to the offset value of 10 seconds and for the other less congested condition that offset value is 0 seconds. The reason for this is that after those offset values, the conditions at the downstream approach (i.e., queue length and average speed at link) start replicating regardless of offset, therefore the average d4 value become insensitive to the offset. Replication of traffic conditions at the downstream approach start because of the fixed signal timing at both approaches and the continuous traffic demand at the upstream approach. The other observation is that for the

most congested condition, the point where d4 becomes insensitive to the offset is a higher offset value as compared to other less congested condition. The reason of this is the lower discharge volume from the downstream approach (i.e., g/c at downstream approach is 0.5 as compared to 0.6), due to which downstream reach equilibrium state at higher offset value as compared to less congested condition. The rate of change of d4 with offset is consistent with the cycle by cycle d4 variation as shown in figures 5.10 to 5.13.

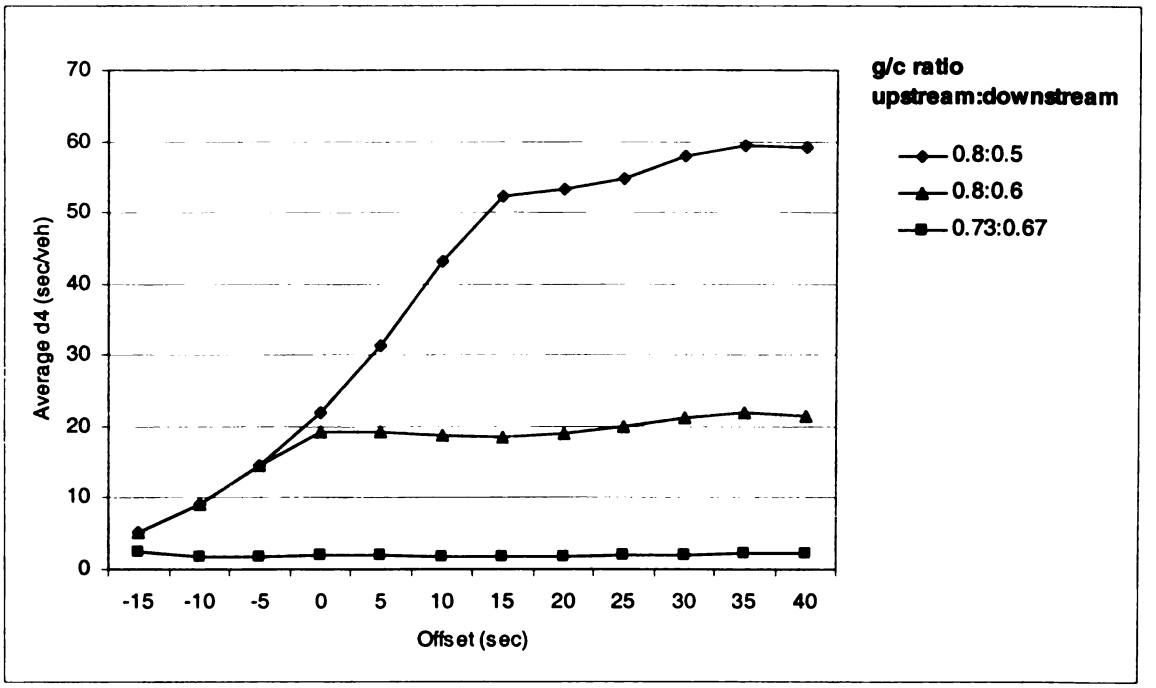

Figure 5.23 Variation of average d_4 with offset (link length is 200m, cycle length 150 sec)

Shorter offsets indicate that the upstream green starts after (negative values) or soon before (positive values) the downstream green, in which cases there is a lower likelihood that the upstream arriving vehicles will be blocked, or, if blocked, the duration of blockage will be shorter. For the cases of longer offsets, the green at the upstream approach starts much earlier than the green at the downstream approach. Thus the chance

for traffic to arrive downstream, stop and then spillback is greater (since the green at the downstream approach does not start soon enough).

5.5 Summary of sensitivity analysis of d4 model

The following points summarize the findings of this chapter

- The amount of d_4 depends on signal control and coordination parameters
- d_4 changes with each cycle and reaches equilibrium once traffic flow, downstream queues, and signal control measures stabilize and start replicating over cycles
- The amount of d4 experienced by the vehicles at the upstream approach during the current cycle depends on the traffic flow conditions in the preceding cycle
- d4-model can be applied in a system of multiple signalized intersections. In this case the value of d4 increases in opposite direction of flow. For example for the system shown in figure 4.1, intersection 0 has the highest value of d4 for the eastbound approach as compared to other intersection eastbound approaches
- The g/c ratios at upstream and downstream approaches have significant effect on d_4, as compare to the offset and link length
- An improper offset leads to higher d_4 particularly in congested congestions

CHAPTER 6

Validation of d4 model

6.1 Introduction

Computer simulation for transportation has been a valuable analysis tool for many applications, including the assessment of operations of transportation system. Microscopic simulation is used in this work for the validation of the d_4 model presented in chapter 4. This chapter first provides a brief introduction to various available simulation models and the methodology used for validation of the delay estimation models, which are presented in the previous chapter. Finally a comparison is presented between results from the microscopic simulation and those from the models derived in previous chapters.

6.2 Simulation models

Simulation is defined as a "Numerical technique for conducting experiments on digital computer, which may include stochastic characteristics and involve mathematical models that describe the behavior of a transportation system over extended periods of real time" (32). Computer simulation is becoming common in every field of study because it can simulate complex and costly scenarios without interrupting real life operations. In traffic engineering, simulation models are important tools for traffic control and are useful for analysis and evaluation of complex transportation systems and designs, which are difficult to create or implement in the real world. New designs and improvement alternatives can be evaluated by simulation without any disruption to traffic in a real network and can also avoid costly construction.

Traffic simulation suitability for use depends upon the logic of the models within the simulation program and the real world data, if any, that is used to calibrate the simulation program.

Traffic simulation models can be classified according to the level of detail with which they represent the behavior of units (vehicles or drivers) in the system, into three categories:

- Microscopic
- Macroscopic
- Mesocscopic

6.2.1 Microscopic simulation model

Microscopic simulation models represent vehicles individually with varying operational and driver's characteristics. Vehicle positions are updated using car-following logic and lane changing rules with appropriate stochastic components (for example, variability in driver behavior and vehicle dynamics is explicitly modeled). Microscopic models capture individual vehicle movements and speed characteristics as they pass a given point or traverse a short segment. For example, a lane-change maneuver at a microscopic level could invoke the car-following law for the subject vehicle with respect to its current leader, then with respect to its immediate leader and its follower in the target lane, as well as represent other detailed driver decision processes. Examples of traffic microscopic simulation models include INTRAS, CORSIM, PARAMICS, AIMSUN2, TRANSIMS, INTEGRATION, VISSIM, and MITSIM.

6.2.2 Macroscopic simulation model

In macroscopic simulation models, vehicle movement is based on analytical representation of traffic stream. These models describe entities and their activities and interactions at a low level of detail. No individual vehicles are modeled. For example, the traffic stream may be represented in some aggregate manner, such as a statistical histogram or by scalar values of flow rate, density and speed. Lane change maneuvers would probably not be represented at all; the model may assert that the traffic stream is properly allocated to lanes or employs an approximation to this end (33). Popular macroscopic simulation models include FREFLO, AUTOS, METANET

6.2.3 Mesoscopic simulation model

A mesoscopic model generally represents most entities at a high level of detail but describes their activities and interactions at a much lower level of detail than would a microscopic model (35). In mesoscopic simulation models, vehicles move at the prevailing speed in the section. The speed remains same for all the vehicles in the section and modified when a vehicle exits the section. Individual vehicles are modeled only for their route choice. DYNASMART and DYNAMIT are example of mesocscopic simulation models.

The choice of simulation model depends upon the purpose and scope of the study, measure of effectiveness and level of detail required. For example, if the model is used to analyze weaving sections, then a detailed treatment of lane-change interactions would be required, implying the need for a micro- or mesoscopic model. On the other hand, if the model is designed for freeways characterized by limited merging and no

weaving, describing the lane-change interactions in great detail is of lesser importance, and a macroscopic model may be the suitable choice.

The d_4 model developed in chapter 4, uses a macroscopic approach to estimate the additional delay induced by downstream disturbance on the upstream approach during each cycle. A microscopic model, therefore can be use to validate it. The microscopic model can be used to monitor movements of individual vehicles as they move, stop, and then move again either due to traffic or signal control. With proper experimental setup, it would be possible to isolate the impact of downstream congestion on upstream approach traffic and hence quantify the corresponding delay, which will equivalent to the macroscopic estimation. CORSIM (CORridor SIMulation Model) (36), a microscopic traffic simulation model, is used for the validation of the downstream induced delay, d_4, model. CORSIM is a well known microscopic simulation model in the USA. A number of studies were done to calibrate different parameters of CORSIM with real life data (38, 39).

6.3 CORSIM

CORSIM is a time based microscopic model with stochastic simulation of individual vehicles in traffic controlled urban networks and freeways. It is the component of the TRAF family of models that were developed by the US Federal Highway Administration (FHWA). The CORSIM traffic flow logic performs a full range of controls on vehicles traveling within specific lanes and responding to multiple control devices including fixed time and actuated traffic signals, related surveillance systems, yield and stop signs and ramp transitions (36). Vehicle flow is guided by car following rules, lane changing logic and other driver decision-making processes.

6.3.1 Support programs

Support programs for CORSIM include TSIS (Traffic software integrated system), and TRAFVU. TSIS is windows based modeling platform that provides menu driven access to CORSIM. TRAFVU is an interactive display post processor.

6.3.2 Simulation models

Two simulation models NETSIM and FRESIM are combined in CORSIM.

6.3.2.1 NETSIM

The NETSIM component of CORSIM is a program designed to simulate traffic operations for arteries, isolated intersections and networks. The NERTSIM component of CORSIM is limited to a maximum of 7000 internal nodes, 2000 links and 1000 actuated controllers, 99 bus stops and a maximum of seven lanes per approach with no more than two left and two right turn per approach. The maximum number of vehicles that may be accommodated is 20,000. CORSIM can model a maximum of five approaches per intersection. The size limits for FRESIM applications are higher.

6.3.2.2 FRESIM

FRESIM is one of two microscopic models of the CORSIM simulation package. Simulation is based on time scan with each vehicle status updated every second because of its microscopic and stochastic simulation (36). The run time of FRESIM is considerably slower than macroscopic programs such as FREFLO; FRESIM is designed to analyze operational improvements in freeway networks. FRESIM'S application may include one to five through lane freeway main lines with one to three lane ramps and one to three lane inter freeway connectors, variation in grade, radius of curvature and super elevation on the freeway.

6.3.3 Measure of effectiveness (MOE'S)

CORSIM can report a wealth of MOE's including different types of delay, queue time, stop time, and travel time, speeds, fuel consumption emissions, and other congestion-based measures. These MOE's are calculated by traffic movement and on a lane by lane basis for all intersection approaches.

6.4 Methodology for validation

Three steps were used to complete the validation of d4 and queue models: 1) Coding networks in CORSIM, 2) Check the significance of downstream disturbance on the upstream approach and quantification of additional delay using microscopic simulation, and 3) Validation of downstream induced delay, d4, model using microscopic simulations results.

6.5. Coding networks in CORSIM

Figures 6.1 and 6.2 show snapshots of TSIS and TRAFVU, respectively. All the inputs including volume, number of lanes, signal timing and other geometric characteristics are coded using TSIS. TRAFVU provides animated graphical representation of the traffic network performance, and enables the user to monitor the acceleration, speed, delay experienced by individual vehicles at any time.

For the purpose of validation, two types of networks are coded in CORSIM. One with an isolated signalized intersection and the other with two paired signalized intersections. Traffic volume, geometric properties, and control parameters are kept the same for both networks (for example, signal timing, phasing, traffic demand, number of lanes etc). The only difference between the two networks is that one network contains a single intersection and the other has two signalized intersections. The difference between

delays experienced by vehicles at the subject approach in the isolated signalized and paired signalized networks, will be compared to d4 from the d4 models developed in this research. Traffic and geometric characteristics of each network are explained in the following sections.

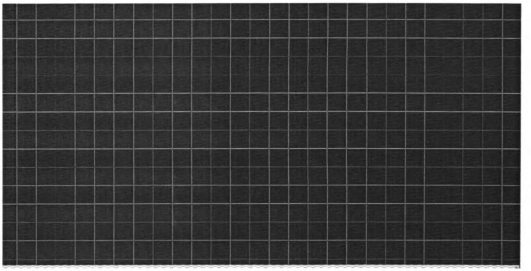

Figure 6.1 Snapshot of TSIS

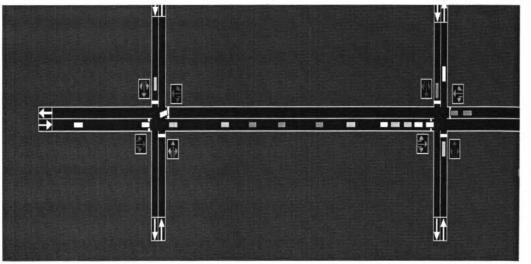

Figure 6.2 Snapshot of TRAFVU

6.5.1 Isolated signalized intersection network

Layout

Isolated intersection means that there is no downstream or upstream disturbance that can cause any interruption to the traffic flow in or out of the intersection. Figure 6.3 shows the layout and movements at the isolated signalized intersection and the subject approach for which control delay is to be calculated. Control delay is a delay caused by control devices, either by a traffic signal or a stop sign. The average control delay is estimated for each lane group and aggregated for each approach and for the intersection as a whole. Components of control delay were already explained in chapter 3.

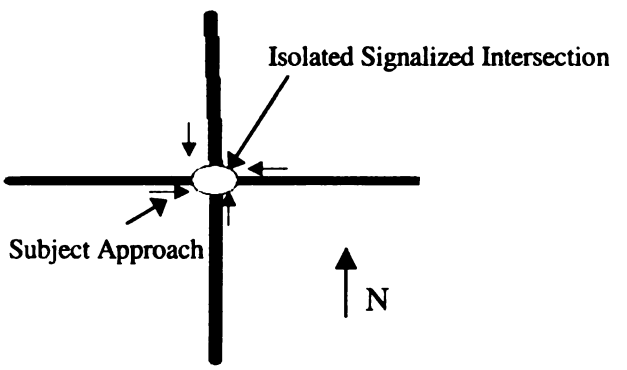

Figure 6.3 Isolated signalized intersection coded in CORSIM

Phasing

Figure 6.4 shows the phasing used for the signalized intersection. Simple two phase scheme was used, considering east-west as the major direction. The volume at the approach is kept such that there is always demand at the subject approach during the eastbound split. It is assumed that an infinite queuing space exists at the subject approach of the signalized intersection.

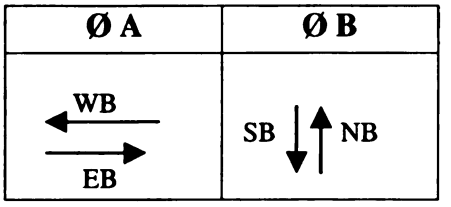

Figure 6.4 Phasing diagram of isolated signalized intersection

MOE observed

Control delay at the subject approach during each cycle was obtained from the CORSIM output. Different experiments were performed by varying signal timing (i.e. cycle length and green split). As discussed earlier, according to the HCM 2000, the analysis period for the calculation of control delay is 15 minutes. Therefore, all cycles that occurred during a 15-minute time interval were included in the calculation of control delay for each experiment. In the first experiment, ten independent runs were made to account for the expected natural variability of traffic data. The sample size needed to evaluate the simulation output with reasonable confidence was determined using the following equation.

$$n = \left(\frac{ts}{\varepsilon}\right)^2$$

Where

n = Required sample size

s= Standard deviation

ε = User specified allowable error

t = coefficient of the standard error of the mean that represents user specified probability level

With 3 sec/veh allowable error for control delay and a 95% confidence level, three runs were found to be sufficient. Therefore, three random runs were made for each of the experiments. Figure 6.5 shows the results of three independent runs for one experiment.

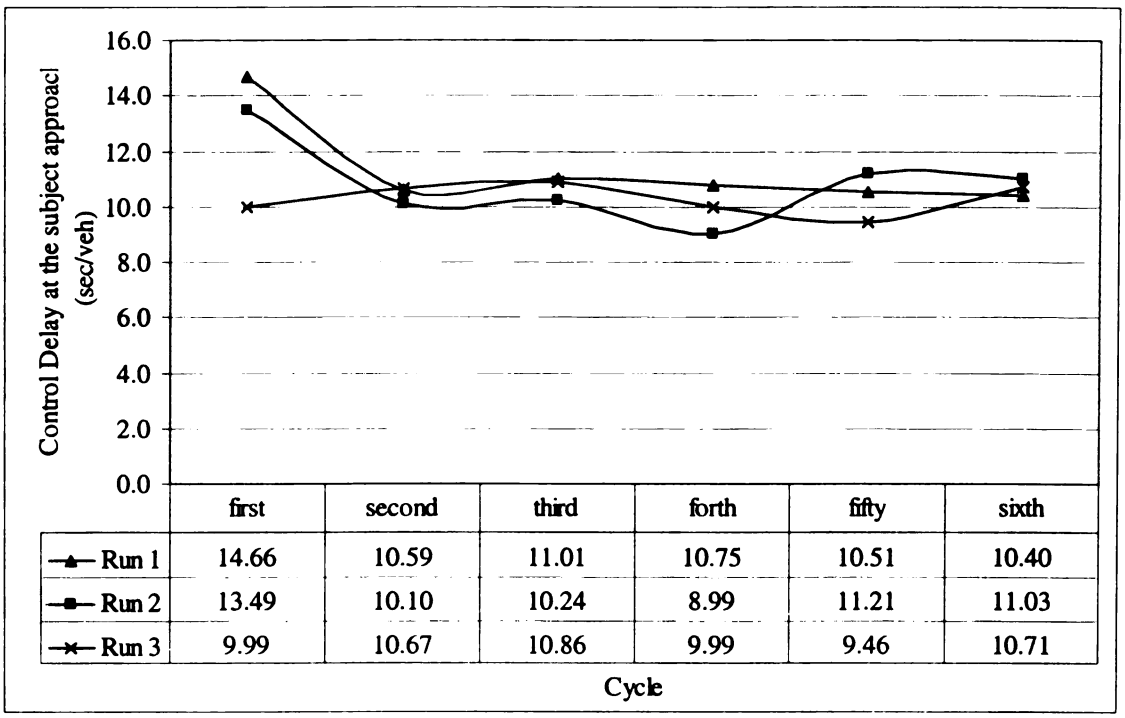

	first	second	third	forth	fifty	sixth
Run 1	14.66	10.59	11.01	10.75	10.51	10.40
Run 2	13.49	10.10	10.24	8.99	11.21	11.03
Run 3	9.99	10.67	10.86	9.99	9.46	10.71

Figure 6.5 Comparison of control delay from the individual runs for the isolated intersection

6.5.2 Paired signalized intersections network

Layout

In this network two closely spaced signalized intersections were coded in CORSIM. Figure 6.6 shows the layout of both signalized intersections and the subject approach for which control delay is to be calculated. "L" is the link length between the two intersections. It is assumed that an infinite queuing space exists at the upstream approach and a finite queuing space exists at the downstream approach.

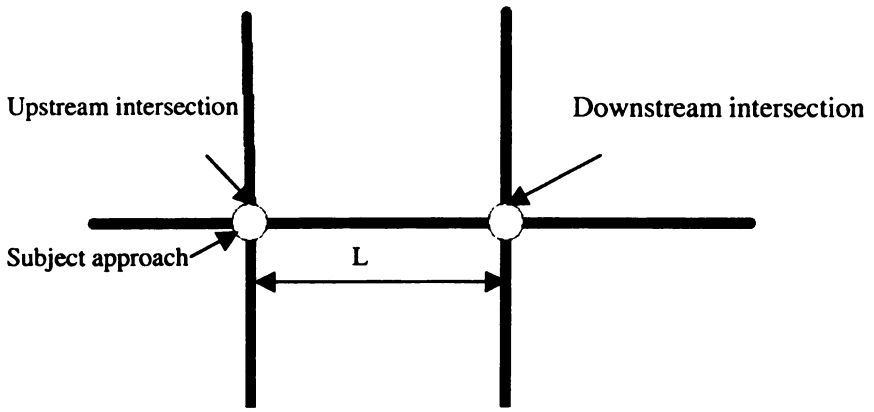

Figure 6.6 Paired signalized intersections coded in CORSIM

Phasing

Figure 6.7 shows the phasing used for both signalized intersections. Upstream intersection acts as the master intersection, and Phase A is the reference phase for the setting of the offset.

	Ø A	Ø B
Upstream Intersection	WB ← → EB	SB ↓ ↑ NB
	Ø A	**Ø B**
Downstream Intersection	WB ← → EB	SB ↓ ↑ NB

Figure 6.7 Phasing diagram of paired signalized intersections network

MOE observed

Control delay at the subject approach during each cycle and the queue length at the downstream link at the start of each cycle of the upstream intersection were observed. Similar to the isolated signalized intersection analysis, the required number of

independent runs was determined to be three for an allowable error of 3sec/veh of control delay and a 95% confidence level. A number of experiments were performed by varying the offset, link length, cycle length, and the g/c of the upstream and downstream approaches.

Note that the only difference between the two networks is that the isolated signalized intersection network consists of one signalized intersection whereas the paired signalized intersection network consists of two closely spaced intersections. All other parameters were similar for both networks. The premise is that if a vehicle at the subject approach in the paired signalized intersection network experienced more delay than at the same approach of the isolated signalized intersection network, then we can conclude that this additional delay is due to the downstream disturbance.

6.6 Significance and quantification of downstream disturbance and additional delay

The two networks, as explained in the previous section, were coded in CORSIM. The isolated signalized intersection network layout is shown in figure 6.3 and the layout of the paired signalized intersections network is shown in figure 6.6. All applicable control, traffic, and geometric variables for both networks were kept the same.

Figures 6.8 through 6.13 show a comparison of operations at the single and two-intersection systems using different MOE's for the subject approach. Note that values shown in those figures are average of three independent runs. The following MOE's are used: vehicle trips, average speed, total time, delay time, queue delay and control delay. Figures 6.8 through 6.13 show the results for scenarios' with the following system parameters: spacing between upstream and downstream intersection is 200m, offset is 0

sec with the upstream eastbound approach taken as a reference phase for the paired signalized intersection system, and the cycle length is 150 sec.

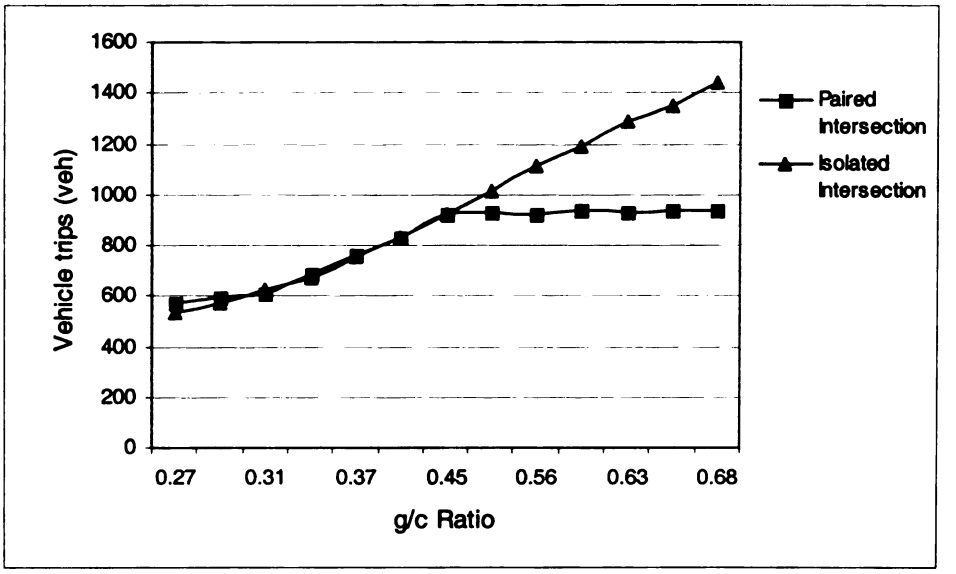

Figure 6.8 Comparison of vehicle trips discharged from the subject approach for the isolated and paired signalized intersection systems

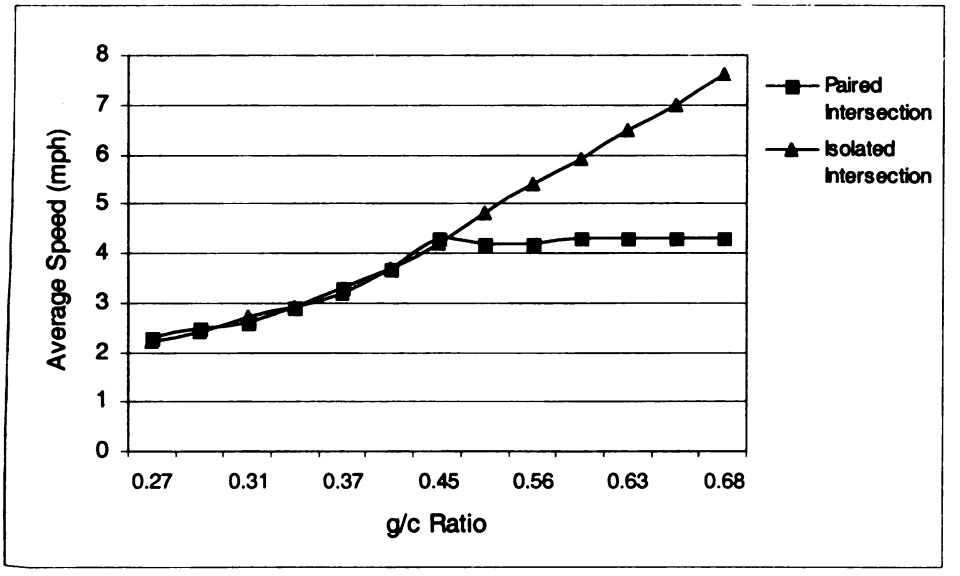

Figure 6.9 Comparison of average speed at the subject approach for the isolated and paired signalized intersection systems

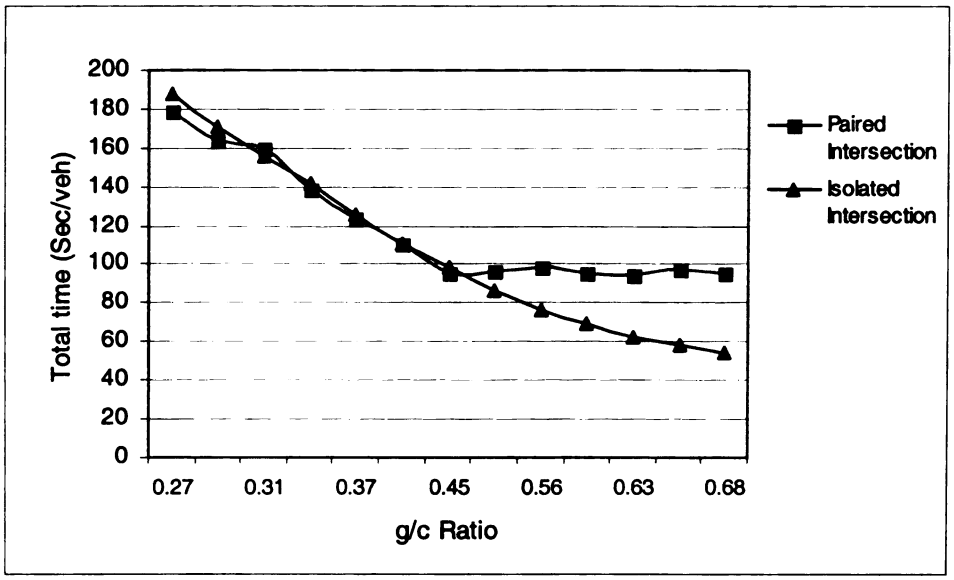

Figure 6.10 Comparison of total time (total time on the link for all vehicles) at the subject approach for the isolated and paired signalized intersection systems

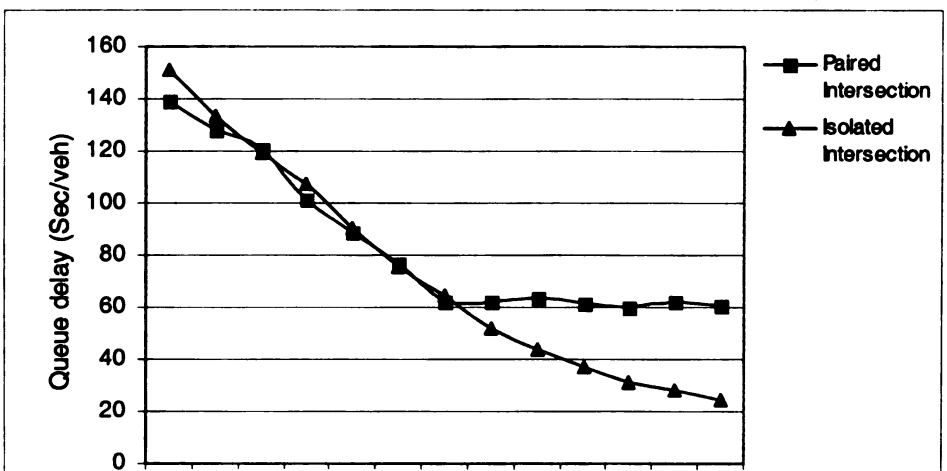

Figure 6.11 Comparison of queue delay at the subject approach for the isolated and paired signalized intersection systems

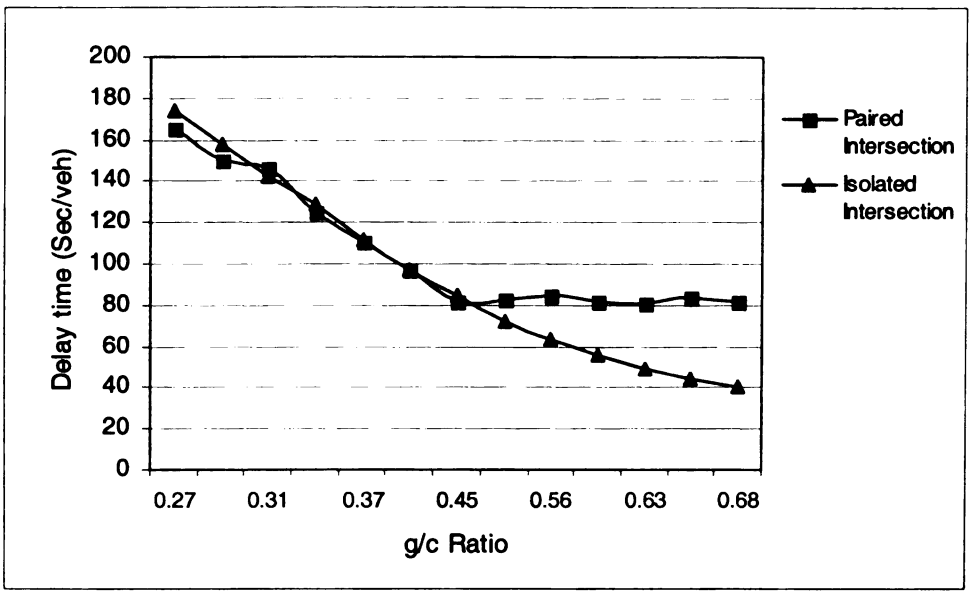

Figure 6.12 Comparison of delay time (total delay per vehicle trip) at the subject approach for the isolated and paired signalized intersection systems

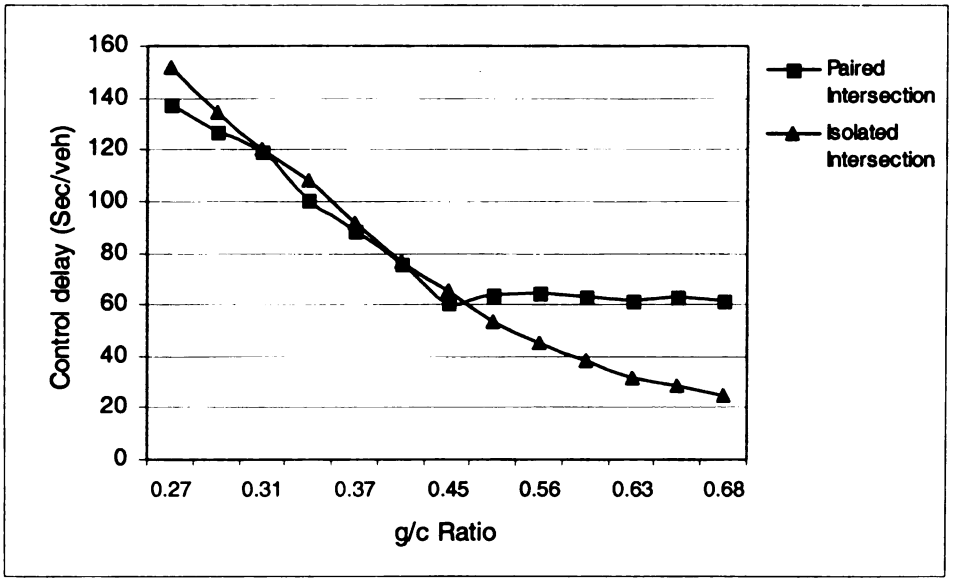

Figure 6.13 Comparison of control delay at the subject approach for the isolated and paired signalized intersections system

For all MOE's, it is clear that the results from the two-intersection system are similar to those of the single intersection system up to the point when the downstream disturbance starts affecting the upstream traffic. For larger g/c ratios (in this case greater than 0.45), the downstream disturbance starts impacting operations at the upstream approach, and the differences between the two systems become obvious. Note that the critical value of 0.45 g/c of upstream approach is only valid for the given experimental setup in which the downstream approach has 0.5 g/c ratio. For other conditions, this critical value can vary depending upon the link length, offset, and the g/c ratio of the downstream approach.

This observed trend is expected because by increasing the g/c of the upstream approach while keeping the downstream approach g/c constant, we are increasing the traffic demand at the downstream link whereas the supply at the same approach is constant (no change in g/c of the downstream approach). Specifically, vehicles at the upstream approach incur additional delay, and the number of vehicles leaving the subject approach is reduced. This additional delay is comparable to the delay from the d4 model formulated and presented in chapter 4. Similar type of trends is observed for other link lengths as presented in Ahmed and Abu-Lebdeh (40)

6.7 Validation of the d4 delay model

The basic premise is that the difference in any of the measures of effectiveness (MOE's), shown in figures 6.8 through 6.13, between the two systems for the subject approach is due to operations at the downstream intersection. Specifically, the difference in control delay between the two systems should be comparable to that from the d_4 model. In the following section, results of the downstream-induced delay, d_4, model are compared with

the CORSIM results, first for each cycle and then for the average of a 15-minute time interval.

6.7.1 Cycle by cycle comparison

Different scenarios were created by varying the g/c ratio, for both upstream and downstream approaches, link length, and the offset to compare the results of the d_4 model with those of CORSIM. Three combinations of g/c ratios of upstream and downstream approaches were used: 0.73-0.67, 0.8-0.6, and 0.9-0.6. Note that 0.73-0.67 means that the g/c of the upstream approach is 0.73 and for the downstream approach is 0.67. By increasing the g/c ratio of the upstream approach and decreasing it for the downstream approach, we are creating more congestion at the downstream link, hence more probability of getting the downstream disturbance to impact the upstream approach. Figures 6.14 through 6.22 show a comparison of the downstream-induced delay, d_4, as predicted by CORSIM to that predicted by the d4 model for different combinations of g/c ratios, offset, and link lengths. Note that the CORSIM delays shown in the figures are calculated as the difference in control delay between the single and the two-intersection systems and each d4 value is the average of three independent runs.

Delays from the d_4 model compare reasonably well with the CORSIM results. The d4 model and CORSIM gave minimum d_4 value for the first cycle for all scenarios. This result is expected because conditions before the first cycle are least congested as compared to other cycles. For both models the system reaches equilibrium after two or three cycle, i.e. when d_4 becomes almost constant. These results were consistent with all scenarios shown in figures 6.14 to 6.22.

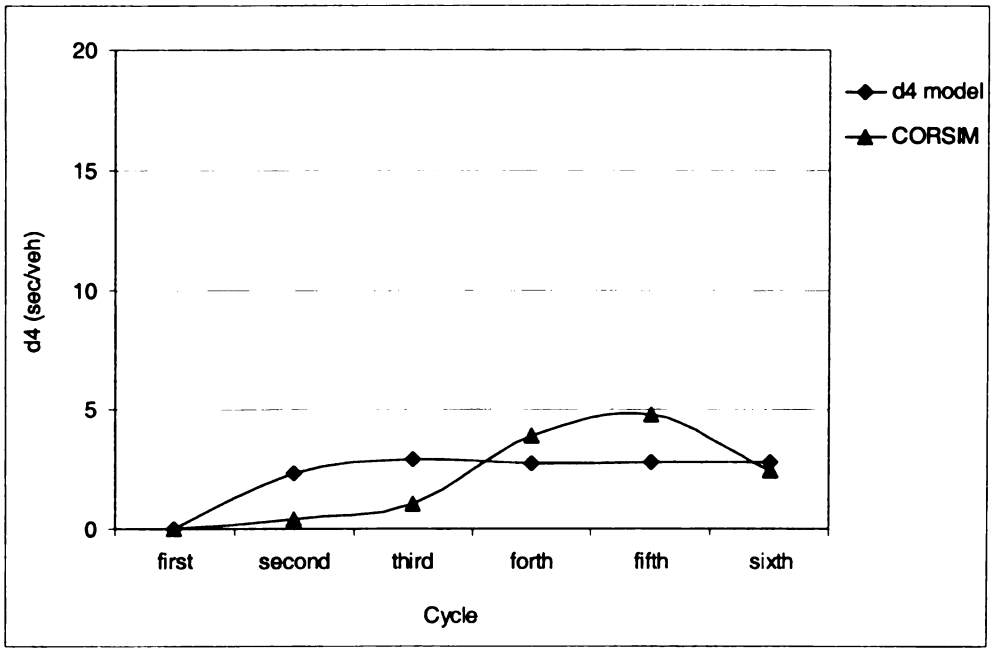

Figure 6.14 Comparison of d_4 values between CORSIM and the d4-model. In this case link length is 300 m, g/c ratios of upstream and downstream are 0.73 and 0.67, respectively; and offset 20 sec

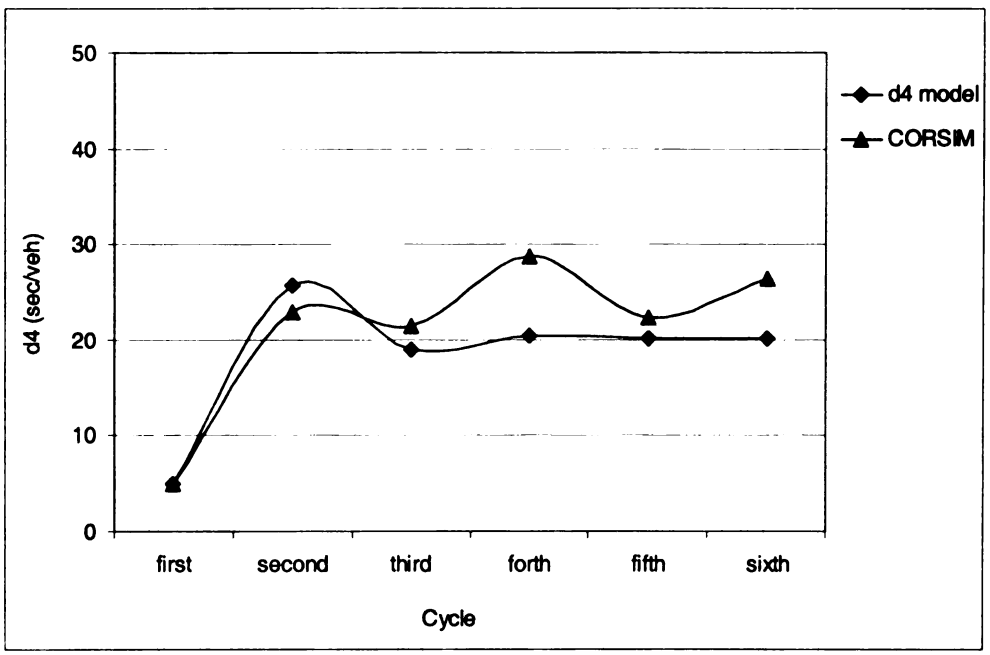

Figure 6.15 Comparison of d_4 values between CORSIM and the d4-model. In this case link length is 300 m, g/c ratios of upstream and downstream are 0.8 and 0.6, respectively; and offset 20 sec.

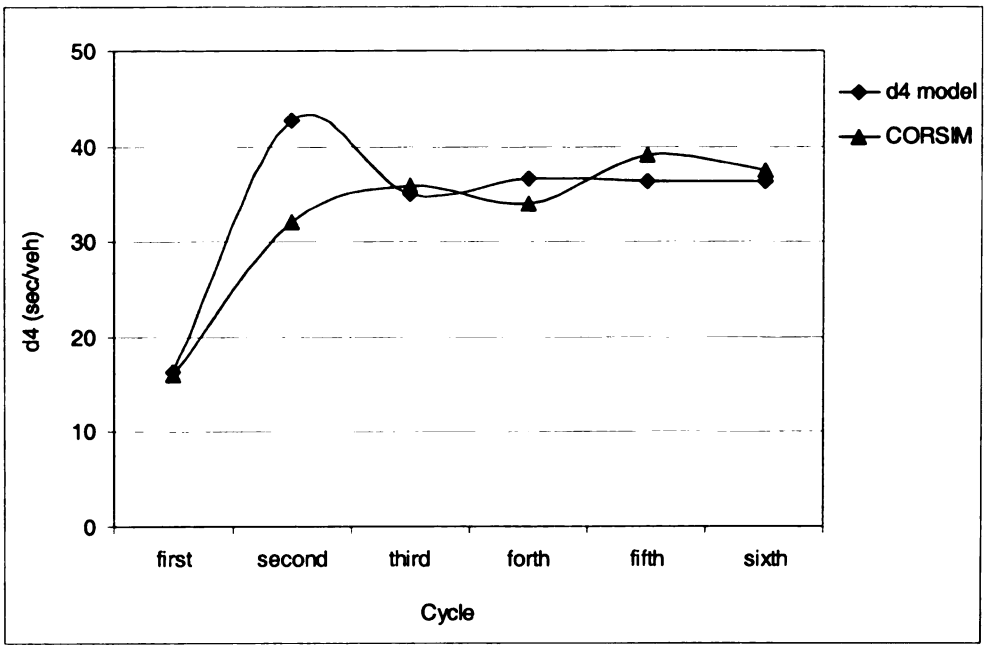

Figure 6.16 Comparison of d_4 values between CORSIM and the d4-model. In this case link length is 300 m, g/c ratios of upstream and downstream are 0.9 and 0.6, respectively; and offset 10 sec.

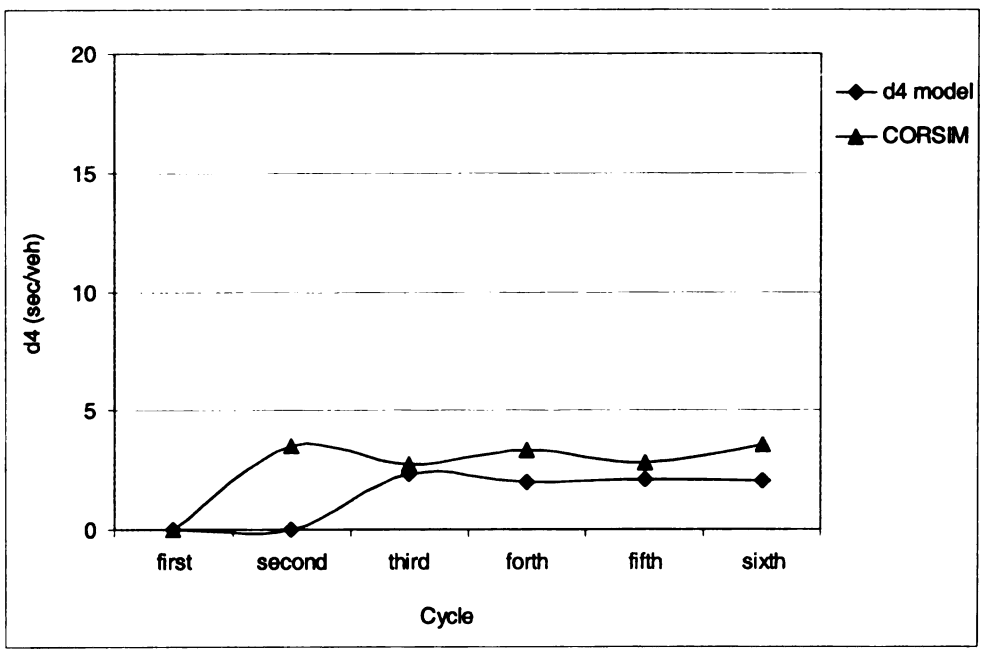

Figure 6.17 Comparison of d4 values between CORSIM and the d4-model. In this case link length is 500 m, g/c ratios of upstream and downstream are 0.73 and 0.67, respectively; and offset 0 sec.

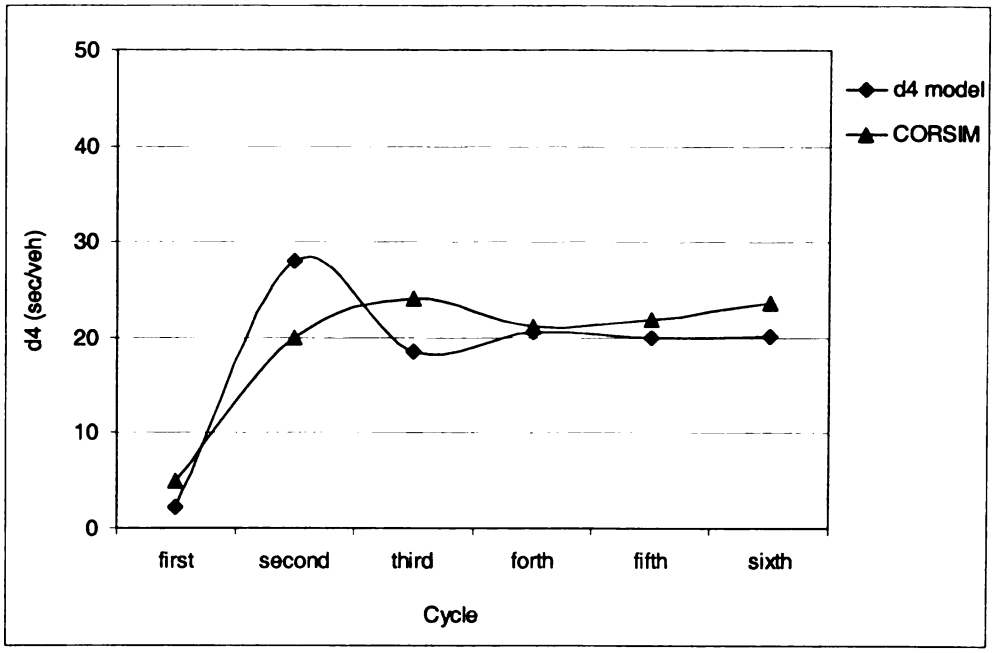

Figure 6.18 Comparison of d4 values between CORSIM and the d4-model. In this case link length is 500 m, g/c ratios of upstream and downstream are 0.8 and 0.6, respectively; and offset 0 sec.

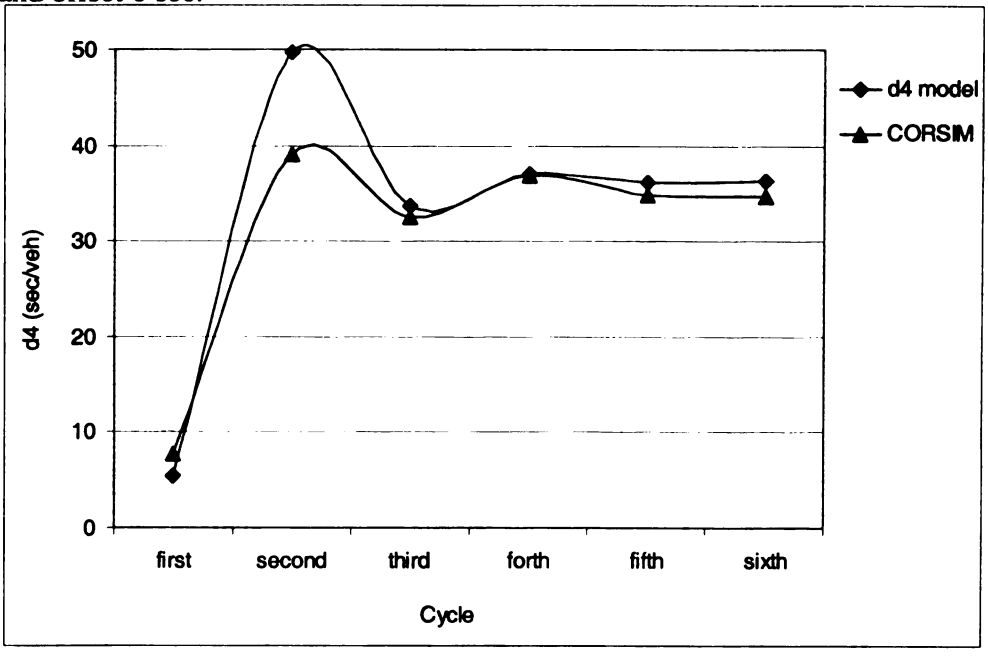

Figure 6.19 Comparison of d_4 values between CORSIM and the d4-model. In this case link length is 500 m, g/c ratios of upstream and downstream are 0.9 are 0.6, respectively; and offset 0 sec.

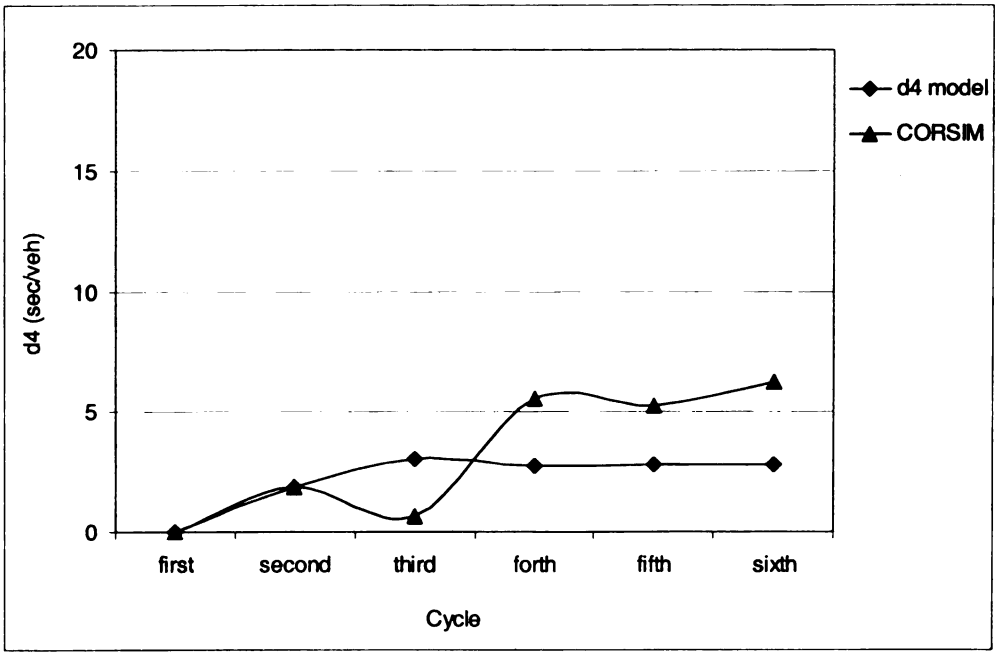

Figure 6.20 Comparison of d4 values between CORSIM and the d4-model. In this case link length is 400 m, g/c ratios of upstream and downstream are 0.73 and 0.67, respectively; and offset 10 sec.

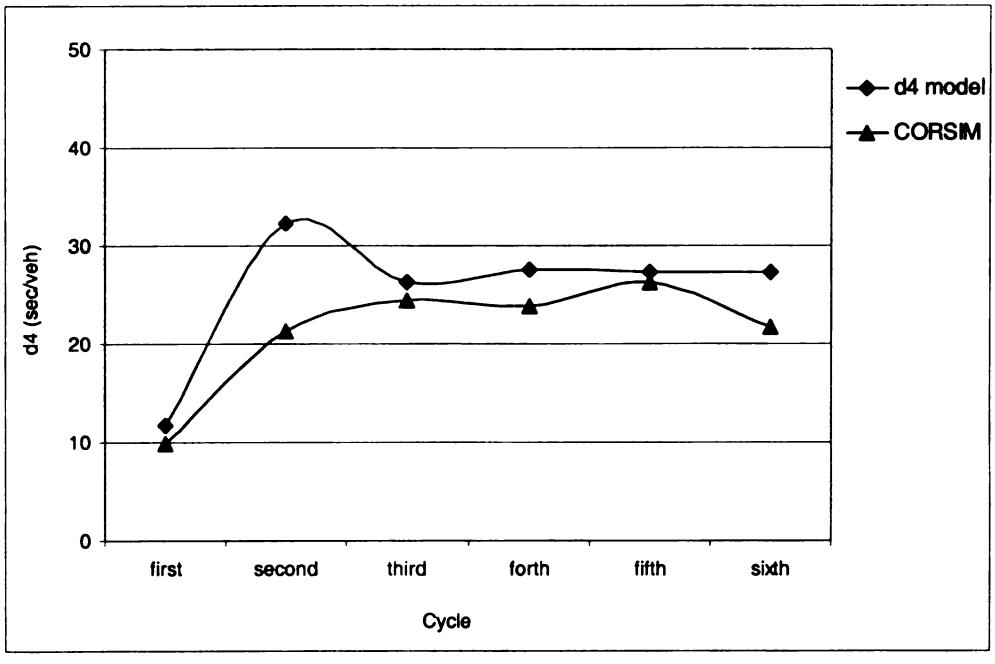

Figure 6.21 Comparison of d_4 values between CORSIM and the d4-model. In this case link is length 400 m, g/c ratios of upstream and downstream are 0.8 and 0.6, respectively; and offset 10 sec.

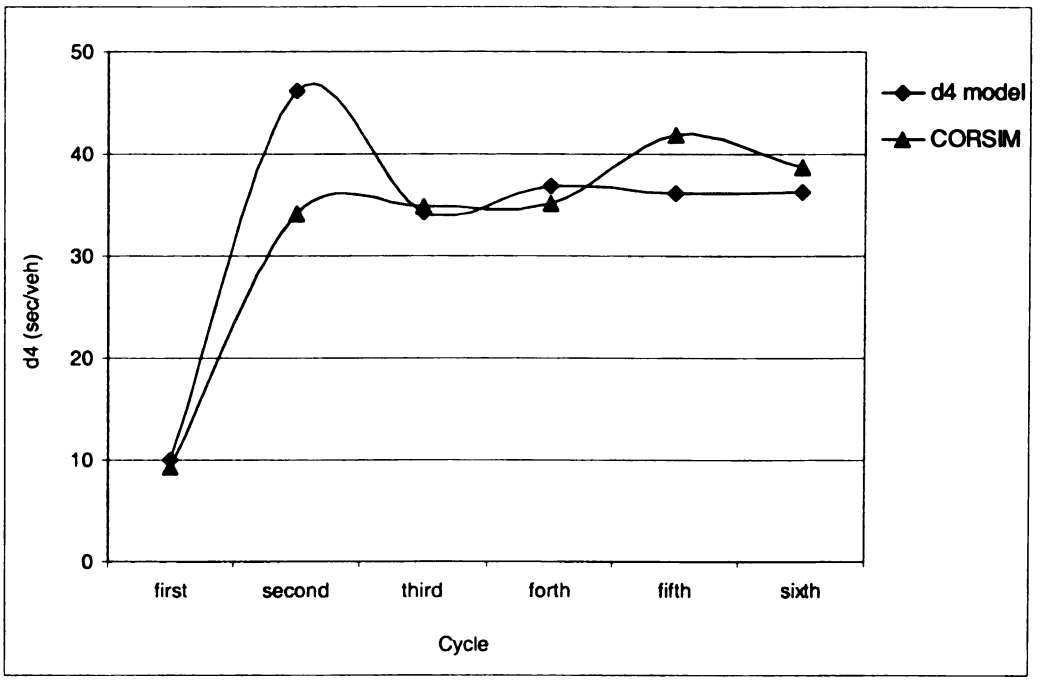

Figure 6.22 Comparison of d4 values between CORSIM and the d4-model. In this case link length is 400 m, g/c ratios of upstream and downstream are 0.9 and 0.6, respectively; and offset 10 sec.

6.7.2 Average d4 value for 15-minute analysis period

The average delay is calculated by taking the arithmetic mean of d_4 values that occurred during each individual cycle. The following sections present the comparison of results given by the d4-model and CORSIM for different input parameters.

6.7.2.1 Varying Link Length

Different conditions were created by changing spacing between the upstream and downstream intersections from 200 m to 500 m in of 100 meters increments. Figures 6.23 through 6.25 show a comparison of d4 from CORSIM and the d4-model. Three cases are shown, each with a different g/c ratio. Figure 6.23 represents the least congested scenario with g/c ratios of 0.73 and 0.67 for the upstream and downstream approaches, respectively. Figure 6.24 shows a relatively more congested condition with g/c ratios of

0.8 and 0.6 for the upstream and downstream approaches, respectively. The most congested condition is shown in figure 6.25 with g/c of 0.9 for the upstream approach and 0.6 for the downstream approach.

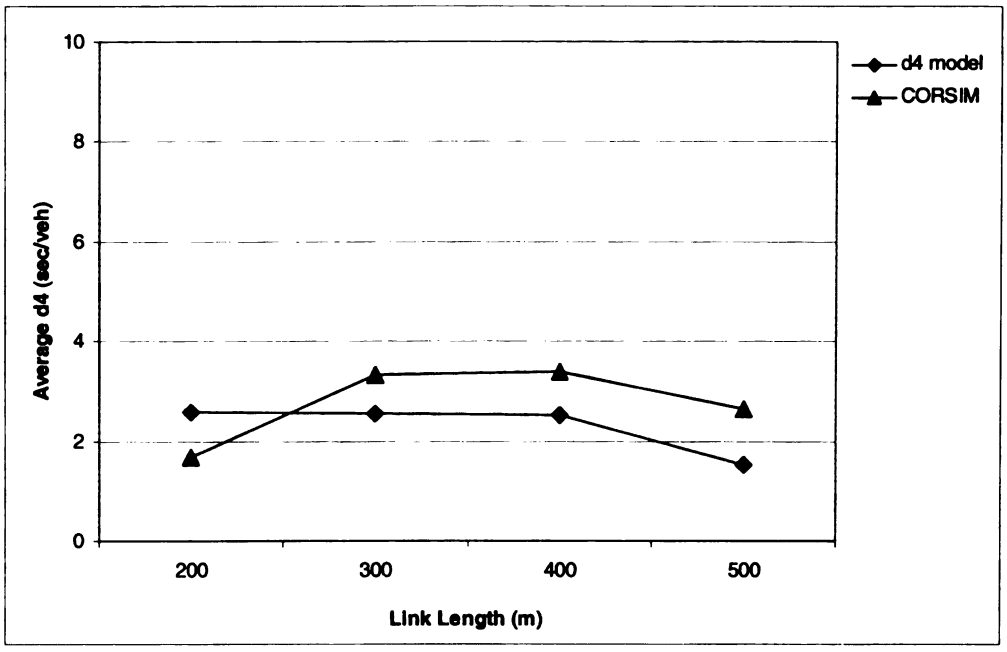

Figure 6.23 Comparison of d_4 values between CORSIM and the d4-model. In this case g/c ratios of upstream and downstream are 0.7 and 0.67, respectively; offset -15 sec, and cycle length 150sec

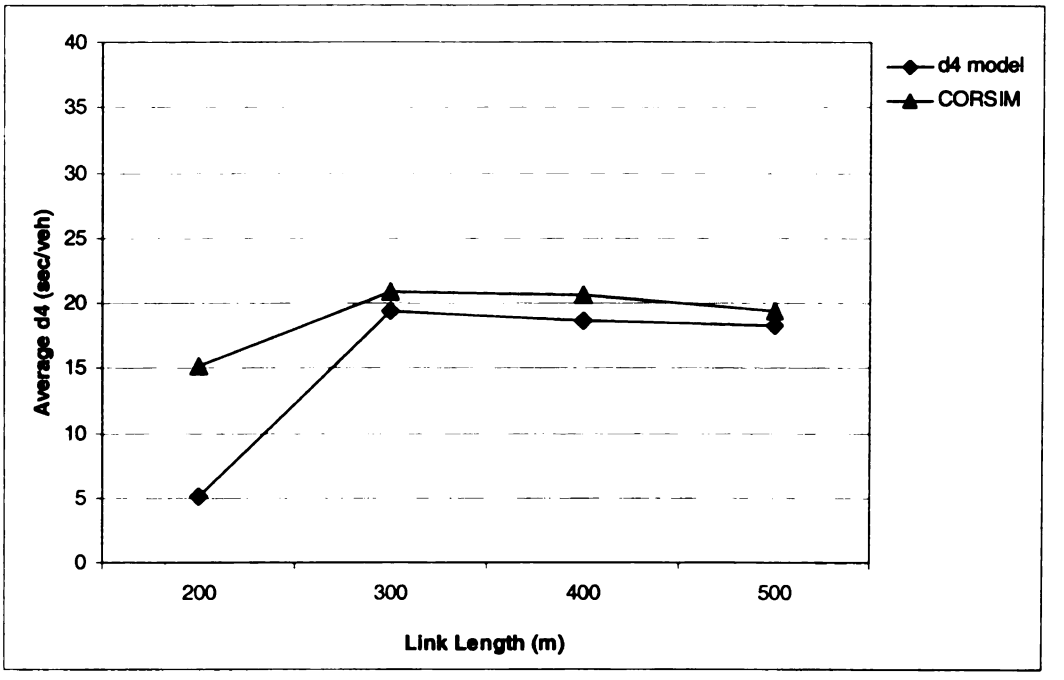

Figure 6.24 Comparison of d_4 values between CORSIM and the d4-model. In this case g/c ratios of upstream and downstream are 0.8 and 0.6, respectively; offset -15 sec, and cycle length 150sec

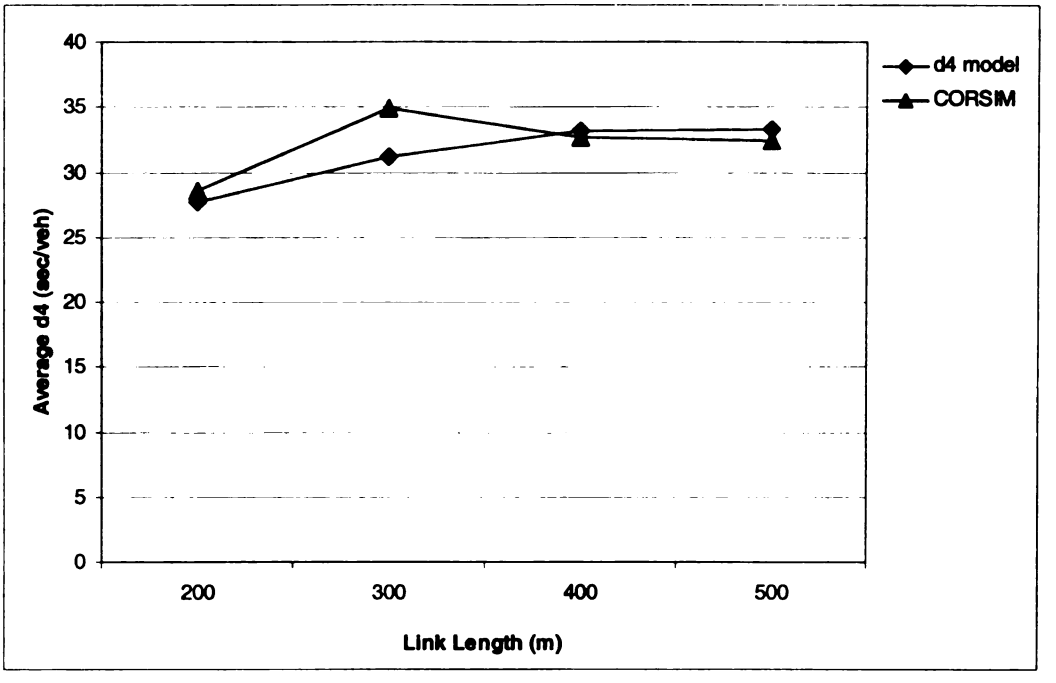

Figure 6.25 Comparison of d_4 values between CORSIM and the d4-model. In this case g/c ratios of upstream and downstream are 0.9 and 0.6, respectively; offset -15 sec, and cycle length 150sec

Both models show comparable results. There are some differences in results between CORSIM and the d4-model specially for uncongested conditions. Table 6.1 shows a statistical comparison between the means of d4 from CORSIM and from the d4-model for the g/c ratio 0.73-0.67 case. All significance levels are greater than 0.05, which means that the difference between the average values of d4 from CORSIM and the d4-model are not statistically significant. There is significant difference between CORSIM and the d4-model for link length 200m, shown in figure 6.24. This finding is specific to this condition. All other results are consistent and comparable, as shown in figures 6.26 to 6.29.

Table 6.1 Comparison of delay between d4-model and CORSIM results (g/c 0.73-0.67)

Link length		**Delay (sec/vehicle)**	**Std. Deviation**	**t statistic**	**Significance**
200	Model	2.58	1.86	-1.79	0.135
	CORSIM	1.66	1.06		
300	Model	2.53	0.95	.84	0.436
	CORSIM	3.34	2.59		
400	Model	2.51	1.29	2.44	0.058
	CORSIM	3.39	1.73		
500	Model	1.51	1.21	2.12	0.088
	CORSIM	2.65	1.34		

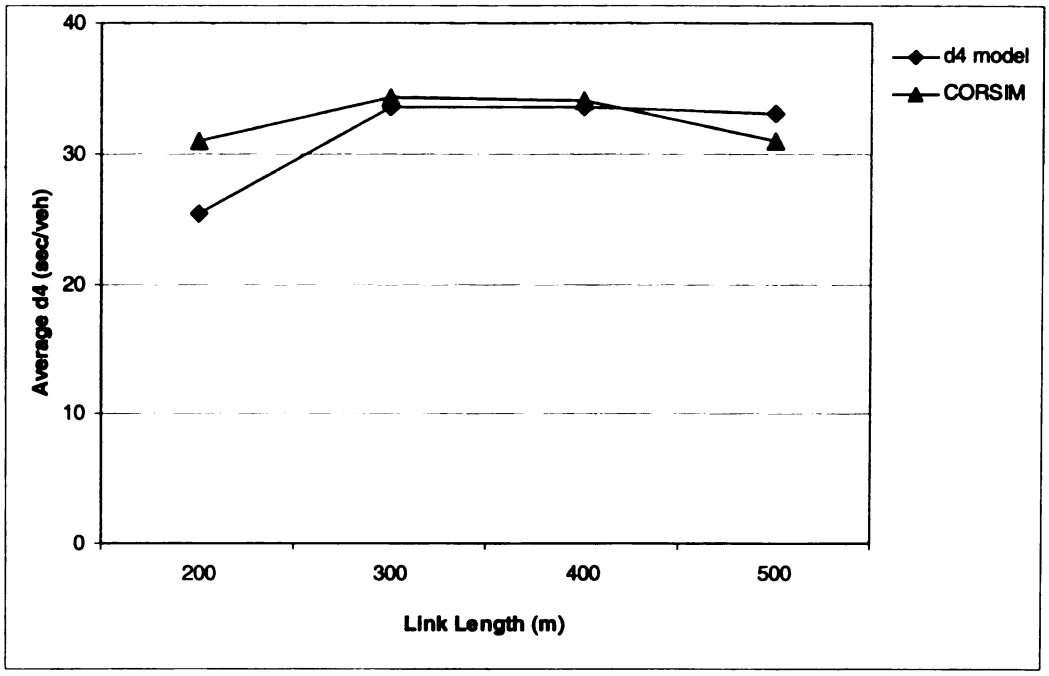

Figure 6.26 Comparison of d_4 values between CORSIM and the d4-model. In this case g/c ratios of upstream and downstream are 0.9 and 0.6, respectively; offset 0 sec, and cycle length 150sec

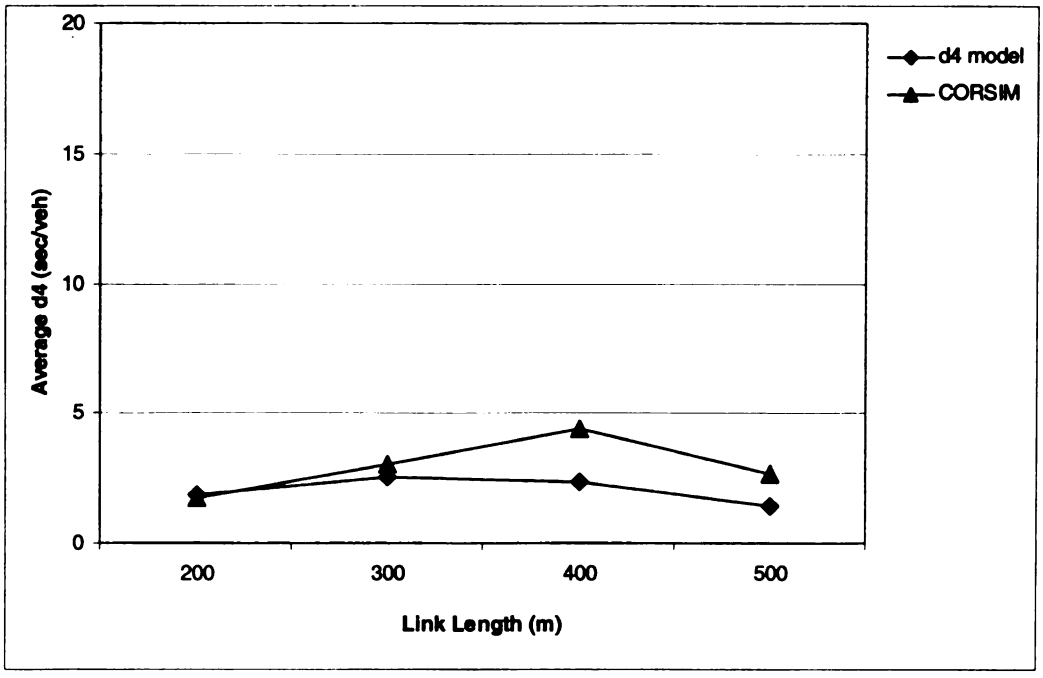

Figure 6.27 Comparison of d_4 values between CORSIM and the d4-model. In this case g/c ratios of upstream and downstream are 0.73 and 0.67, respectively; offset 0 sec, and cycle length 150sec

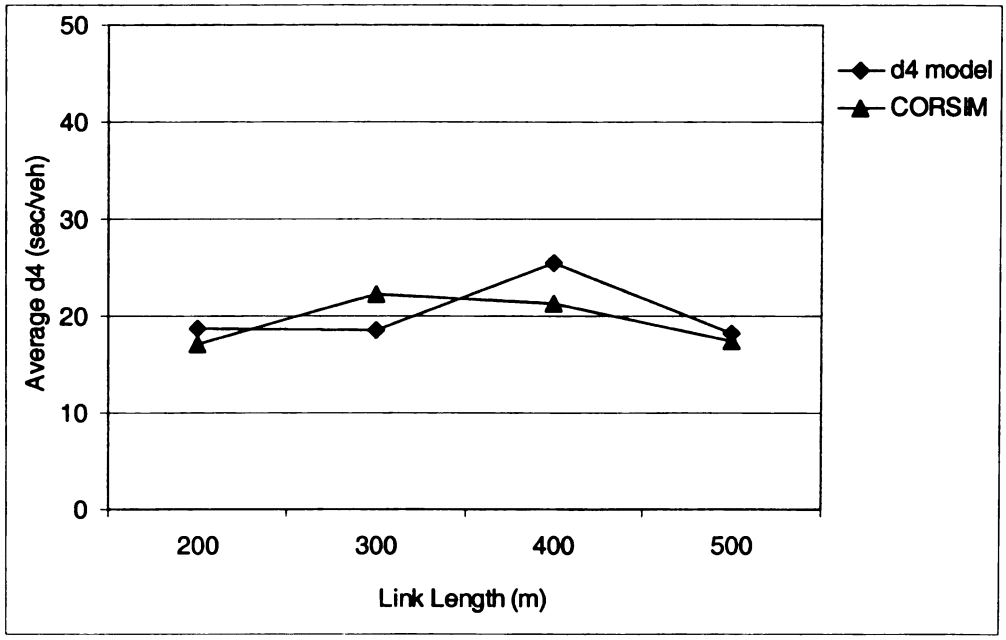

Figure 6.28 Comparison of d_4 values between CORSIM and the d4-model. In this case g/c ratios of upstream and downstream are 0.8 and 0.6, respectively; offset 10 sec, and cycle length 150sec.

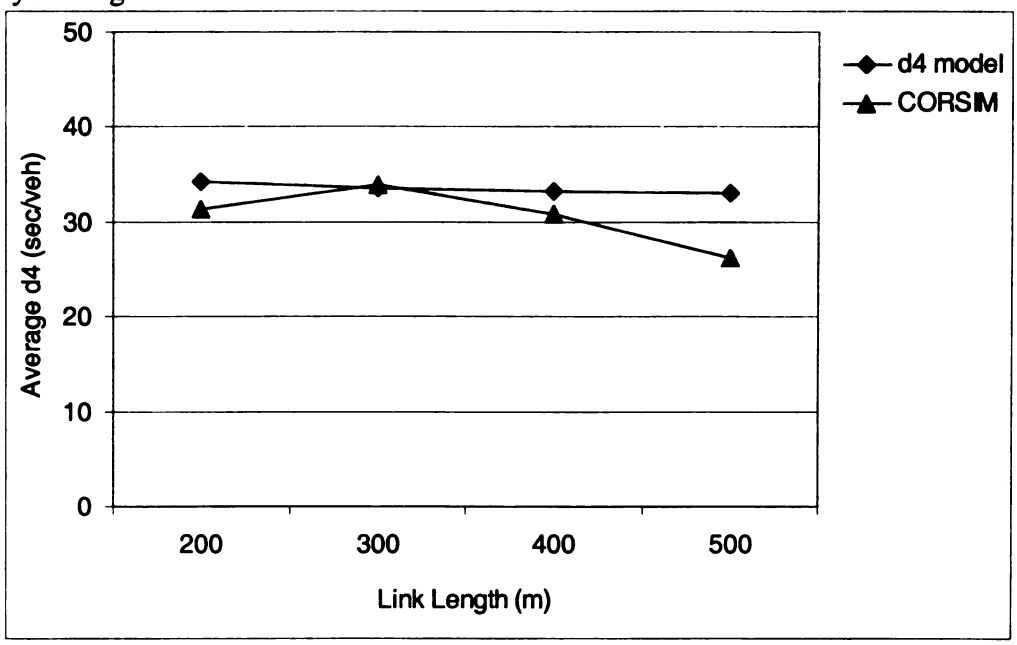

Figure 6.29 Comparison of d_4 values between CORSIM and the d4-model. In this case g/c ratios of upstream and downstream are 0.9 and 0.6, respectively; offset 20 sec, and cycle length 150sec.

6.7.2.2 Varying g/c ratio

Figure 6.30 shows a comparison between the d4 values estimated by the d4-model and CORSIM for different g/c values at the upstream and downstream approaches. Figures 6.30a to 6.30d show the case for which spacing between upstream and downstream intersections is 500m and the offsets are -15, 0, 10 and 20 seconds, respectively. The results from both models are comparable, and the trends also make sense for each scenario. As the g/c ratio of the upstream approach increases, the delay at the subject approach also increases. Similar trends and comparable results are observed for the other scenarios, as shown in figure 6.31.

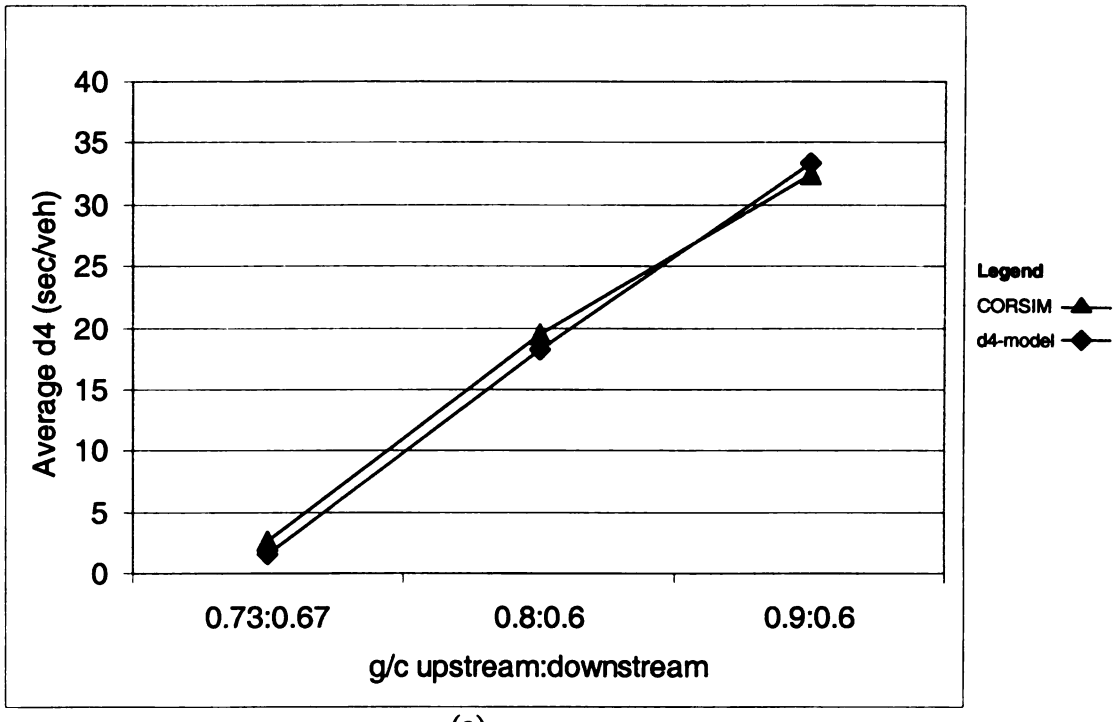

(a)

Figure 6.30a Comparison of average d4 between CORSIM and d4-model. In this case link length is 500m and offset = -15sec,

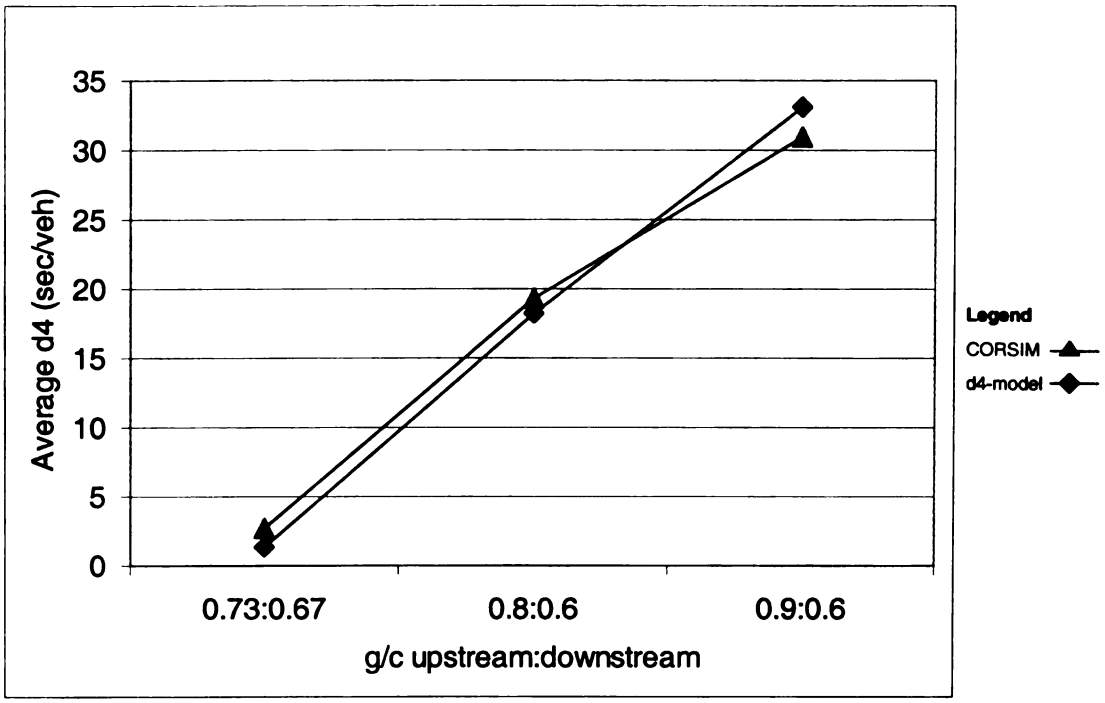

Figure 6.30b Comparison of average d4 between CORSIM and d4-model. In this case link length is 500m and offset = 0sec,

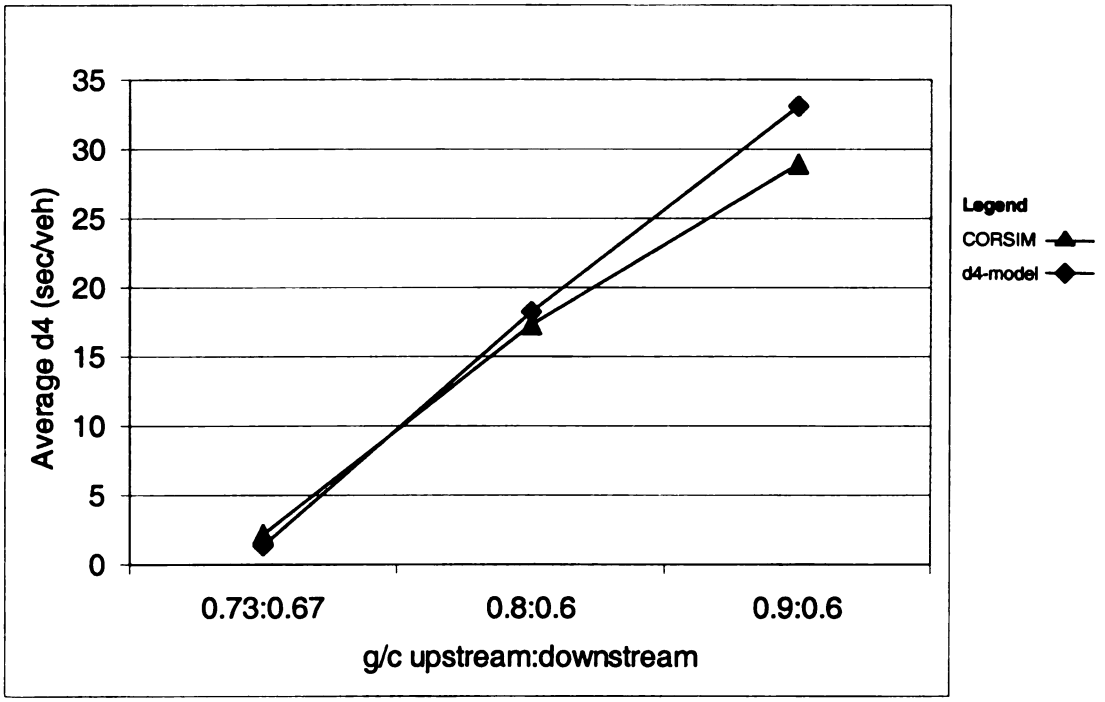

Figure 6.30c Comparison of average d4 between CORSIM and d4-model. In this case link length is 500m and offset = 10sec,

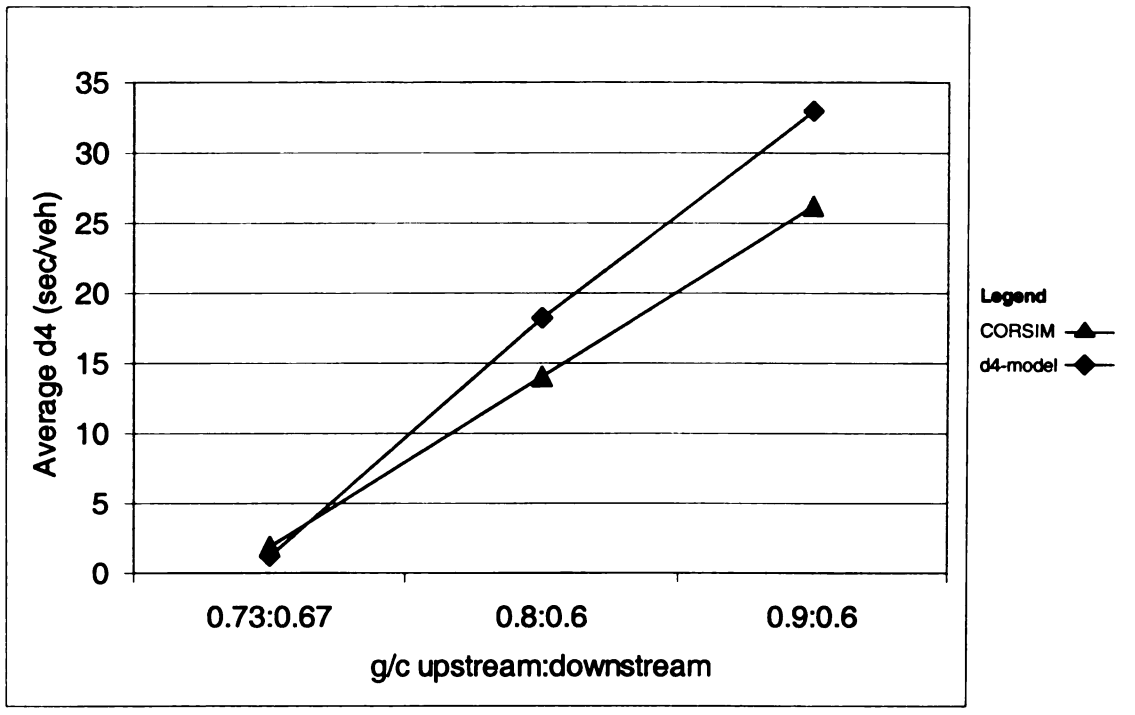

Figure 6.30d Comparison of average d4 between CORSIM and d4-model. In this case link length is 500m and offset = 20sec,

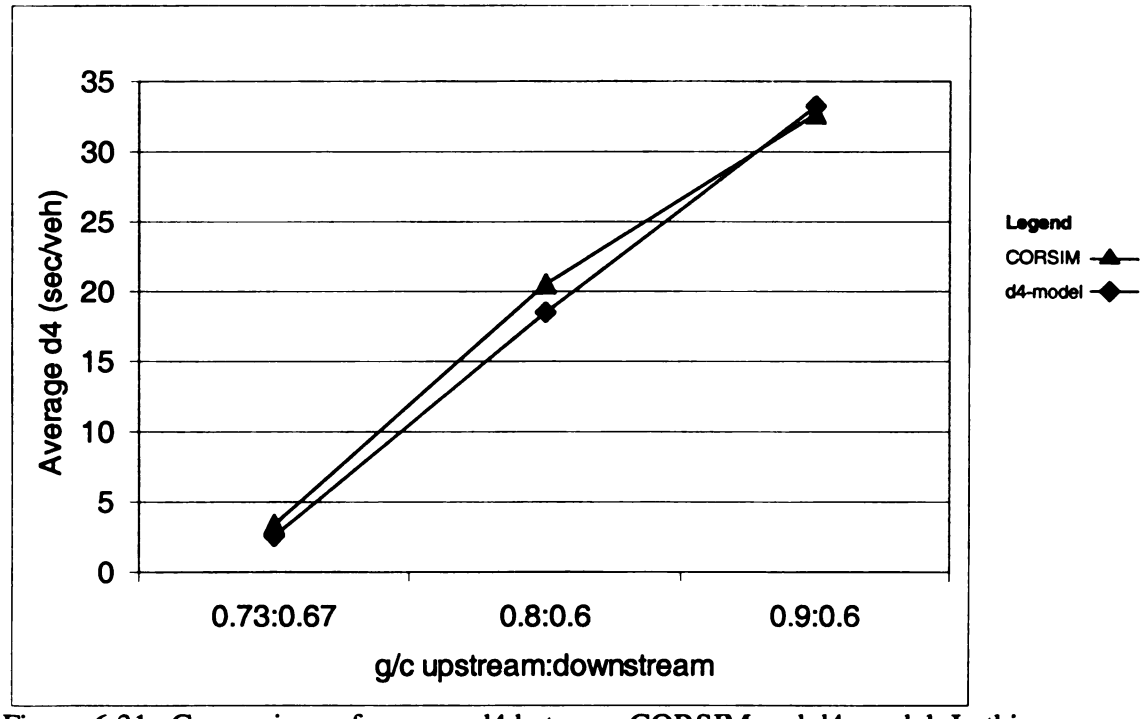

Figure 6.31a Comparison of average d4 between CORSIM and d4-model. In this case link length is 400m and offset = -15sec,

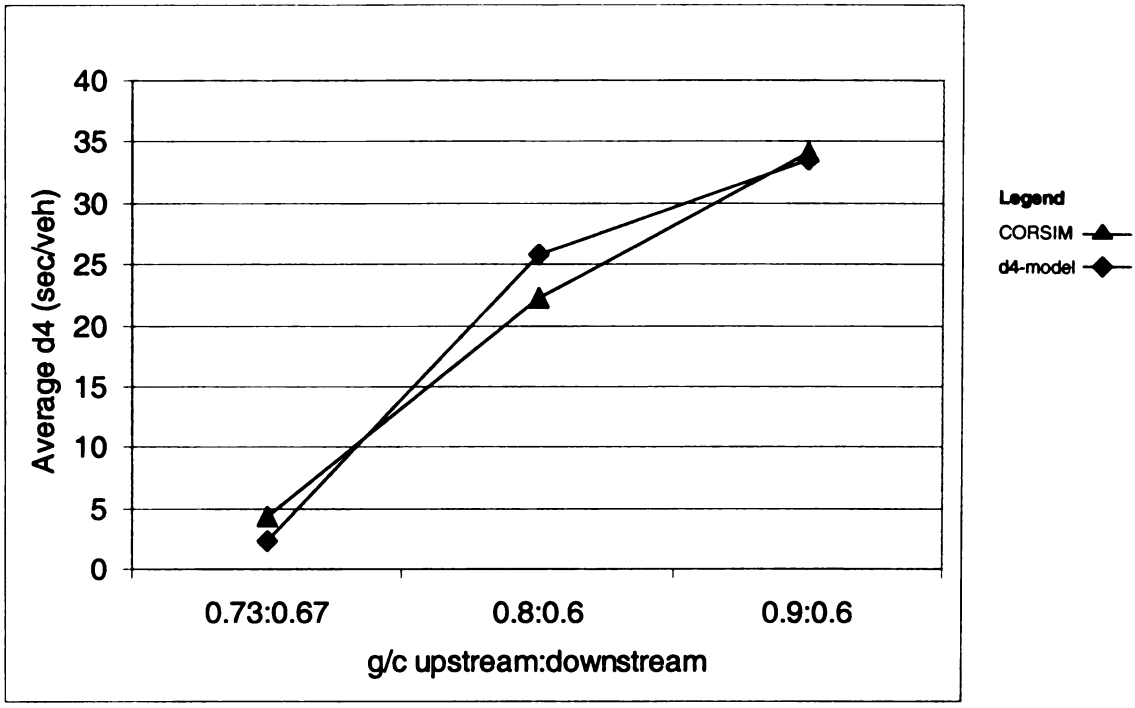

Figure 6.31b Comparison of average d4 between CORSIM and d4-model. In this case link length is 400m and offset = 0sec,

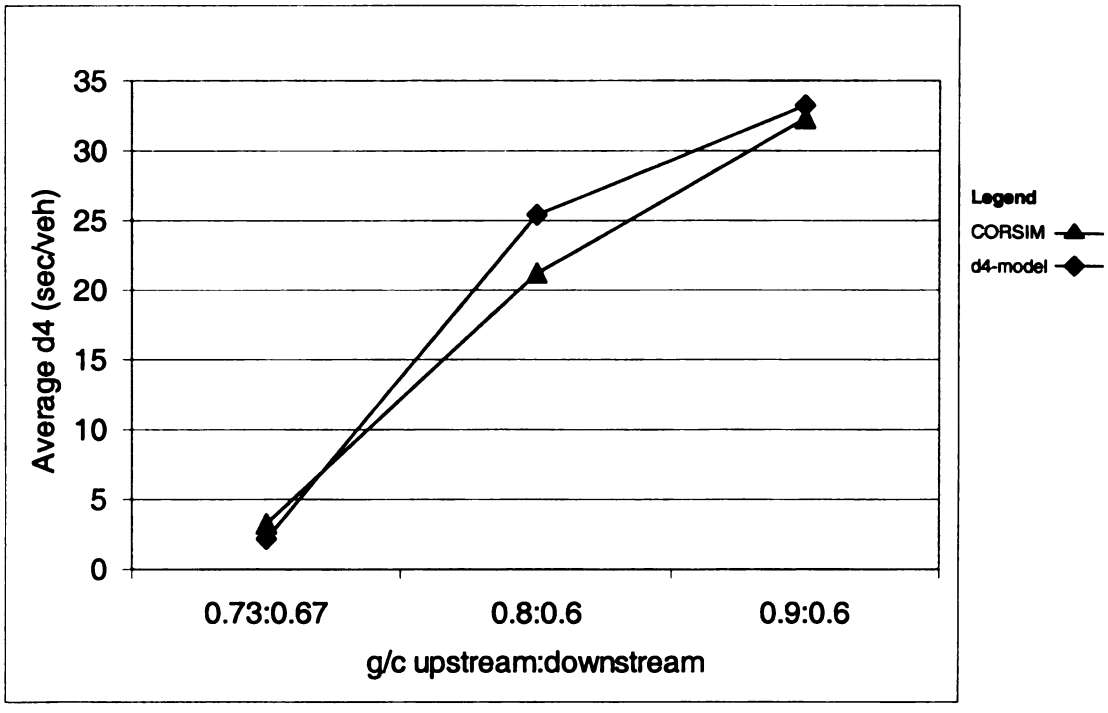

Figure 6.31c Comparison of average d4 between CORSIM and d4-model. In this case link length is 400m and offset = 10sec,

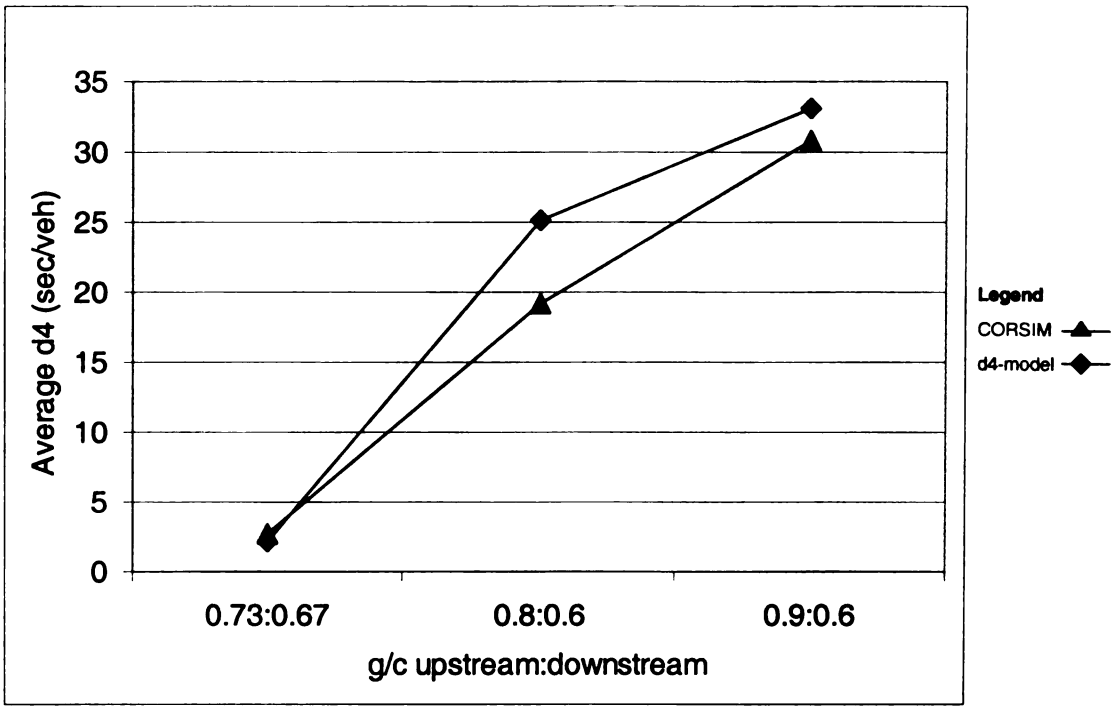

Figure 6.31d Comparison of average d4 between CORSIM and d4-model. In this case link length is 400m and offset = 20sec,

6.8 Summary of validation of d4 model

This chapter compares the d4 values obtained from the d4-model and CORSIM. The d4-model is macroscopic model to estimate downstream-induced delay, and CORSIM is a microscopic simulation model. Different scenarios were created by varying g/c ratios of the upstream and downstream approaches, link lengths and offset. d4 at the upstream subject approach is calculated for all cycles occurred during 15-minute time interval. The results from the d4-model and CORSIM are comparable. The main conclusions are:

- CORSIM and d4-model show downstream traffic disturbance cause significant additional delay at upstream approach
- CORSIM shows similar trends of d4 at the upstream approach as the d4-model.
- There is no significant difference between the d4 values estimated from d4-model and CORSIM except for some specific conditions.

CHAPTER 7

Conclusion and Recommendations

7.1 Introduction

Current standard models for signalized intersection delay ignore the impact of downstream conditions on upstream intersection operations. There are cases where such conditions do impact operations at the upstream intersection. One example is congested conditions where downstream queues extend upstream and cause additional delay and reduction in capacity. As congested conditions become more prevalent, it is imperative that suitable models be developed to reliably handle congested conditions.

This research presents models to estimate delay that is incurred by traffic of upstream approach due to downstream traffic disturbances. The models were formulated in terms of traffic flow, control, and geometric properties that are normally available or can be easily collected. The models distinguish between cases where downstream disturbances cause additional delay and others where they do not. Properties of stopping and starting shockwaves were used for this purpose. Where additional delay occurs, it is quantified using control and flow parameters and shockwave properties. The models distinguish between various flow and queue formation conditions. The models presented in this research are a step in the direction to understand the traffic flow characteristics at upstream intersections in closely spaced signalized intersection networks. They supplement existing models that estimate the impact of congestion on capacity, but not on delay.

7.2 Conclusions

Following are the main conclusions of this research

- Disturbance caused by the downstream at upstream approach in closely spaced signalized intersection system can be significant, depending upon the offset, link spacing, signal timing or combination of these factors. Downstream disturbance induces additional delay at upstream approach. The operational characteristics of such approach cannot be observed or assessed independently. For upstream approach of such system, models are needed to capture the share of delay that is induced by downstream disturbances.
- Significant downstream disturbance caused by queues or otherwise affects the discharge volume at upstream and downstream approaches and average speed at downstream link. These factors contribute to enhance the additional delay at upstream approach.
- Additional delay "d_4", caused by downstream disturbance on upstream approach can be significant and depends upon the geometric, signal control, and coordination parameters. Queue length at downstream link, g/c ratio of upstream and downstream approaches, offset and spacing between intersections are prominent parameters.
- d_4 changes with each cycle and reach equilibrium once traffic flow and downstream queues stabilize and start replicating over cycles. The traffic demand and signal timing at the upstream intersection remain the same throughout the cycles; therefore the value of d4 for each cycle becomes steady as soon as the queue length at the downstream link starts repeating itself during subsequent cycles.

- Queue length at downstream at the start of cycle depends upon traffic flow conditions during the preceding cycle, and hence should be included in estimation of d4. The increase of queue length on the downstream link at the start of a cycle heightens the value of d4. Arriving vehicles from upstream approach reach the back of queue quickly and increase the probability of blockage and value of d4 at the upstream approach.
- Improper offset leads to higher d4 value. For congested conditions, shorter offsets have lesser d4 value than higher ones'. For shorter offsets, there is lower likelihood that the upstream arriving vehicles will be blocked or if blocked, the duration of blockage will be shorter, which decrease the d4 values. In case of longer offsets, green at the upstream approach starts much earlier than green at the downstream approach, which enhance the probability of blockage at downstream link and leads to higher d4 value.
- Increase of g/c ratio at the upstream approach relative to g/c at the downstream approach increase value of d_4 for each cycle. By increase of g/c at the upstream approach, more vehicles are fed into the downstream link and at the same time decreasing or keeping g/c ratio constant for downstream approach reduces the traffic output from downstream approach and increase probability of getting longer queues at downstream link and higher d4 value for the upstream approach.
- Average speed at downstream link depends upon the queue length at downstream intersection and remaining space. Increase in average speed decrease d4 value.

- Control parameters (g/c, offset), geometry (link length), and traffic queues interact in a complex way to impact d4. It is not possible to check the effect of individual parameter without looking at other parameters.
- The proposed models were validated using well-established microscopic traffic simulation model i.e. CORSIM. The validation results show close agreement between the outcomes of the models of this paper and those of the microscopic simulation models.
- d4-model supports what Prosser and Dunne, Messer, and Rouphail and Akcelik concluded in their work even though neither of group intended to isolate d4 or its equivalent.
- The d4-model is applicable to any system size; the system can be divided into subsystems each consists of two paired signalized intersections. When we have a system, the increase in delay due to downstream queues at different approach cannot be simply added together to get d4 for the system. It all depends on how the delay of the system is to be calculated, whether the system has an odd or even number of intersections, whether and where traffic starvation occurs, and whether turns from upstream intersections and mid-block sources are to be considered.
- d4 model is macroscopic model and estimate additional delay at upstream approach caused by downstream traffic disturbance. The d4-model use basic traffic flow, geometric properties and control parameters at neighboring intersections. Whereas CORSIM is a microscopic simulation model, which estimate delay for individual vehicles in a system. CORSIM does not provide additional delay at upstream approach due to downstream disturbance but can be

estimated numerically. d_4 model results are consistent with microscopic simulation model output.

- The models presented in this dissertation were tested on a hypothetical signalized system and different control conditions. The results show that the delay induced by downstream conditions can be significant and that it depends on signal control and coordination parameters. The results were evaluated for consistency and were found to agree with expectation.

7.3 Recommendations for further studies

New delay term "d_4" is proposed, which should be added in already existing HCM 2000 control delay formula after some refinement and validation from field data. Following are some suggestion for further research:

- Evaluation of sink source consequence on downstream induced delay. The volume will have to be reliably estimated through sound models that would be incorporated in the overall procedures presented in this research. Inclusion of sink and source only affect the queue estimation model at start of each cycle. The d4 model and its parameters will remain same.
- Non-through traffic need to be incorporated. The proposed d4 model only consider through traffic from upstream and downstream approach. Left and right turns volumes from upstream intersecting streets can be included easily through a term (or terms) in d4 and queue estimation models.
- Delay model can be calibrated for multiple lanes by including lane-changing parameters. Numbers of lane changing models are already available and evaluated on field data which can be used to elaborate proposed delay d4 model.

- Modification need to be done to the d4 model to make it applicable to adaptive controllers which change signal timing according to the traffic demand.
- The proposed models used some simplifying but reasonable assumptions. While some of these simplifications and assumptions are practically inconsequential others need to be revised and the models refined to make them useable for variety of traffic and roadway conditions. Before the models of this research are finally adopted more consistency tests and evaluations will have to be conducted including field validation.
- A comprehensive research is recommended through the National Cooperative Highway Research Program (NCHRP) to expand on the d4-model such that all limitations are addressed, other conditions are considered and accounted for, and all parameter sensitivities are investigated using real world data.

References

1. Weisbrod, G; Vary, D; Treyz, G. (2003); Measuring Economic Costs Of Urban Traffic Congestion To Business. In *Transportation Research Record: Journal of the Transportation Research Board No. 1839*, TRB, National Research Council, Washington, D.C. pp 98- 106

2. The Costs of Traffic Congestion in America, (2001), American Road & Transportation Builders Association, Washington, D.C

3. Urban Roadway Congestion Annual Report – 1998, Texas Transportation Institute,

4. Highway Capacity Manual, (2000) Transportation Research Board, National Research Council, Washington, D.C.

5. Akchlik, R. and Rouphail, N.M. (1992); A Preliminary Model of Queue Interaction at Signalised Paired Intersections. Proceedings of Australian Road Research Board, Vol. 16, Part 5, Vermont South, Victoria, pp. 325-345

6. Prosser, N, and M. Dunne. (1994); A Procedure for Estimating Movement Capacities at Signalised Paired Intersections. Proceedings of the 2nd International Symposium on Highway Capacity, Vol. 2, Sydney, Australia, pp. 473-492.

7. Messer, C. J. (1998); Extension and Application of Prosser-Dunne Model to Traffic Operation Analysis of Over saturated Closely-Spaced Signalized Intersections. Paper presented at the 77th Transportation Research Board Annual Meeting, Washington, D.C.

8. Johnson, B, and Akchlik, R. (1992); Review of Analytical Software for Applicability to Paired Intersections. Proceedings of the 16th Australian Road Research Broad, Proceeding; Vol.16, Perth, Western Australia, pp. 347-367.

9. Abu-Lebdeh, G and Benekohal, R.F. (2000); Signal Coordination and Arterial Capacity in Over saturated Conditions. In *Transportation Research Record: Journal of the Transportation Research Board No. 1727*, TRB, National Research Council, Washington, D.C. pp 68- 76

10. Gazis, D.C. (1964); Optimum Control of a System of Oversaturated Intersections. *Operations Research*, vol. 12, pp. 815-831

11. Longley, D. (1968); A Control Strategy for a Congested Computer-Controlled Traffic Network. *Transportation Research*, vol. 2, pp. 391-408

12. Singh, M.G. and Tamura, H. (1974); Modeling and Hierarchical Optimization of Oversaturated Urban Road Traffic Networks. *Int'l Journal of Control*, vol. 20, no. 6, pp. 913-934

13. Michalopoulos, PG and Stephanapoulos, G. (1977); Oversaturated Signal System with queue length constraints-II. *Transportation Research.*, vol. 11, pp. 423-428

14. Michalopoulos, PG & Stephanapoulos, G. (1978) Optimal Control of oversaturated intersections: Theoretical and practical considerations. *Traffic Engineering and Control*, vol. 19, no. 5, pp. 216-222

15. Vaughan, R. & Hurdle, V.F. (1992); A Theory of traffic flow for congested conditions on urban arterial streets I: Theoretical developments. *Transportation Research-B*, vol.26B, no. 5, 1992, pp. 381-396

16. Gal-Tzur, A.; Mahalel, D.; & Prashker, J.N. (1993); Signal Design for Congested Networks Based on Metering. *In Transportation Research Record 1398*, TRB, Washington, D.C., pp. 111-118

17. TRANSYT-7F Users Guide. (1991); Center for Microcomputers in Transportation, Univ. of Florida, Gainesville, Florida.

18. Hadi, M.A. & Wallace, C.E. (1995); Treatment of Saturated Conditions using TRANSYT-7F. Compendium of technical papers.

19. Rathi, A.K. (1988); A control scheme for high traffic density sectors. *Transportation Research-B*, vol. 22B, no.2, pp. 81-101

20. Shibata, J. & Yamamoto, T. (1984); Detection and control of congestion in urban road networks. Traffic *Engineering and Control*, vol. 2, no. 9, pp. 438-444

21. McGhee, CC; Arnold, ED, Jr. (1997); Review and Evaluation of Methods for Analyzing Capacity at Signalized Intersections. In *Transportation Research Record: Journal of the Transportation Research Board No. 1572*, TRB, National Research Council, Washington, D.C. pp 160- 166

22. Dowling, RG. (1994); Use of Default Parameters for Estimating Signalized Intersection Level of Service. In *Transportation Research Record: Journal of the Transportation Research Board No. 1457*, TRB, National Research Council, Washington, D.C. pp 82- 95

23. Rouphail, NM (1989); Progression Adjustment Factors At Signalized Intersections. In *Transportation Research Record: Journal of the Transportation Research Board No. 1455*, TRB, National Research Council, Washington, D.C. pp 82- 95

24. Teodorvic, D. (1990); Analysis of Delay and Level of Service at Signalized Intersections in Delaware. Delaware Transportation Center, Civil Engineering Department, University of Delaware. August 1990.

25. Englebrecht, RJ; Fambro, DB; Rouphail, NM; Barkawai, AA (1997); Validation of Generalized Delay Model for Oversaturated Conditions. In *Transportation*

Research Record: Journal of the Transportation Research Board No. 1572, TRB, National Research Council, Washington, D.C. pp 122-130.

26. Kovvali, V. (2001); Development of Robust Arterial Signal Coordination Software. PhD Thesis. Texas A&M University. December 2001.

27. Daniel, J; Fambro, DB; Rouphail, NM (1996); Accounting for Nonrandom Arrivals in Estimate of Delay at Signalized Intersections. In *Transportation Research Record: Journal of the Transportation Research Board No. 1555*, TRB, National Research Council, Washington, D.C. pp 9-16.

28. Rouphail, N.M. (1993); Cycle-by-Cycle Analysis of Congested Flow at Signalized Intersections. *ITE Journal*, Vol. , No. March 1993, pp. 33-36.

29. Pignataro, L.J.; McShane, W.R.; Crowley, K.W.; Lee, B.; & Casey, T.W. (1978); Traffic Control in Oversaturated Conditions. NCHRP Report # 194, TRB, D.C.

30. Papacostas, C.S. and Prevedouros, P.D, *Transportation Engineering & Planning*, Third Edition, Prentice Hall, Inc., NJ, 2001

31. Khisty, C.J. and Lall, B.K, *Transportation Engineering An Introduction*, Third Edition, Pearson Education, Inc., NJ, 2003

32. May, A.D., *Traffic Flow Fundamentals*, Pearson Education, Inc., NJ, 1990

33. Dion, F, Rakha, H, Kang, Y.S' (2004); Comparison of Delay Estimation at under-Saturated and Over-Saturated Pre-timed signalized intersection. In Transportation Research Board, Vol. 32, No. 2, National Research Council, Washington, D.C. pp. 99-122

34. ITE (1995), "Canadian Capacity Guide for Signalized Intersection", Second Edition, S. Teply Editor, Institute of Transportation Engineers, District 7, Canada.

35. Kang, Youn-Soo, (2000), Delay, Stop and Queue Estimation for Uniform and Random Traffic Arrivals at Fixed-Time Signalized Intersections. PhD Thesis. Virginia Polytechnic Institute and State University, April 2000

36. TSIS version 5.1 user manual, ITT industries, Inc., Systems Division, 2003

37. Abu-Lebdeh, G. & Benekohal, R.F. Ahmed, K. (2003); Modeling of Traffic Signal Output for Design of Dynamic Intelligent Control in Congested Conditions. Proceedings of the 83rd Transportation Research Board Meeting, Washington D.C., January 04.

38. Rilett L. R. and Ok Kim Kyu. Comparison of TRANSIMS and CORSIM traffic signal simulation modules. In *Transportation Research Record: Journal of the Transportation Research Board No. 1748*, TRB, National Research Council, Washington, D.C., 2001, pp 18- 25

39. Bloomberg Loren and Dale Jim. Comparison of VISSIM and CORSIM Traffic Simulation Modules on a Congested Network. In *Transportation Research Record: Journal of the Transportation Research Board No. 1727*, TRB, National Research Council, Washington, D.C., 2000, pp 52- 60

40. Ahmed, K. & Abu-Lebdeh, G. (2005): "Modeling of Delay Induced By Downstream Traffic Disturbances At Signalized Intersection". Proceedings of the 84th Transportation Research Board Meeting, Washington D.C., January 05 (will be published in upcoming TRR Journal 05)


MICHIGAN STATE UNIVERSITY LIBRARIES
3 1293 02845 5214